Reinforcement Learning Applied to Forex Trading

João Maria Branco Carapuço

Thesis to obtain the Master of Science Degree in

Engineering Physics

Supervisor(s): Prof. Rui Fuentecilla Maia Ferreira Neves
Prof. Maria Teresa Haderer de la Peña Stadler

Examination Committee

Chairperson: Prof. Maria Joana Patrício Gonçalves de Sá
Supervisor: Prof. Rui Fuentecilla Maia Ferreira Neves
Member of the Committee: Prof. Rui Manuel Agostinho Dilão

November 2017

To my mother Cristina.

Without her life would be much darker.

Acknowledgments

I would like to thank my supervisor, professor Rui Neves, for his patience and dedication. All the best for future friday afternoon meetings and new students!

A word of appreciation for all my family, truly a part of my life that has been most fortunate. In particular: my grandparents António, Zizi, Nini and Lu, all are truly important to me and fill me with wonderful memories, my sister Maria, the day she was born I received presents and missed school and although the following 19 years haven't been nearly as good, I still love her, my mother Tita, to whom I dedicate this thesis, a small drop in the ocean of love and support that I still have to pay back, and last but certainly not least my father António, whose company has taught me so much and who I will always look up to.

Finally, I would like to mention those friends that were more present during this phase of my life: António Ornelas, always my MEFT comrade, Teresa, Ricardo and Bernardo, awesome company, anywhere, anytime, Galileu, consistently terrible company, Cláudio and Nones, always make me smile and laugh, Yanne, hour-long conversations that go by in five minutes.

Resumo

Nesta tese é descrita a implementação de um sistema que efectua transacções automáticas no mercado de moeda com o intuito lucrar com flutuações de cotação com aprendizagem por reforço e redes neuronais.
O funcionamento de um sistema de aprendizagem por reforço pode ser resumido em três sinais: uma representação do estado do ambiente dada ao sistema, a acção que este toma nesse estado e uma recompensa por essa acção. Uma rede neuronal é composta por neurónios artificiais interconectados que apesar de simples, como um todo estabelecem uma relação complexa e não-linear entre entradas e saídas. Essa relação pode ser ajustada para diferentes fins num processo de treino com aprendizagem automática.
O sistema transaccional concebido consiste numa rede neuronal com três camadas ocultas de 20 neurónios ReLU cada e uma camada de output com 3 neurónios lineares, treinada para funcionar sob o paradigma de aprendizagem por reforço. A rede recebe o estado do mercado, composto por características extraídas do histórico de preços e volumes, e dá como saída o valor Q de cada acção possível nesse estado. Valor Q é uma estimativa, construída no processo de treino, das recompensas que uma acção num dado estado vai acumular no futuro. A escolha da acção com melhor valor Q leva ao maior lucro futuro quando os valores estimados de Q têm qualidade.
No mercado EUR/USD desde 2010 a 2017 este sistema obteve em 10 testes com diferentes condições iniciais um lucro total médio de 114.0$\pm$19.6%, ou seja, uma média de 16.3$\pm$2.8% por ano.

Palavras-chave: Aprendizagem de máquina, Redes neuronais, Aprendizagem por reforço, Q-learning, Mercado de moeda

Abstract

This thesis describes the implementation of a system that automatically trades in the foreign exchange market to profit from price fluctuations with reinforcement learning and neural networks.
A reinforcement learning system can be summed up by three signals: a representation of the environment's state given to the system, the action it chooses for that state and a reward for the chosen action.
A neural network is a group of interconnected artificial neurons, which albeit individually very simple, as a whole establish a complex non-linear relationship between input and output. This relationship can be molded through an automatic training process.
The trading system described in this thesis is a neural network with three hidden layers of 20 ReLU neurons each and an output layer of 3 linear neurons, trained to work under the reinforcement learning paradigm, more precisely, under the Q-learning algorithm. This network receives as input a state signal from the market environment, comprised of features extracted from the history of prices and volumes, and outputs the Q-value of each action available for that state. Q-value is an estimate, built during the training process, of the amount of reward an action performed in a given state may accumulate in the future. Choosing the action with the best Q value leads to the largest future profit when Q-value estimates are accurate.
In the EUR/USD market from 2010 to 2017 the system yielded, over 10 tests with varying initial conditions, an average total profit of 114.0±19.6%, an yearly average of 16.3±2.8%.

Keywords: Machine learning, Neural networks, Reinforcement learning, Q-learning, Foreign exchange market

Contents

List of Tables

List of Figures

Nomenclature

Reinforcement Learning

γ	Reinforcement learning's discount-rate parameter.
$\mathbb{A}$	The set of all actions.
$\mathbb{E}$[X]	Expectation of random variable X.
$\mathbb{S}$	The set of all states.
π	A policy.
$\pi(s)$	Action taken in state s under deterministic policy π.
π_*	The optimal policy.
a	An action.
A_t	The action at step t.
G_t	Cumulative discounted reward following step t.
$p(s', r \mid s, a)$	Probability of transition to state s' with reward r, from state s taking action a.
$Q(s, a)$	Array estimate of an action-value function q_π or q_* for state s and action a.

$Q(s, a; \theta)$	Function approximation estimate of an action-value function q_π or q_* for state s and action a with parameters θ.
$q_*(s, a)$	Value of taking action a in state s under the optimal policy.
$q_\pi(s, a)$	Value of taking action a in state s under policy π.
r	A reward.
R_t	Reward at step t.
s, s'	States.
S_t	The state at step t.
$v_\pi(s)$	Value of state s under policy π.

Financial

A_i	The ask price from tick i in the dataset.
B_i	The bid price from tick i in the dataset.
T_i	The tick i in the dataset.
Va_i	The trading volume at the ask price from tick i in the dataset.
Vb_i	The trading volume at the bid price from tick i in the dataset.

Neural Networks

α	Learning-rate parameter.
$\mathbb{S}_k$	The subsample of cases for update k with mini-batch gradient descent.

$\mathbb{W}_k$	The set of all weights in the network at iteration k.
$\mathbf{a}^l$	The vector of all activations from the l^{th} layer.
$\mathbf{b}^l$	The vector of all biases in the l^{th} layer.
$\mathbf{d}_p$	The desired output for input $\mathbf{z_p}$.
$\mathbf{net}^l$	The vector of all total inputs to the l^{th} layer.
$\mathbf{z}_p$	The input from training case p.
a_j^l	The activation of the j^{th} neuron in the l^{th} layer.
b_j^l	The bias of the j^{th} neuron in the l^{th} layer.
$E(\mathbb{W})$	Total error between desired and actual output for set of weights $\mathbb{W}$.
$E_p(\mathbb{W})$	Error between desired and actual output for training case p and set of weights $\mathbb{W}$.
net_j^l	The total input to the j^{th} neuron in the l^{th} layer.
W^l	The matrix containing all weights for all neurons in the l^{th} layer.
w_{jk}^l	The weight the j^{th} neuron in the l^{th} layer gives to the part of its input that comes from the k^{th} neuron in the $(l-1)^{th}$ layer.

Glossary

Action-value function

Measures how good it is to perform a certain action in a given state, based on expected future reward.

Ask

In the context of Forex, it is the price at which a broker is willing to sell a unit of base currency, in units of counter currency.

Backpropagation

A widely used procedure to obtain the error contribution from each of a neural network's parameters.

Bid

In the context of Forex, it is the price at which a broker is willing to buy a unit of base currency, in units of counter currency.

Deep Network

A neural network with more than two non-linear layers.

Environment

That with which the RL agent interacts with.

Feedforward

The property of a neural network whose connections never form a cycle.

Forex/FX

The foreign exchange market.

Long

In the context of Forex, it is a trading position that entails buying units of the base currency while creating debt in the counter currency.

MSE

Mean squared error.

Policy

A mapping from states of the environment to actions to be taken when in those states.

Q-learning

An RL algorithm meant to estimate the optimal action-value function.

Q-network

A neural network designed to work under the Q-learning algorithm.

Q-value

An output of the action-value function obtained with the Q-learning algorithm.

RL

Reinforcement learning. A machine learning paradigm meant to create systems that learn from interaction to achieve a goal.

RMSProp

Root Mean Square Propagation, a gradient descent implementation with adaptive learning rate.

ReLU

Rectified linear unit, a type of artificial neuron.

Recurrent

The property of a neural network whose connections form a cycle.

Return

The relative difference between two prices and, consequently, the relative change of unrealized profit of an open position.

Reward

One of the input signals of a reinforcement learning system. Should relay to the system what is its objective by providing feedback on its performance.

Short

In the context of Forex, it is a trading position that entails buying units of the counter currency while creating debt in the base currency.

State-value function

Measures how good it is to be in a given state, based on expected future reward.

State

One of the input signals of a reinforcement learning system. Should include all relevant information about the environment for decision making.

Tick

The smallest granularity of foreign exchange data.

Topology

The frame of neurons and their interconnection structure in a neural network.

Unrealized Profit

The profit that a open position would provide if it was closed at this moment.

Value

In the context of RL, is the amount of reward the system is expected to accumulate in a given state.

Volume

Number of units traded at a certain price or during a certain time period.

Chapter 1

Introduction

In order to obtain an edge over their competitors, financial institutions and other market participants have been devoting an increasing amount of time and resources to the development of algorithmic trading systems. Algorithmic trading refers to any form of trading using algorithms to automate all or some part of the trade cycle, which includes pre-trade analysis, generation of the trading signal and execution of the trading signal. For example, an algorithm focused on pre-trade analysis could output price predictions, while an algorithm for trading signal generation would take it a step further and decide when to open or close positions in the market and finally a trade execution algorithm would have the ability to further optimize trading signals by deciding how large those positions should be and how to place them in the market.

The use of algorithmic trading began in the U.S. stock market more than 20 years ago and has nowadays become common in major financial markets [1]. The adoption of algorithmic trading in the foreign exchange market (Forex or FX), the market this thesis deals with, is a more recent phenomenon since the two major trading platforms for currency only began to allow algorithmic trades in the last decade. But it has grown extremely rapidly, and presently a majority of foreign exchange transactions involve at least one algorithmic counterparty, as shown in Figure 1.1. Despite concerns there is no evident causal relationship between algorithmic trading and increased market volatility. If anything, the presence of more algorithmic trading appears to lead to lower market volatility and increases liquidity during periods of market stress [1]. Although algorithmic trading was initially reserved for financial institutions and other major players in the markets, an increase in the availability of information, ease of access to the market and computational power of commercial computer technology has expanded this phenomenon to the retail trading and academic worlds.

This thesis describes the development of an algorithmic system that generates trading signals for the foreign exchange market using recent developments from the field of machine learning. These developments concern the use of Q-learning, an algorithm from the reinforcement learning (RL) paradigm, in tandem with neural networks (NNs), a computational tool that mimics biological brains, to create what is known as a Q-network. Enveloping the Q-network, the system's core, is a simulated market environment of our design that provides a widely applicable framework for efficient usage of market data in training

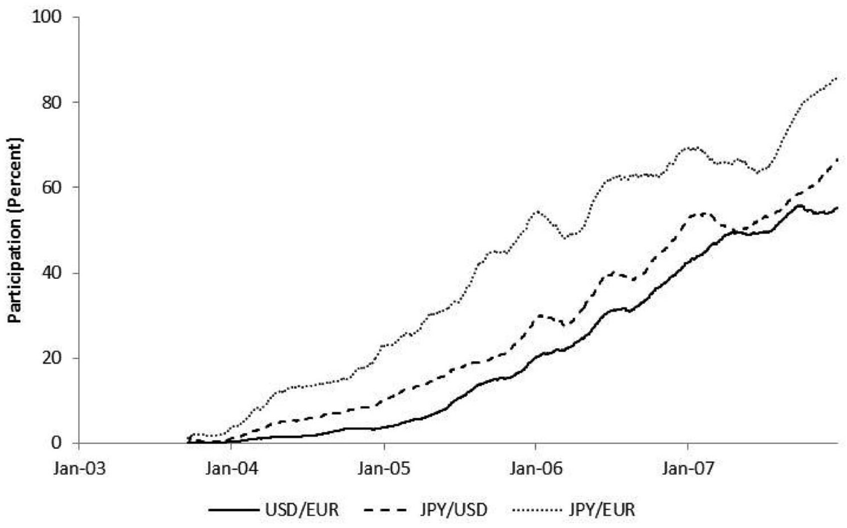

Figure 1.1: 50-day moving averages of the percent of total volume with at least one algorithmic counterparty, for three of the most commonly traded currencies. [1]

and testing a system for financial trading.

In this first chapter we introduce the foreign exchange market (section 1.1) followed by a concise overview of the machine learning field focusing on the approaches used in this thesis (section 1.2). We close the chapter by discussing the objectives and challenges of this work (section 1.3), our contributions (section 1.4) and the layout of the rest of the thesis (section 1.5).

1.1 Foreign Exchange Market

A financial market is a broad term describing any aggregate of possible buyers and sellers of assets and the transactions between them. Common usage of the term typically implies some characteristics such as having transparent pricing, basic regulations on trading, costs and fees. The assets traded in financial markets are intangible, their value is derived only from contractual claim. They can be roughly divided into three categories, commodities, securities and currency. Commodities represent the promise of delivery of a certain good, be it coal, gold, oranges, coffee, etc., that meets certain standards of quality that make each of its units interchangeable, thus facilitating trade. The legal definition of securities varies for different jurisdictions, but they can be broadly divided into debt securities, which represent borrowed money with specific repayment parameters, and equity securities, representing partial ownership of an entity. Stocks, usually the asset most associated with financial trading, fall into the category of equity securities. Finally, the market that will be focused on in this thesis is that of currency, which is simply money represented, sustained and given value by a certain central bank/government and which can be traded by its equivalent from another nation. This is the foreign exchange market, which exists to assist international trade and investments by enabling currency conversion.

Since currencies are the basis on which value is assigned to an asset they can only be measured in comparison with another currency, thus all currencies are traded in pairs. Figure 1.2 shows an example of price quotes displayed for traders in real time for four different currency pairs: EUR/JPY (Euro-

Japanese Yen), EUR/USD (Euro-US Dollar) pair, GBP/USD (British Pound-US Dollar) and NZD/USD (New Zealand Dollar-US Dollar). When the price is quoted, the first currency is the base and the se-

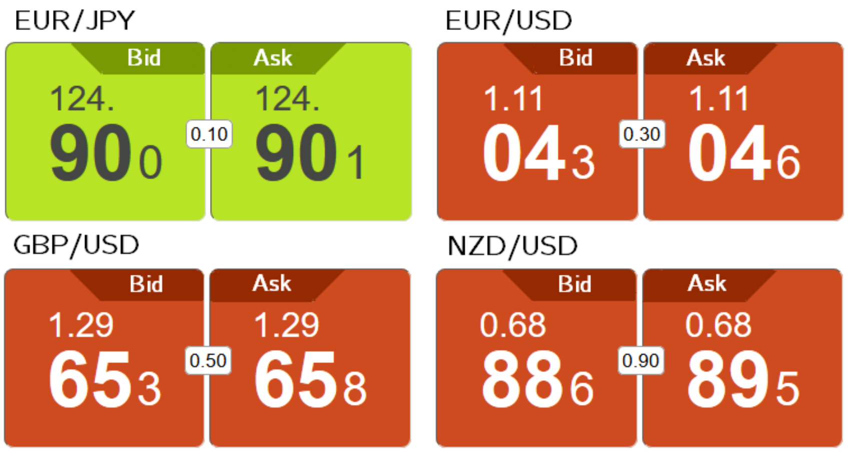

Figure 1.2: Price quotes from the swiss broker Duskacopy. Green means price has gone up since the last value, and red means it has gone down. Traditionally price quotes had five significant figures of which the last digit was known as a pip, the smallest possible price change at the time. Recently some brokers added one more digit of precision, known as fractional pip, which is shown here in a smaller font in reference to the traditional pip. The spread, the number in the small white box between the Bid and Ask prices, is also typically given in units of pips.

cond is the counter. The prices are always in terms of amount of counter currency for one unit of base currency. So the bid represents how much the broker offers in counter currency for one unit of base and the ask is how much the broker wants in counter currency for one unit of base. Spread is the difference between them and is always lost by the trader when he opens and then closes a position, acting as a commission for the trade.

While stock trading is centralized in stock exchanges, meaning all orders are routed to the exchange where a company is listed and then are matched with an offsetting order, with no other competing market, the Forex market operates very differently. There is no one location where currencies are traded. Without a central exchange, the trading rates are set by market makers, firms that stand ready to buy and sell currency held in inventory, on a regular and continuous basis at a publicly quoted price. They quote both a price a bid and an ask, hoping to make a profit on the price differential, the spread. At the highest level these market makers are huge banks selling and buying to mostly other banks, thus being commonly called the interbank market. Other than banks, only the largest hedge funds and large multinational companies can directly access the interbank market as it deals only with very large orders. There is little oversight, but fierce competition ensures fair pricing and small spreads. Retail level trading is mediated through brokers, companies which have access to this interbank market and act as the middle man for smaller traders. In this thesis we use historical datasets from Duskacopy, a swiss bank and broker.

The system developed in this thesis could theoretically be adapted to any financial market, but there is a particular reason why we chose to focus on foreign exchange during its development and subsequent testing. Forex is by far the largest financial market in terms of volume traded. According to the Bank for International Settlements, in the 2016 Triennial Central Bank Survey [2], trading in foreign exchange markets averaged 5.1 trillion $ per day in April 2016. To put this number into perspective, the New York

Stock Exchange, one of the the world's largest stock exchanges, has an average daily trading value of approximately 169 billion $, about 30 times smaller volume of trade. And while this trading volume in NYSE is spread over a couple of thousand companies represented in the exchange, Forex trading is heavily concentrated in just a few currency pairs, most notably among them the EUR/USD pair (see Table 1.1). This is of utmost importance because with high levels of liquidity we can be reasonably

Currency Pair	**2004**		**2007**		**2010**		**2013**		**2016**	
	Amount	%	Amount	%	Amount	%	Amount	%	Amount	%
EUR/USD	541	28.0	892	26.8	1,099	27.7	1,292	24.1	1,172	23.1
USD/JPY	328	17.0	438	13.2	567	14.3	980	18.3	901	17.8
USD/GBP	259	13.4	384	11.6	360	9.1	473	8.8	470	9.3

Table 1.1: Trade volume for the three most traded currency pairs. Daily averages for the month of April, in billions of US dollars and percentage of total volume. Note that over the past decade the EUR/USD pair has accounted for almost a quarter of total foreign exchange daily volume. [2]

confident that, when testing the system on data from the past, our hypothetical orders would be fulfilled in a timely fashion and at a price similar to what the price history shows, and we would not significantly influence the market. As the liquidity gets lower, this assumption holds up less and less. Thus, to ensure the most reliable results, our tests will be performed on the EUR/USD pair. Other advantages of the foreign exchange market include 24 hour trading, meaning larger amounts of data, and low transaction costs compared to other forms of financial trading.

1.2 Machine Learning

Machine learning is a sub-field of computer science that aims to build systems which automatically learn from experience and, at a deeper level, aims to find the fundamental laws that govern all learning processes. A machine is said to learn with respect to a particular task T, performance metric P, and type of experience E, if the system reliably improves P when performing T, after experiencing E [3]. Systems created under this field are able to infer patterns from observational data which has resulted in systems that can, for example, recognize objects in photographs or transcribe speech with considerable precision. In fact, machine learning systems have surpassed humans in some benchmarks such as recognizing handwritten digits [4] or traffic signs on a road [5], just to name a few. Machine learning truly shines in problems that are too complex for manually designed algorithms.

As it stands now, machine learning can be roughly divided into three approaches: supervised, unsupervised and reinforcement learning. In supervised learning an agent is given a number of inputs labeled with a desired output, and it is tasked with inferring the relationship between them so it can produce accurate outputs for further examples. In unsupervised it is given only the input with no labels at all and tasked with finding structure in that input, such as grouping by similitude for example. The third approach, reinforcement learning, is somewhat between supervised and unsupervised learning. Some of its inputs contain labels, but unlike the meticulous labels set by the supervisor in supervised learning, these are sparse and time-delayed, automatically generated from the environment where the system is operating. These labels are scalars called rewards, received as feedback after an RL agent chooses actions in a given environment. The agent learns desired behavior by trying to maximize the reward it receives. This approach is particularly suited for the development of control systems. With recent advances it has been leveraged to the development of agents that can learn behaviors with unprecedented intelligence, reaching and sometimes surpassing human decision making, all directly from data, without explicitly programmed responses.

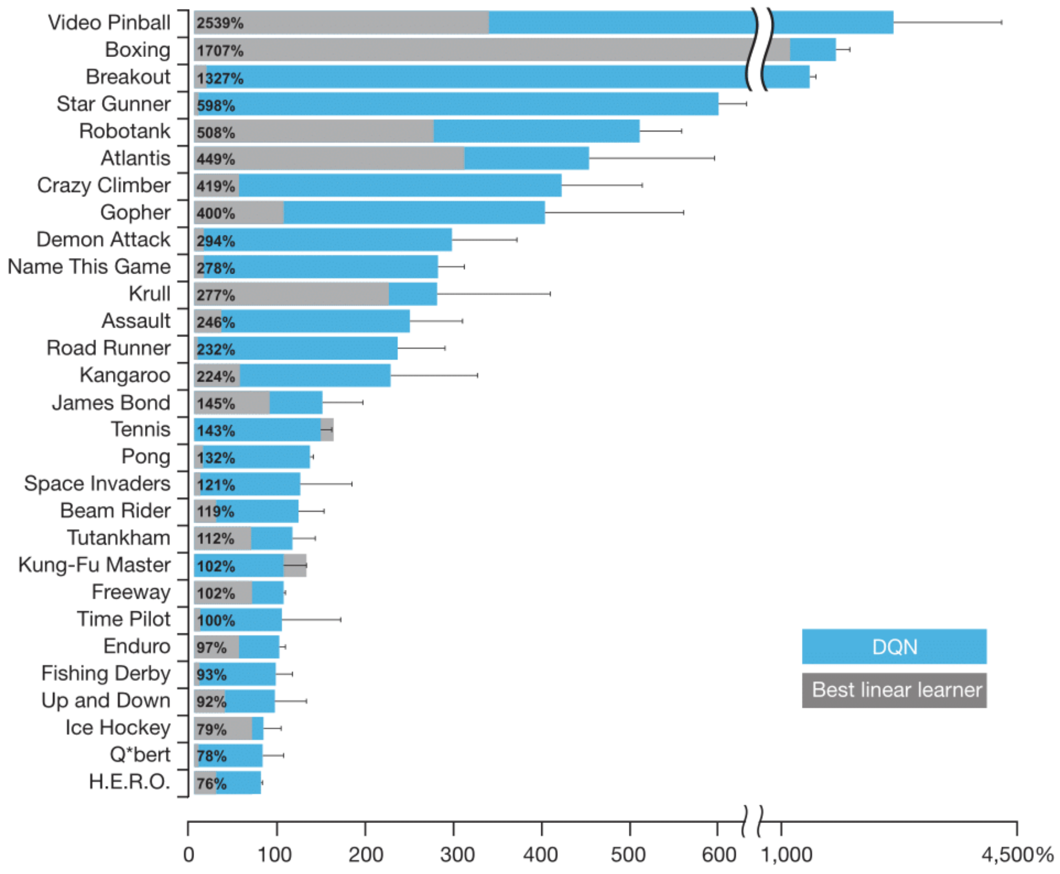

Figure 1.3: Performance of Deepmind reinforcement learning system on various Atari games. Performance is normalized with respect to a professional human games tester (100%) and random play (0%): $100 \cdot$ (score $-$ random play score)$/$(human score $-$ random play score). Error bars indicate standard deviation across 30 evaluation episodes, starting with different initial conditions. [6]

Reinforcement learning is actually far from new, one of its earliest successes was all the way back in 1995, a backgammon playing program by Gerald Tesauro [7]. But the field has of late come into a sort of Renaissance that has made it very much cutting-edge. Some high-profile successes ushered this new era of reinforcement learning. First, in 2013 a London-based artificial intelligence company (AI) called Deepmind stunned the AI community with a computer program based on the RL paradigm that had taught itself to play nearly 7 different Atari video-games, 3 of them at human-expert level, using simply pixel positions and game scores as input and without any changes of architecture or learning algorithm between games [8]. Deepmind was bought by Google, and by 2015 the system was achieving a performance comparable to professional human game testers in over 20 different Atari games [6], which are listed in Figure 1.3. Then, that same company achieved wide mainstream exposure when its Go-playing program AlphaGo, which uses a somewhat similar approach to the Atari playing system, beat the best Go player in the world in an event that reached peaks of 60 million viewers.

This reinforcement learning Renaissance was made possible by the use of techniques from another field of machine learning, neural networks. Neural networks consist of interconnected artificial neurons inspired by biological brains which provide computing power. In the examples cited above, and in this thesis' system, NNs are used with an RL algorithm called Q-learning, creating a Q-network. This combination has been used before, but often proved troublesome, especially for more complex neural networks. Contributions from Mnih et al. [8] and many others afterwards helped alleviate stability issues, allowing for more powerful Q-networks.

From the point of view of reinforcement learning neural networks provide much needed computational power to find patterns for decision making that lead to greater reward. From the point of view of neural networks, reinforcement learning is useful because it automatically generates great amounts of labelled data, even if the data is more weakly labeled than having humans label everything, which is usually a limiting factor for neural networks [9].

1.3 Objectives

The major challenges with this thesis come from the quality, or lack thereof, of financial markets data in regards to its use in predicting future developments of the market. The data is non-stationary and very noisy [10] which makes extracting usable patterns from it particularly difficult. Furthermore, neural networks require large amounts of data to learn, which may present a problem considering there is a single fixed market history with no possibility of generating more data. Also, the Q-network architecture itself is known to be difficult to train, requiring careful management over its inputs and hyper-parameters. With these challenges with mind, we have three main objectives for our system:

- Create a Q-network that is able to stably, without diverging, learn and thus improve its financial performance on the dataset it is being trained on;
- Show that the Q-network's learning has potential to generalize to unseen data;
- Harness generalization capabilities to generate profitable training decisions on a realistic simulation of live trading.

1.4 Contributions

In this section we briefly outline the contributions we hope to have provided with this thesis.

- A widely applicable framework for trading systems, supported by positive results in the EUR/USD currency pair over a large time frame;

- First adaptation of various state of the art reinforcement learning methodologies to foreign exchange trading, namely:
  - Use of a deep neural network topology as function approximator of action value function, enabled by the use of ReLU neurons and a gradient descent algorithm with adaptive learning rate;
  - Use of the experience replay mechanic and auxiliary Q-network for update targets introduced by Mnih et al. [8];
  - Use of the double Q-learning adaptation introduced by van Hasselt et al. [11];
- Introduced a novel framework for trading using tick market data:
  - Customizable preprocessing method, shown to provide features that induce stable learning which consistently generalizes to out-of-sample data;
  - Method for more efficient use of historical tick data resulting in both better training and more accurate testing;
- Introduced a reinforcement learning reward function for trading that induces desirable behavior and alleviates the credit assignment problem, leading to faster training;
- Introduced an easily customizable reinforcement learning state function with proven out-of-sample efficacy;

1.5 Outline of Contents

We conclude this introductory chapter with a brief outline of the contents of this thesis. In chapter 2 we provide the theoretical framework that supports the trading system. We start by discussing in section 2.1 the environment the system will be in, that of financial trading. Then in section 2.2 we introduce reinforcement learning, the paradigm that drives the system, and more specifically the algorithm of Q-Learning. We establish that reinforcement learning by itself is not enough for a problem of this complexity, leading to the introduction of neural networks in section 2.3, which will be the workhorse of the system.

We continue in chapter 3 by describing how we leveraged the theoretical tools introduced in the previous chapter to design the trading system. In section 3.1 a concise overview of the whole system is provided, introducing its three main pillars which are detailed in the following sections: a preprocessing stage, section 3.2, the simulated market environment, section 3.3, and the Q-network, section 3.4. We close this chapter with a word on hyper-parameter selection in section 3.5.

In chapter 4 the testing procedure is described and used to assess the validity of the proposed architecture using data the EUR/USD currency pair. Finally, chapter 5 provides some concluding remarks and a brief discussion of possible future developments for the proposed trading system.

Chapter 2

Background

In this chapter the theoretical foundations for the trading system are laid down. These can be separated into three essential pillars

- **Financial Trading:** the necessary knowledge from the domain of application (section 2.1);
- **Reinforcement Learning:** the paradigm guiding the trading system (section 2.2);
- **Neural Networks:** the computational tools that allow implementation of the paradigm (section 2.3).

2.1 Financial Trading

There are many approaches to financial trading, but they can be broadly categorized as belonging to one of four main types: hedge, arbitrage, investment or speculation. With hedge trading the aim is to open positions in the market that offset the risk of a trader's other business ventures. Arbitrage takes advantage of price differences between markets, objective mispricing, or any combination of factors that allow for risk-free profit. The last two, investment and speculation, have a much blurrier line dividing them. The distinction between them is one of risk and time frame. Investors tend to open bigger positions with a more in-depth analysis, and therefore supposedly with less risk, intended to stay open for longer periods, long enough to take advantage of the underlying financial attributes of the instrument such as capital gains, dividends, or interest. Speculators usually operate on smaller timeframes, and thus don't benefit from either such an in-depth research or the underlying financial attributes of the instrument, and care only for profits acquired through fluctuations of the asset's market value. The system developed in this thesis acts as a speculator.

Speculation is obviously dependent on having some form of price prediction capability so that decisions are correct more times than they are wrong to a degree that they compensate for transaction costs and allow for profit. Literature divides the methods for price prediction into two categories, technical and fundamental analysis, based on the data they analyze.

Technical analysis uses historical market data to find predictive patterns in an asset's price fluctuations. Market data is the sequence of prices the market went through and the respective number of units of the asset that were traded at those prices, known as the volume. This data is usually curated into fixed time intervals, such as hourly, daily or weekly, but these common depictions of market data are actually compressions of its true granularity, known as tick data, which will be used by this trading system. Whenever the market updates prices, which may happen several times in a second or just a couple of times in a minute depending on market activity and the broker's methods, a new tick is put out. Each tick contains the bid price and ask prices at the time it was put out and volume of trades that were executed at those prices, the bid volume and ask volume. Table 2.1 shows an excerpt of tick data for the EUR/USD currency pair.

Date	Bid	Ask	Bid Volume	Ask Volume
...	...	...	...	...
2012.04.04 15:30:26.520	1.31241	1.31248	2.40	1.50
2012.04.04 15:30:28.150	1.31241	1.31251	3.75	4.88
2012.04.04 15:30:28.576	1.31241	1.31251	4.13	4.88
2012.04.04 15:30:29.388	1.31247	1.31253	1.50	1.88
2012.04.04 15:30:29.800	1.31246	1.31253	1.13	1.13
2012.04.04 15:30:29.878	1.31245	1.31253	3.49	1.88
2012.04.04 15:30:30.301	1.31249	1.31256	1.50	2.78
2012.04.04 15:30:30.929	1.31249	1.31257	1.50	3.15
...	...	...	...	...

Table 2.1: Excerpt of tick data for the EUR/USD currency pair with the Duskacopy broker. Volume is in millions of units traded.

Fundamental analysis focuses on assessing the intrinsic value of the asset with the expectation that the market value will tend towards it. For a stock this would be ascertained by analyzing the company's financial statements, its market share, outlook of the sector, etc. The same principle of analysis holds for currency, but since currency reflects not a company but a whole country it is even vaster in scope, and includes information such as GDP growth, unemployment rates, interest rates, central bank monetary policies, debt, geopolitical landscape, etc.

Fundamental analysis of a currency is thus not easily curated to serve as machine learning input: data is often subjective and almost always very context-dependent. Besides, its strength usually lies in the medium to long term investments [12, 13, 14], meaning several months or years, while this system will focus on narrower time windows. For these reasons, our focus in this thesis will be on technical analysis, which we will explore further in the next section.

2.1.1 Technical Analysis

Trading under this discipline traditionally relies on technical indicators and technical rules. A technical indicator is simply a formula applied to a sequence of prices and/or volumes, with the aim of extracting some insight into the most likely evolution of prices in the future. Typically, simple descriptive statistics are applied in a sliding window of a certain number of market data entries preceding the current one.

Then, these are combined in a variety of manners to make up the different technical indicators. Technical rules turn indicators into trading decisions by triggering the opening or closing of positions based on their value or the configuration of values of a set of indicators.

There are many such indicators and rules, each with its own logic behind it. The focus of this thesis is not to explore these rules and their rationale, our interest in them is indirect. Evidence that classical technical indicators and rules produce results, supports the core concept of past market data having predictive value. Thus their building blocks, descriptive statistics of market data, could be used as inputs for our trading system.

Researchers have demonstrated that simple technical were able to generate excess returns over a long period during the 1970s and 1980s. These returns for the simpler rules had disappeared by the early 1990s, but returns for more complex or sophisticated rules persisted [15, 16]. Among a total of 95 modern[1] studies compiled by Park and Irwin [17] in 2007, 56 studies find positive results regarding technical trading strategies and 19 studies indicate mixed results. Surveys show that 30% to 40% of foreign exchange traders around the world believe that technical analysis is the major factor determining exchange rates in the short run up to 6 months [18, 13]. In their survey, Gehrig and Menkhoff [13] state that technical analysis is the main approach for foreign exchange traders.

Various theoretical and empirical explanations have been proposed to explain technical trading profits. In theoretical models, profit opportunities arise from noise in current equilibrium prices, traders' cognitive bias, herding behaviour, market power or chaos, while empirical explanations focus on central bank interventions, order flow, temporary market inefficiencies, risk premiums or market micro-structure deficiencies [17, and references therein]. It is not within the purvey of this thesis to explore the causes behind technical analysis' efficacy, but one explanation in particular needs further consideration.

It has been proposed that the apparent profits from technical trading could be spurious, an artifact of the research process resulting from data dredging. Whenever a good forecasting model is obtained by searching the data, there is always the possibility that the observed performance is simply due to chance rather than any merit inherent to the method yielding the results. In analysis of financial data only a single history measuring a given phenomenon of interest is available for analysis so the same data will be more extensively searched, which justifies the concerns with data dredging.

Tests were conducted by Hsu et al. [19] and Neely et al. [16] specifically to address this hypothesis. Hsu et al. [19] created 'data-snooping adjusted' p-values and their results support the notion that technical rules truly have significant predictive ability, but that their predictive power has declined over time. Neely et al. [16] takes a different approach in trying to extract results not contaminated by data snooping. They select trading methods that prominent literature had previously found to be profitable, and test their true out-of-sample performance by using datasets that did not yet exist at the time of their publication. They conclude that profits were not a result of data snooping. But in line with Hsu et al. [19] they also conclude profit opportunities from technical rules have declined over time, although complex strategies appear to survive longer than simple strategies. Overall using market data as a basis for trading decisions seems to be justified by evidence, with the worrying caveat that its efficacy has declined

[1]A study by Lukac et al. in 1988 is regarded by Park and Irwin [17] as the first modern work as it is among the first to substantially improve upon early studies in several important ways.

significantly over time.

2.1.2 Positions

As we discussed in section 1.1, currency is always traded in pairs, with a base currency and a counter currency. Two prices are displayed, the bid represents how much the broker offers in counter currency for one unit of base currency and the ask is how much the broker requires in counter currency for one unit of base. There are two positions a trader may take in a currency pair: long or short. Opening a long position in a currency pair implies buying the base currency while creating debt in the counter currency, while shorting the pair implies creating debt in the base currency and buying the counter. Opening a position of size K in units of the base currency at the instant t:

- Long position: buys K units of base currency creating debt of $K \times Ask_t$ units of the counter currency;
- Short position: creates debt of K units of base currency by acquiring $K \times Bid_t$ units of the counter currency;

When these positions are subsequently closed, the debt will be settled using the current value of the acquired currency. If the Ask and Bid moved favorably, the surplus is added to the trader's account otherwise the difference is removed from the trader's account. So an open position has an unrealized profit[2] at instant $t + k$:

- Unrealized profit of an open long position: $K \times (Bid_t - Ask_{open})$ units of the counter currency;
- Unrealized profit of an open short position: $K \times (Ask_t - Bid_{open})$ units of the base currency;

which becomes actual profit when it is closed.

Usually to open a position of size K it would be necessary to have an amount K in the trader's account to use as collateral, however this is not the case when brokers offer the use of leverage. When trading with leverage L, its possible to open a position of size $L \times K$ using that same collateral K. Most brokers allow traders to open positions with leverage as high as $L = 50$, or even higher. Thus the unrealized profit of such a position is L times higher, greatly enhancing our potential profits. The caveat is that our collateral must always cover possible negative profits, thus our position is automatically closed when the negative unrealized profit reaches a safety threshold, usually 50%, of our collateral. Since the position size is $L \times K$ rather than K, this can happen very easily and quickly for large L, leading to a higher risk / higher reward situation.

2.2 Reinforcement Learning

As Sutton and Barto [20] put it in their highly regarded 'Reinforcement Learning: An Introduction':

[2]We consider losses as simply negative profits.

Reinforcement learning, like many topics whose names end with “ing”, such as machine learning or mountaineering, is simultaneously a problem, a class of solution methods that works well on the class of problems, and the field that studies these problems and their solution methods.

The problem in RL is, to put it succinctly, that of learning from interaction how to achieve a certain goal. We frame this problem by identifying within it two distinct elements and detailing their interactions. The elements are the learner/decision-maker which we call the agent, and that with which the agent interacts, known as the environment. Their interactions consist of actions taken by the agent and the response of the environment following those actions (see 2.1).

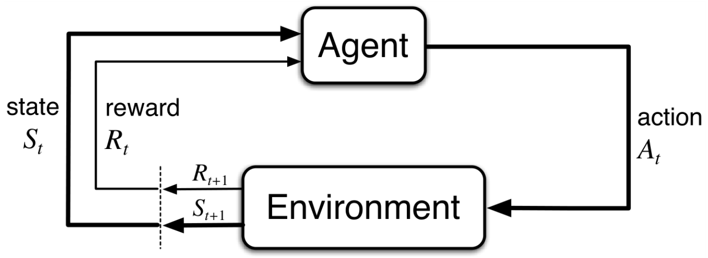

Figure 2.1: The RL learning framework. [21]

Formally, considering discrete time steps $t = 0, 1, 2, 3, ...$, at each t the agent receives some representation of the environment's state, $S_t \in \mathbb{S}$, where $\mathbb{S}$ is the set of possible states, and uses that information to select an action $A_t \in \mathbb{A}(S_t)$, where $\mathbb{A}(S_t)$ is the set of actions available in state S_t. The agent chooses an action according to its policy π_t, where $\pi_t(s)$ represents the action chosen if $S_t = s$ for a deterministic policy[3]. On the next time step $t+1$, the agent receives its reward R_{t+1} as a consequence of action A_t, and information about the new state S_{t+1}.

Coming back to the initial citation, we now have the class of solution methods for the problem of learning from interaction to achieve a goal. It is those that whatever the details of a specific problem, reduce it to the three signals mentioned – reward, state and action - being communicated between agent and environment. This framework has proven widely useful and applicable [20]. These signals can be implemented in a variety of ways, and the performance of the RL agent will be greatly dependent on this choice. A deeper look at each of them will provide direction and a basis for the choices to come later in this work.

2.2.1 State

In the RL framework the agent makes its decisions based on the condition of the environment, of which it only knows whatever the state signal contains. It is thus of utmost importance that this signal is competently crafted. If we imagine an agent that has to navigate the real world using some sort of sensor, it is obvious that the state at time t should include whatever immediate sensory measurements

[3]A deterministic policy is assumed throughout this chapter to lighten the notation, but all expressions are easily generalized to the stochastic case, where $\pi_t(a|s)$ is the probability that $A_t = a$ if $S_t = s$.

are coming from the sensor, but it can contain much more than that. The same way that after looking around a room we are only actually seeing whatever our eyes are looking at in the moment and still we know there is a red chair to the right, a double bed behind us, etc., the agent would be more effective if the current state could contain information from previous sensory measurements. In a similar spirit, an agent that deals with speech and tries to maintain a conversation, when hearing the word “no” at certain moment t should consider itself in completely different states depending on the words that preceded this input, which is done by including past information in S_t. This basically amounts to giving context to the present, if it did not have that context included its state signal, the “no” alone would probably become a less meaningful piece of information.

What these examples mean to convey is that ideally we want a state signal that summarizes the past in such a way that all relevant information is retained. Such a signal is said to have the Markov property. Only all relevant information is needed for a Markov state, not a full history of past sensations. A good example of this distinction would be a state containing the current configuration of pieces on a checkers board. It does not contain all information about the sequence of events that led to it, the configuration of pieces 5 or 6 moves ago cannot be ascertained, but in terms of future developments it contains everything relevant.

With a Markov state the environment’s response at $t+1$ depends solely on the state and action on the previous time step t. Thus, the dynamics of a general, causal environment’s response at time $t+1$ to the action taken at time t that would otherwise need to account for everything that has happened earlier with a complete conditional probability such as:

$$Pr\{S_{t+1} = s', R_{t+1} = r \mid S_0, A_0, R_1, ..., S_{t-1}, A_{t-1}, R_t, S_t, A_t\}, \tag{2.1}$$

can now be reduced to simply:

$$Pr\{S_{t+1} = s', R_{t+1} = r \mid S_t = s, A_t = a\} \doteq p(s', r \mid s, a), \tag{2.2}$$

for all r, s', s and a.

The theoretical framework of RL relies on 2.2, meaning it assumes Markov states. In many cases this is only an approximation since a true Markov state is not easily achieved, but RL systems still work very well for many problems that do not strictly fulfill this requirement. Nevertheless, as the state signal approaches Markov property it becomes a better basis for predicting future rewards and for selecting actions, which will generally mean better performance [20]. It is unfeasible to construct a true Markov state for financial trading, there are too many factors that influence markets. But within the realm of an asset’s market data we can hope to construct a state that compactly stores most of the relevant information. In section 3.2 we will explore the creation of such a state.

2.2.2 Reward

The use of a reward signal to represent the idea of a goal is among the most distinctive features of reinforcement learning. This signal is extracted from the environment and given to the agent after it performs an action. This idea can be stated as the reward hypothesis [20]:

> All of what we mean by goals and purposes can be well thought of as maximization of the expected value of the cumulative sum of a received scalar signal: the reward.

It is thus critical that the rewards we set up truly indicate what we want accomplished. It is also important that they don't communicate *how* it should be accomplished, just *what*. For example, if we want an agent to learn how to administer medicine, we should reward it only for curing a patient, not for eliminating each of the particular symptoms. Otherwise, an agent might find a way to maximize the received reward by repeatedly achieving these sub-goals without completing the ultimate goal, letting the patient stay sick and maybe eventually die.

Now, lets say our agent has cured the patient and receives its reward. In the process of curing it tried a thousand different medicines, which ones had the desired effect? Which ones should it associate with the desired outcome? This is the credit assignment problem, a problem at the core of reinforcement learning. As the delay between action and reward grows, credit assignment becomes more and more difficult. In subsection 3.3.2 we discuss the implementation of a reward function that facilitates credit assignment without restricting the system's behaviour.

2.2.3 Actions

With reinforcement learning we aim to perform the action most suited to achieving our goals when presented with the environment in a certain state. In RL terms, this means we want to find a policy π for our agent, that obtains as much reward as possible over its lifetime. The sequence of rewards an agent will receive after time step t is denoted as $R_{t+1}, R_{t+2}, R_{t+3}, \ldots,$. We want to maximize:

$$G_t = R_{t+1} + \gamma R_{t+2} + \gamma^2 R_{t+3} + \cdots = \sum_{k=0}^{\infty} \gamma^k R_{t+k+1}, \tag{2.3}$$

the sum of those rewards with a chosen discount rate γ. The discount rate allows for a prioritization of immediate versus future rewards according to the specific purpose of the agent.

To relate the discounted sum G_t with a policy π, we use value functions. There are two value functions, firstly the state-value function:

$$v_\pi(s) \doteq \mathbb{E}_\pi[G_t \mid S_t = s] = \mathbb{E}_\pi[\sum_{k=0}^{\infty} \gamma^k R_{t+k+1} \mid S_t = s], \tag{2.4}$$

which, qualitatively, tells us how good we expect it is to be in a certain state s for a policy π. Secondly, the action-value function:

$$q_\pi(s,a) \doteq \mathbb{E}_\pi[G_t \mid S_t = s, A_t = a] = \mathbb{E}_\pi[\sum_{k=0}^{\infty} \gamma^k R_{t+k+1} \mid S_t = s, A_t = a], \tag{2.5}$$

which tells us how good we expect it is to perform a certain action a in a given state s and following policy π thereafter. Throughout this thesis we often refer to values of a action-value function as Q-values.

To make a human analogy, rewards are somewhat like pleasure (if high) and pain (if low), whereas values correspond to a more refined and farsighted judgment of how pleased or displeased we are that our environment is in a particular state. We seek actions that bring states of highest value, not highest reward, because these actions will obtain the greatest amount of reward for us in the long run. We can tune what constitutes ”the long run” by changing the discount rate γ.

If a policy is better than all others then the value of each state for that policy must be higher, as it is expected to accumulate the most reward when starting from it. The goal in RL can be restated as trying to find such a policy, usually known as the optimal policy:

$$\pi_* = \arg\max_\pi v_\pi(s), \forall s \in \mathbb{S}, \tag{2.6}$$

where the $\arg\max$ operator, short for ”arguments of the maxima”, returns the arguments or inputs at which the function has its maxima. The value functions associated with the optimal policy are denoted as $v_*(s)$ and $q_*(s,a)$. A well-defined notion of optimality organizes the approach to learning, although it is rarely reached in most problems as it would require extreme computational cost.

2.2.4 Q-Learning

Most algorithms in RL involve finding value functions, from which a policy can be derived, rather than directly searching for the policy. The algorithm used throughout this thesis is called Q-Learning, and relies on estimating the optimal state-action value function. To do this, we first need to look at a fundamental property of value functions, a recursive relationship known as Bellman equations [22]. We derive these equations for q_π from its definition, by expanding the right side of 2.5:

$$\begin{aligned}
q_\pi(s,a) &= \mathbb{E}_\pi[G_t \mid S_t = s, A_t = a] \\
&= \mathbb{E}_\pi[\sum_{k=0}^{\infty} \gamma^k R_{t+k+1} \mid S_t = s, A_t = a] \\
&= \mathbb{E}_\pi[R_{t+1} + \gamma \sum_{k=0}^{\infty} \gamma^k R_{t+k+2} \mid S_t = s, A_t = a] \\
&= \sum_{s'} \sum_{r} p(s', r \mid s, a)[r + \gamma \mathbb{E}_\pi[\sum_{k=0}^{\infty} \gamma^k R_{t+k+2} \mid S_{t+1} = s']] \\
&= \sum_{s',r} p(s', r \mid s, a)[r + \gamma v_\pi(s')] \\
&= \sum_{s',r} p(s', r \mid s, a)[r + \gamma q_\pi(s', \pi_t(s'))], \\
&= \mathbb{E}_\pi[R_{t+1} + \gamma q_\pi(S_{t+1}, \pi(S_{t+1}))]
\end{aligned} \tag{2.7}$$

where $\pi_t(s')$ is the action chosen by the policy π for a state s'. The Bellman equations state that the value of a starting state must be equal to the discounted value of the expected next state, plus the reward expected to be received between them.

Explicitly solving these equations is one route to finding an optimal policy, and thus to solving the RL problem. However, this solution is not useful to us. It is akin to an exhaustive search, which for any complex problem is unfeasible as it requires immense computational power. Furthermore, we would need $p(s', r \mid s, a)$ for all r, s', s and a, or in other words, a complete and accurate knowledge of the dynamics of the environment, which we do not have in our problem of foreign exchange markets. So we need an alternative way to obtain solutions, and when facing a recursive relationship an obvious path is to turn it into an update rule and build that solution iteratively from an arbitrary initial value. Using the last line of 2.7 as a target we obtain the update rule:

$$q_{k+1}(s,a) = \sum_{s',r} p(s', r \mid s, a)[r + \gamma q_k(s', \pi_t(s'))], \tag{2.8}$$

which belongs to a class of methods known as dynamic programming, a close cousin to RL. It is important to point out that the action value for a new state s' and action $\pi_t(s')$, $q_\pi(s', \pi_t(s'))$, is something we don't know, we are doing this to find the value function after all. So we simply used our current estimate, $q_k(s', \pi_t(s'))$, in the update to $q_k(s,a)$, an approach called bootstrapping.

However, while this method makes approximating a solution more computationally tractable, it still requires, like the analytical approach, complete and accurate knowledge of the environment's dynamics, making it unusable[4]. We side-step this problem by using actual experienced transitions in place of knowledge of the expected transitions. In fact, we use only the current observed transition as an estimate:

$$q_{k+1}(s,a) = (1-\alpha) q_k(s,a) + \alpha[r + \gamma q_k(s', \pi_t(s'))], \tag{2.9}$$

[4]This is not strictly true, in some problems the complete dynamics are not known or not tractable, but a simplified model can be developed and a useful value function derived from it. Such a thing could be attempted for financial markets, but I feel the financial theoretical framework is far from being robust enough.

where α is the learning rate, allowing us to adjust how much we want to update the estimate at each observation. We have derived the RL update rule known as SARSA, named after its use of the events $s, a, r, s', a' = \pi_t(s')$. This update rule is but a short step from the one used in this thesis.

The difference is in the bootstrapping element: $\gamma q_k(s', a' = \pi_t(s'))$. When SARSA bootstraps, it does so assuming the next action taken is the one given by the policy, $\pi_t(s')$, which means that q_k is an approximation of q_π. This kind of algorithm is known as on-policy, while Q-Learning is an off-policy algorithm. A Q-learning agent also performs its actions following a policy π, but updates to q_k are meant to approximate q_*. Thus, the update rule is:

$$q_{k+1}(s, a) = (1 - \alpha) q_k(s, a) + \alpha[r + \gamma \max_{a'} q_k(s', a')]. \tag{2.10}$$

In essence, $q_{k+1}(s, a)$ values in Q-Learning represent taking action a in state s and then following the optimal policy, while SARSA's represent taking action a in state s' and then following the same policy that generated a. The classic implementation of this algorithm is a table where each state-action pair has a corresponding tabulated value $Q(S_t, A_t)$ initialized arbitrarily and then updated with 2.10.

The use of bootstrapping or a single observation as an estimate of transition dynamics may seem like far-fetched approximations, but over many visits to a state s and subsequent transitions from it, those errors balance themselves off, and Q can indeed be proven to converge to q_* with Q-Learning under a few simple assumptions (see [23]).

2.2.5 Policy

The purpose of control algorithms is to find a policy that performs as desired. Q-Learning is no exception, although the search for a policy is done indirectly through the value function. When our system has finished learning and we have our estimate for $q_*(s, a), \forall s \in \mathbb{S}, \forall a \in \mathbb{A}(s)$, the policy becomes implicitly defined by $\pi_*(s) = \arg\max_a q_*(s, a), \forall s \in \mathbb{S}$. While learning however, such a policy does not suit our purposes because we want to discover the relations between states, actions, and rewards, which entails exploration by choosing actions not currently seen as optimal. On the other hand, we need to leverage some of the knowledge acquired thus far, since the states encountered during training are dependent on the actions taken and we want the system to experience states similar to those it will encounter afterwards. Common approaches to balance these two conflicting needs include:

- ϵ-greedy action selection method, whereby the action with highest value (greedy), is selected with probability $1-\epsilon$ and an exploratory action, randomly chosen among all actions available, is selected with probability ϵ;
- Greedy action selection with optimistic initial estimates for the value function. For any actions already taken, value estimates have already been adjusted downwards from their optimistic initialization, so greedy action selection leads to exploring novel actions;
- Softmax action selection where actions are given a probability of being chosen according to their current estimated value, using a Gibbs or Boltzmann distribution for example [20].

Note that for financial trading this dependence of states encountered during training on the actions taken is weaker in comparison to other more common reinforcement learning environments, since actions are assumed to have no effect on the market. But there is still a dependence since a certain portion of the market history may be reached with or without a position open, with a different type of position open, and with positions opened at different points in the past.

2.2.6 Limitations of Reinforcement Learning

The classic tabular implementation of Q-learning, where each entry corresponds to the current estimate for a given state-action pair (s, a), is only possible for cases where the state and action spaces consist of a small, finite number of discrete elements [24]. As state-action spaces become larger such a representation for Q-values requires larger and larger portions of memory. Furthermore, since each state-action pair has to be visited a number of times to accurately fill the entries, it requires more and more time and interactions to do so, in what is commonly called the sample problem. Finally, there is a problem of optimization as the maximization over the action variable in 2.10 has to be solved for every sample considered. In large or continuous action spaces, this maximization can lead to impractical computational requirements. This limitation is a central challenge in RL, and one we have to overcome.

For the action space a simple but effective solution is discretization. Discretization of an action-space into a small number of values solves the optimization problem and greatly alleviates the sample problem by turning a potentially very large number of available actions in each state into only a few state-action pairs per state to explore. Discretization lends itself quite naturally to our trading system, since we do not optimize order execution we are only interested in knowing when system thinks it is a good time to open a position rather than its size. Thus, the actions can be discretized into simple dichotomies of buy/sell as detailed in chapter 3.

Discretization of the state space on the other hand, is not advantageous. Firstly, it is not needed to solve the optimization problem. Secondly, while action signal discretization comes naturally, streamlining the problem without drawbacks, state signal discretization degrades the information given to the system. An alternative is function approximation, which works by taking examples from a desired function and attempting to construct an approximation of the entire function. This effectively solves the representation problem by replacing the table with an approximately equivalent function $Q(s, a; \theta)$, where θ is the set of parameters of the function approximator. Furthermore, it provides an essential contribution towards the sample problem: generalization power. An approximator can be designed so that changes to the value function in each state influences the value function in other, usually nearby states[5]. Then, if good estimates are available in a certain state, the algorithm can also make reasonable control decisions in nearby states.

Neural networks acting as function approximators are known for their capacity to process both linear and nonlinear relationships and for being the best available method for generalization power [9]. While trading we will never see the same exact state twice, so power of generalization is essential. Thus, the action-value function in our reinforcement learning system is embodied in a neural network, which

[5]This requires the assumption of a certain degree of smoothness.

is usually dubbed a Q-network. Classically, Q-Learning updates a previous tabulated estimate for the value of an action-state pair by observing the result of each state transition. With function approximation it simply provides that same information as a training example to the NN instead.

2.3 Neural Networks

Neural networks are a computational approach loosely modeled after biological brains. Brains can be seen as an interconnected web of neurons transmitting elaborate patterns of electrical signals: dendrites receive input signals and, based on those inputs, fire an output signal via an axon. NNs mimic this effect via artificial neurons connected in what can be mathematically described as a graph.

NNs receive input from the outside world into their input neurons and perform a forward propagation: the input is propagated to other neurons in the network and each neuron changes the signal according to its internal set of rules until the signal goes through the whole structure, culminating in an output to the exterior from its output neurons. This creates a complex relationship between the input it receives and the output it generates, and that relationship can be shaped to suit a variety of purposes.

2.3.1 Neurons

A given neuron j has a number of other neurons with a connection to it, i.e., which transfer their output to j. These inputs $x_1, x_2, ..., x_n$, coming from neurons $i \in 1, 2, ..., n$ are received by the neuron j's propagation function which transforms them according to the weight of the connection between j and i, w_{ji}, into the total input net_j. There are some exotic propagation functions, but the one almost all NNs use, and the one used throughout this thesis, is a weighted sum in the form:

$$net_j = \sum_{i=1}^{n} x_i w_{ji} + b_j \tag{2.11}$$

where b_j is an adjustable bias. It is clear from 2.11 that the weights w_{ji} determine the strength of one neuron's influence on the other, i.e. the strength of the connection between them. The total input net_j is then transformed by neuron j's activation function f_j, as depicted in Figure 2.2, resulting in the activation a_j:

$$a_j = f_j(net_j) = f_j(\sum_{i=1}^{n} x_i w_{ji} + b_j). \tag{2.12}$$

a_j is outputted from neuron j either to be used as input by other neurons in the network or as output of the whole network if j is an output neuron. Since the propagation function is almost always assumed to be a weighted sum, it is its activation f_j that defines a neuron.

Almost any function can be used as activation although it should be non-linear to introduce non-linearity into the network, allowing it to model a response variable that varies non-linearly with its explanatory variables [25]. But if other neurons in the network are already non-linear, linear neurons are acceptable as well. Some activation functions are noteworthy, either for their historical importance or

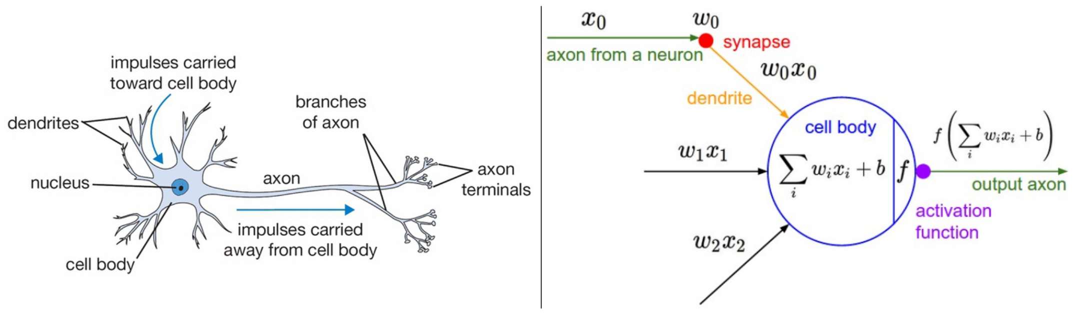

Figure 2.2: A very simplified drawing of a biological neuron (left) and its mathematical model (right). [26]

their widespread use. The simplest activation is an Heaviside function:

$$a_j = \begin{cases} 1, & \text{if } net_j > 0 \\ 0, & \text{otherwise} \end{cases} \tag{2.13}$$

whereby the neuron either fully activates or it does not activate at all. Networks with this activation function are called perceptrons, they are historically relevant since the first neural networks belonged to this category. However, this function is not differentiable therefore, as we will see in subsection 2.3.3, it cannot be used in most modern implementations of neural networks.

After the initial period of perceptrons the most common activation function, and still used to this day, became the logistic function, usually simply referred to as the sigmoid function σ:

$$a_j = \sigma(net_j) = \frac{1}{1+e^{-net_j}} = \frac{1}{1+e^{-\sum_{i=1}^{n} x_i w_{ji} + b_j}}. \tag{2.14}$$

It takes a real-valued number and "squashes" it into range between 0 and 1. In particular, large negative numbers become 0 and large positive numbers become 1. It is a logical step from the perceptron: it is similar to the Heaviside function but with the added benefits of a region of uncertainty and an easily computable derivative. A common variation of this standard sigmoid, is the $\tanh$ function:

$$a_j = \tanh(net_j) = \tanh(\sum_{i=1}^{n} x_i w_{ji} + b_j), \tag{2.15}$$

which squashes a real-valued number to the range [-1, 1]. It is just a rescaled version of the sigmoid:

$$\tanh(net_j) = \frac{e^{net_j} - e^{-net_j}}{e^{net_j} + e^{-net_j}} = 2\sigma(\frac{net_j}{2}) - 1, \tag{2.16}$$

but this makes its output zero-centered, which is usually preferred.

Finally, an activation function that has been gaining traction over the last few years is ReLU, short for rectified linear unit:

$$a_j = \max(0, net_j) = \max(0, \sum_{i=1}^{n} x_i w_{ji} + b_j), \tag{2.17}$$

whose non-linearity comes from its behavior at 0. These are some of the most widely used functions, but there many many others. Neural networks with any of these activation functions are universal approximators [27], even the very simple Heaviside step. This means any of them can theoretically perform the task we need. This is not to say they are guaranteed to do so, at all. Learning in neural networks is a complex task that can fail in many ways, so in practice networks built using different neurons outperform each other depending on the application. They may learn faster, generalize better to test data, be easier to implement, require less input treatment, and many other practical considerations.

2.3.2 Topology

The topology of a neural network is both the frame of neurons and their interconnection structure. To guide the effort of building a network the frame of neurons rather than being an amorphous blob is very often organized into distinct layers. With this structural approach there is always an input layer and an output layer, any additional layers are placed between those two and referred to as hidden layers.

Each neuron in the input layer represents a dimension of the input, which it feeds to whichever neurons it has a connection to. Generally input neurons are passive, they simply distribute the inputs without transforming them through an activation function. Neurons in the hidden layers are invisible in the sense that they have no interaction with the outside world, their inputs come from other neurons in the network, are transformed, and their output goes to other neurons in the network. They exist to add complexity and representational power. Neurons in the output layer also transform the input they receive and their activation corresponds to a dimension of the output of the whole network, so their activation function should be chosen in accordance with the kind of output we want our network to produce.

As for interconnection structure there are two fundamentally distinct types of neural networks, feedforward and recurrent (see Figure 2.3). Feedforward networks have an unidimensional flow of information from input to output layer, a neuron never feeds its output to a neuron in the same or previous layer and so its units never form a cycle. Recurrent networks are networks that have at least one such connection, forming a directed cycle. In this thesis we focus on feedforward networks, in particular feedforward networks with no skip connections: connections between neurons that are more than one layer apart.

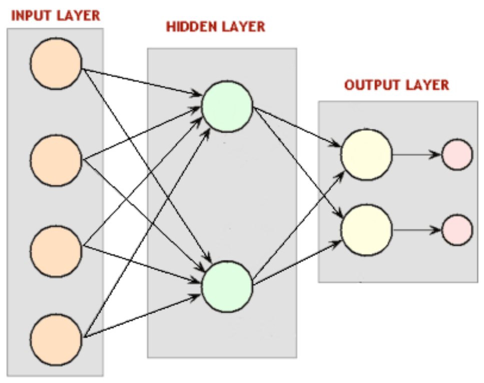

(a) A feedforward neural network.

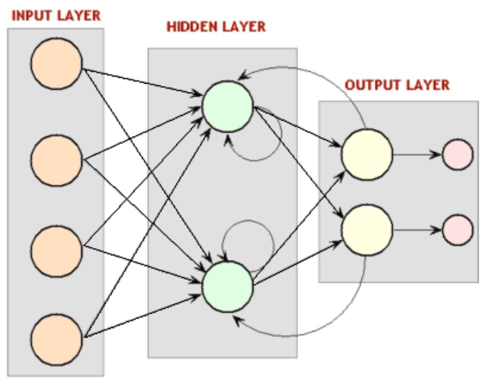

(b) A recurrent neural network.

Figure 2.3: Example of feedforward and recurrent neural networks with one hidden layer. [28] (modified)

These constraints to the topology allow for an improvement over the notation introduced in subsection 2.3.1, which will be useful in discussing the NNs learning mechanism in the next section:

- a^l_j is the activation of the j^{th} neuron in the l^{th} layer and $\mathbf{a}^l$ is the vector of all activations from the l^{th} layer;
- net^l_j is the total input to the j^{th} neuron in the l^{th} layer and $\mathbf{net}^l$ is the vector of all total inputs to the l^{th} layer;
- b^l_j is the bias of the j^{th} neuron in the l^{th} layer and $\mathbf{b}^l$ is the vector of all biases in the l^{th} layer;
- w^l_{jk} is the weight the j^{th} neuron in the l^{th} layer gives to the part of its input that comes from the k^{th} neuron in the $(l-1)^{th}$ layer and W^l is the matrix containing all such weights for all neurons in the l^{th} layer;

This notation and the type of neural network topology considered is exemplified for a small network in Figure 2.4.

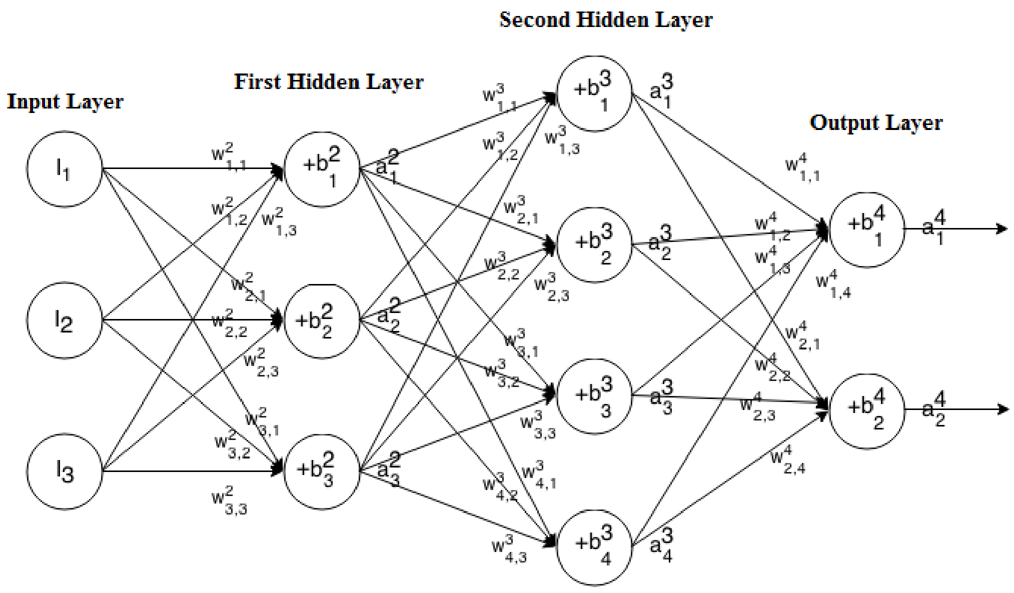

Figure 2.4: A fully-connected feed-forward neural network with two hidden layers and no skip connections. [29] (modified)

Having discussed topology, an addendum to the statement of neural networks being universal approximators can be made. As stated, this property holds for an arbitrary activation function, the defining trait is topology: a neural network needs to have at least one hidden layer to have the potential for universal approximation [27].

2.3.3 Backpropagation

A neural network is configured for a specific application, such as pattern recognition or data classification, through a learning process as opposed to explicit programming. Learning in neural networks is achieved by changes in the network as an automated response to stimuli. Like biological brains, which can learn by adjusting synaptic connections between the neurons, NNs change the strength of connections between their neurons.

Formally, a neural network computes a function, which we refer to as $M(\mathbf{z}_p; \mathbb{W}_k)$, where $\mathbf{z}_p$ is the p^{th} input pattern and $\mathbb{W}_k$ is the set of weights[6] in the network at iteration k. This function is evaluated regarding its discrepancy towards $\mathbf{d}_p$, the desired output for input $\mathbf{z}_p$, as measured by a cost function[7] $E_p(\mathbb{W}_k) := C(M(\mathbf{z}_p; \mathbb{W}_k), \mathbf{d}_p)$ over a training set $\{(\mathbf{z}_1, \mathbf{d}_1), ..., (\mathbf{z}_P, \mathbf{d}_P)\}$.

The problem of learning then becomes one of optimization, we want to find the set of weights $\mathbb{W}$ that minimizes the total error $E(\mathbb{W})$. Throughout this thesis the total error is defined through the mean squared error (MSE):

$$\begin{aligned} E_p(\mathbb{W}_k) &= \|\mathbf{a}^L_{p,k} - \mathbf{d}_p\|^2 \\ E(\mathbb{W}) &= \sum_{p=1}^{P} \frac{E_p(\mathbb{W})}{P} \end{aligned} \tag{2.18}$$

where $\mathbf{a}^L_{p,k}$ is the activation vector the output layer L for $\mathbb{W}_k$ and $\mathbf{z}_p$.

There can be easily millions of weights in the set $\mathbb{W}$, so solving this optimization problem analytically is unfeasible [30]. The alternatives include using genetic algorithms to evolve the weights, Hebbian learning or even, in some specific and small problems, exhaustive search. But the method that has been by far most effective on the majority of problems is gradient descent. Gradient descent methods work on the basis that if the multi-variable function $E(\mathbb{W})$ is defined and differentiable in a neighborhood of a point a, then $E(a)$ decreases fastest if one goes from a in the direction of the negative gradient $-\nabla_{\mathbb{W}} E(a)$. To repeatedly use gradient descent to train a neural network, an efficient way to find $\nabla_{\mathbb{W}} E(\mathbb{W})$ is required. This need was answered by a method known as backpropagation.

To intuitively demonstrate backpropagation it is introduced below in a similar manner to how it was described by Rumelhart et al. [31], often cited as the source of this procedure. In this proof of concept the sigmoid is the activation function for all neurons[8] in a network with L layers. This network receives an input $\mathbf{z}_p$ from the training set, performs a forwards propagation and delivers an output corresponding to the activations of the last layer $\mathbf{a}^L_p$. With squared error as the cost function, for an input/desired output pair p:

$$E_p(\mathbb{W}_k) = \frac{1}{2}\|\mathbf{a}^L_{p,k} - \mathbf{d}_p\|^2 = \frac{1}{2}\sum_j (a^L_j - d_j)^2_{p,k} \tag{2.19}$$

where j is an index over the neurons in the output layer and $\frac{1}{2}$ is included here only to simplify notation for derivatives. For notational clarity indexes p and k are suppressed from all variables except $E_p(\mathbb{W}_k)$ for the rest of this proof of concept.

As the name suggests, backpropagation finds $\nabla_{\mathbb{W}} E_p(\mathbb{W}_k)$ starting from how the weights in the output layer influence $E_p(\mathbb{W}_k)$ and propagating that influence backwards. Thus, it starts by the effect on $E_p(\mathbb{W}_k)$ of changing the activation of an output neuron:

$$\frac{\partial E_p(\mathbb{W}_k)}{\partial a^L_j} = a^L_j - d_j. \tag{2.20}$$

[6]Which includes all the biases b^l_j as well.
[7]Sometimes referred to as a loss or objective function.
[8]Note that backpropagation works with any input-output function which has a bounded derivative.

Applying the chain rule extracts the influence that inputs to an output neuron have on $E_p(W_k)$:

$$\frac{\partial E_p(\mathbb{W}_k)}{\partial net_j^L} = \frac{\partial E_p(\mathbb{W}_k)}{\partial a_j^L}\frac{da_j^L}{dnet_j^L}, \tag{2.21}$$

which with 2.14 and:

$$\frac{da_j^L}{dnet_j^L} = \frac{d\frac{1}{1+e^{-net_j^L}}}{dnet_j^L} = \frac{e^{net_j^L}}{(e^{net_j^L}+1)^2} = \frac{1}{1+e^{-net_j^L}}(1-\frac{1}{1+e^{-net_j^L}}) = a_j^L(1-a_j^L), \tag{2.22}$$

can be rewritten as:

$$\frac{\partial E_p(\mathbb{W}_k)}{\partial net_j^L} = \frac{\partial E_p(\mathbb{W}_k)}{\partial a_j^L}a_j^L(1-a_j^L). \tag{2.23}$$

Knowing how the cost changes when the total input net_j^L to an output layer neuron j is changed, the effect of changing a weight w_{ji}^L is within reach. With 2.11:

$$\frac{\partial E_p(\mathbb{W}_k)}{\partial w_{ji}^L} = \frac{\partial E_p(\mathbb{W}_k)}{\partial net_j^L}\frac{\partial net_j^L}{\partial w_{ji}^L} = \frac{\partial E_p(\mathbb{W}_k)}{\partial net_j^L}a_i^{L-1}, \tag{2.24}$$

where a_i^{L-1} is the activation of a neuron i in the previous layer $L-1$. With 2.23 and 2.20 we simplify the equation above to:

$$\frac{\partial E_p(\mathbb{W}_k)}{\partial w_{ji}^L} = (a_j^L - d_j)a_j^L(1-a_j^L)a_i^{L-1}. \tag{2.25}$$

This gives us a means to find $\nabla_{\mathbb{W}^L}E_p(W_k)$, but we need to propagate this process further backwards to find $\nabla_{\mathbb{W}}E_p(\mathbb{W}_k)$.

To compute 2.25 we simply built upon our knowledge of $\frac{\partial E_p(\mathbb{W}_k)}{\partial a_j^L}$, so it stands to reason that to prove it is possible to recursively use the process for any number of layers, we must now obtain $\frac{\partial E_p(\mathbb{W}_k)}{\partial a_i^{L-1}}$. To do so, we take advantage of the fact that a_i^{L-1} is part of the input net_j^L for a neuron j to which it connects. This means a_i^{L-1} has an effect on net_j^L, which in turn has an effect on $E_p(\mathbb{W}_k)$ that we already found in 2.23. We can describe this chain with:

$$\frac{\partial E_p(\mathbb{W}_k)}{\partial net_j^L}\frac{\partial net_j^L}{\partial a_i^{L-1}} = \frac{\partial E_p(\mathbb{W}_k)}{\partial net_j^L}w_{ji}^L. \tag{2.26}$$

This is the indirect effect of a_i^{L-1} on $E_p(\mathbb{W}_k)$ by way of j. We can piece together the total influence of a_i^{L-1} by accruing all such indirect effects derived from each connection it has to neurons in layer L:

$$\frac{\partial E_p(\mathbb{W}_k)}{\partial a_i^{L-1}} = \sum_j \frac{\partial E_p(\mathbb{W}_k)}{\partial net_j^L}w_{ji}^L. \tag{2.27}$$

Thus, we have a way to compute $\frac{\partial E_p(\mathbb{W}_k)}{\partial a_i^{L-1}}$ for any i just knowing $\frac{\partial E_p(\mathbb{W}_k)}{\partial a_j^L}$ for all j. This procedure can be repeated for successively earlier layers, computing $\nabla_{W^l}E_p(W_k)$ along the way until we have $\nabla_{\mathbb{W}}E_p(\mathbb{W}_k)$. After this more intuitive view of the backpropagation process we can state its more general, matricial form:

$$\begin{aligned}\frac{\partial E_p(\mathbb{W}_k)}{\partial \mathbf{net}^l} &= \frac{\partial \mathbf{a}^l}{\partial \mathbf{net}^l}\frac{\partial E_p(\mathbb{W}_k)}{\partial \mathbf{a}^l}\\ \frac{\partial E_p(\mathbb{W}_k)}{\partial W^l} &= \mathbf{a}^{l-1}\frac{\partial E_p(\mathbb{W}_k)}{\partial \mathbf{net}^l}\\ \frac{\partial E_p(\mathbb{W}_k)}{\partial \mathbf{a}^{l-1}} &= (W^l)^T\frac{\partial E_p(\mathbb{W}_k)}{\partial \mathbf{net}^l}.\end{aligned} \tag{2.28}$$

2.3.4 Gradient Descent

We now have a procedure to obtain $\nabla_{\mathbb{W}} E_p$ for each case p in the training set, allowing us to perform gradient descent updates on the set of weights $\mathbb{W}$. Two classic implementations of gradient descent are the stochastic gradient descent:

$$\mathbb{W}_{k+1} \leftarrow \mathbb{W}_k - \alpha \nabla_{\mathbb{W}_k} E_p(\mathbb{W}_k),\ p \in \{1, ..., P\} \tag{2.29}$$

where α is the learning rate which defines how fast we move in the weight space and p is an index over a training set of size P. And the batch gradient descent:

$$\mathbb{W}_{k+1} \leftarrow \mathbb{W}_k - \frac{\alpha}{P}\sum_{p=1}^{P} \nabla_{\mathbb{W}_k} E_p(\mathbb{W}_k). \tag{2.30}$$

Each update with the first method is cheaper computationally, while each update with the second method is presumably a better step. But since batch updates can take advantage of the speed-up of matrix-matrix products over matrix-vector products [32] they somewhat lessen the computational cost gap. Thus, for convex, or relatively smooth cost manifolds batch updates may be preferred. But since gradients only represent the steepest descent locally, when the cost manifolds are highly non-convex even an error-less gradient update may not have the desired direction so batch updates lose some of their advantage. In fact, it may become helpful to have some noise in the gradient updates, updates with less error will discover the minimum of whatever basin the weights are initially place in, while noisier updates can result in the weights jumping into the basin of another, potentially deeper local minimum [25].

With these two opposing effects, it is doubtful either stochastic or batch are the optimal approach. A third method known as mini-batch gradient descent offers a compromise between these opposing approaches by computing the gradient using only a subset of the training cases $\mathbb{S}_k$ at a time:

$$\mathbb{W}_{k+1} \leftarrow \mathbb{W}_k - \frac{\alpha}{|\mathbb{S}_k|}\sum_{p=1}^{|\mathbb{S}_k|} \nabla_{\mathbb{W}_k} E_p(\mathbb{W}_k) \tag{2.31}$$

This approach is reduced to stochastic when $|\mathbb{S}_k| = 1$ and to batch when $|\mathbb{S}_k| = P$. A good balance is struck when the mini-batch size is small enough to avoid some of the poor local minima, but large enough that it does not avoid the global minima or better-performing local minima[9] and reaps advantage of matrix-matrix computational gains. Typically there is a U-curve of performance versus $|\mathbb{S}_k|$ with an

[9]This assumes that the best minima have a larger and deeper basin of attraction, and are therefore easier to fall into.

optimal choice at a certain value [32]. Our system uses a mini-batch approach, with a fixed, empirically chosen value for $|\mathbb{S}|$.

The mini-batch implementation of gradient descent can be further improved concerning the size of each update. Using a fraction α of the gradient offers some basic level of control over the size of the updates, but there are many alternatives to this basic approach that fine tune the update size and can substantially improve learning. In this thesis we use a method known as RMSProp, short for root mean square propagation, an unpublished method introduced by Tieleman and Hinton [33] which has been shown to work very well in a variety of benchmarks and practical applications [34, 35] and has been successfully utilized for Q-Networks [6].

RMSProp adapts the learning rate for each parameter with the net effect of greater progress in the more gently sloped directions of parameter space. For a given parameter $\theta_{i,k} \in \mathbb{W}_k$, its learning rate is adjusted with a exponentially decaying average of squared previous gradients v_k:

$$\begin{aligned} v_k &= 0.9 v_{k-1} + 0.1\left(\frac{\sum_{p=1}^{|\mathbb{S}_k|} \nabla_{\theta_{i,k}} E_p(\mathbb{W}_k)}{|\mathbb{S}_k|}\right)^2 \\ \theta_{i,k+1} &= \theta_{i,k} - \frac{\alpha}{v_k} \frac{\sum_{p=1}^{|\mathbb{S}_k|} \nabla_{\theta_{i,k}} E_p(\mathbb{W}_k)}{|\mathbb{S}_k|} \end{aligned} \tag{2.32}$$

Intuitively this increases the learning rate for sparser parameters and decreases the learning rate for less sparse ones. This adaptive behavior greatly alleviates the burden of optimizing the learning rate hyper-parameter, with default or slightly adjusted from default settings usually exhibiting desired behavior.

2.3.5 Deep Networks

A machine learning approach is dubbed ”deep” based on the number of sequential instructions that must be executed to evaluate the whole architecture. We can think of it as the length of the longest path through a flow chart that describes how to compute each of the model’s outputs given its inputs [35]. For a neural network designed with a layered framework, this equates to the number of layers excluding the input layer, which does not perform computations. There is no consensus on the depth needed for a system to be considered ”deep”, but for feedforward neural networks most researchers agree on more than 2 nonlinear layers, and those with more than 10 are ”very deep” [36].

It was mentioned that a neural network with a single hidden layer is a universal approximator, so this discussion of depth may seem unnecessary. But while that result is interesting and it does showcase the power of neural networks, the single hidden layer approach is inefficient for many complex problems. By inefficient we mean that functions which can be represented by just a few computational elements, neurons, in a depth k architecture might require an exponential number of computational elements to be represented by a depth $k-1$ architecture [37]. So even if the right shallow neural network is guaranteed to exist, it may be unfeasible to find and use. As a result deep networks consistently outperform shallow ones on a variety of tasks and datasets. Theoretical results on this power are limited by the composition of nonlinear functions in deep models which makes mathematical analysis difficult [38] but recently works such as those by Pascanu et al. [38] and Montúfar et al. [39] have shown that for piecewise linear activations, such as the widely used ReLU, deep networks are able to separate their input space into exponentially more linear response regions than their shallow counterparts, despite using the same number of computational units, which indicates greater flexibility and capacity to compute highly complex and structured functions (see Figure 2.5).

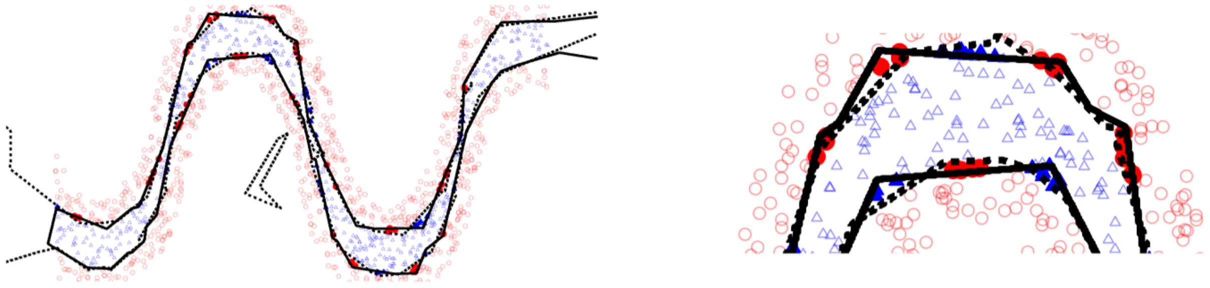

Figure 2.5: Binary classification using a shallow model with 20 hidden units (solid line) and a deep model with two layers of 10 units each (dashed line). The right panel shows a close-up of the left panel. Filled markers indicate errors made by the shallow model. The learnt decision boundary illustrates the advantage of depth, it captures the desired boundary more accurately, approximating it with a larger number of linear pieces. [39]

This power of deep networks not only allows us to design networks that learn a previously unfeasible task, but also the quality of learning is generally superior than what it would have been if we managed to solve it with a shallow architecture. Since it learns the same problem using fewer computational elements, it stands to reason that they offer better generalization [37]. We can roughly illustrate this concept by imagining a perceptron with a very large number of neurons compared to the number of points in the training dataset and another with a smaller number. The one with a very large number can afford to dedicate a unique pattern of activation in the first layer for each input and then learn an output to that specific pattern in the output layer. This means its effectively memorizing the answers for each input. The smaller perceptron however, cannot assign a unique pattern to each input, it needs to group inputs it observes as similar and give the same pattern to each element in a group, which leads to generalization and useful learning.

While deep networks are often superior to shallower topologies, the fact is that deep networks have only recently began to attract widespread attention, and shallow networks have been the conventional approach for a long time. The reason is that although backpropagation allows for deep networks in principle, they become increasingly hard to train as they grow deeper. For a long time practitioners found no performance benefits from adding layers, and thus they found solace on the universal approximator theorem and stuck to shallow architectures [36]. Explaining in detail the specific problems created by deep architectures is beyond the scope of this thesis (Glorot and Bengio [40] is a good starting point on the subject), it is a multi-faceted issue and it is still a subject of on-going research. While they remain quite difficult to train much progress has been made, particularly through the use of ReLU neurons, gradient descent algorithms with adaptive learning rates such as RMSProp and generally higher computational power. This has allowed us to use a deep network for this trading system, as described in section 3.4.

2.4 Related Work

In this section we briefly discuss some previous applications of RL to financial trading. Table 2.2 summarizes the results obtained by those systems which were tested in the foreign exchange market. Unfortunately, these are few and far between, most systems focus solely on stock trading. Overall, the overwhelming majority of systems rely on technical analysis in their state signal, typically simply a number of past returns[10], and use either profit or risk-adjusted profit as their reward signal.

Paper	Asset	Time Frame	Annualized Profit
Learning to trade via direct reinforcement [41]	USD/GBP	First 8 months of 1996	15%
FX trading via recurrent reinforcement learning [42]	Average over 10 currency pairs	Full year of 1996	4.2%
An automated FX trading system using adaptive reinforcement learning [43]	EUR/USD	January 2000 to January 2002	26%
An investigation into the use of reinforcement learning techniques within the algorithmic trading domain [44]	EUR/USD	January 2014 to December 2014	1.64%

Table 2.2: Summary of performance obtained by RL trading systems tested on the foreign exchange market.

Direct Reinforcement

Direct reinforcement approaches disregard the use of value functions, and simply optimize the policy directly under the discussed RL framework. This is a popular approach for financial trading agents, since Moody and Saffell [41] in 2001 introduced a direct reinforcement approach dubbed recurrent reinforcement learning (RRL) which outperformed a Q-learning implementation on some benchmarks. Moody's RRL trader is simply a threshold unit representing the policy, in essence a one layer NN, which take as input the past eight returns and its previous output. Its parameters are updated through a process similar to backpropagation, with the aim of maximizing a function of risk-adjusted profit. This trader was tested on the first 8 months of 1996 with the currency pair USD/GBP, half-hourly data, using a rolling window scheme. The trader was initially trained on the first 2000 data points, tested on the following two weeks of data, then the training window was shifted to include the tested data, system was retrained and tested on the next two weeks and so on achieving an annualized profit of 15%. Gold [42] further tested the RRL approach on other currency markets, with half hourly data from the entire year of 1996. Final profit level

[10]In this context, returns are the relative difference between two consecutive price points.

varied considerably across the different currency pairs, from -82.1% to 49.3%, with an average of 4.2% over ten pairs: AUD/USD, DEM/ESP, DEM/FRF, DEM/JPY, GBP/USD, USD/CHF, USD/FIM, USD/FRF, USD/NLG, USD/ZAR.

In 2004 Dempster and Leemans [43] introduced what they dubbed as adaptive reinforcement learning (ARL), which was built upon the RRL approach. Using a RRL trader at its core, also with returns as the input, their system had an added risk management layer and dynamic optimisation layer as shown in Figure 2.6. While the RRL core makes the recommendations for trading decisions, it is the risk layer that

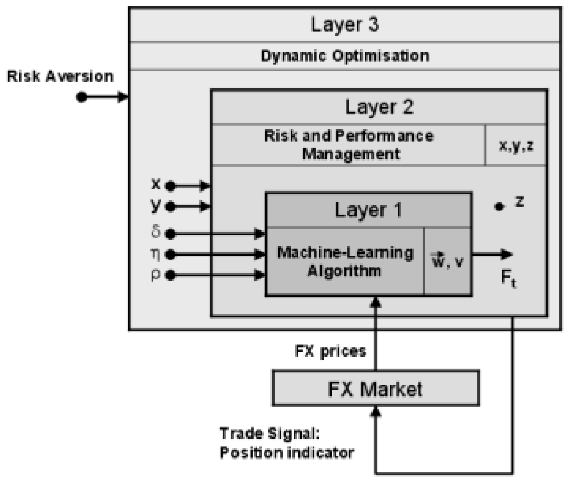

Figure 2.6: Adaptive reinforcement learning (ARL). [43]

decides whether to actually act upon those instructions by considering additional risk and performance factors that are hard to include in the trading model itself. These include a stop-loss that is set and adjusted so that a position is always x under or above the highest price ever reached during its life, a validation system that looks at the strength of the RRL's recommendation and only acts when the signal is stronger than y and a procedure that initiates a system shutdown when the total profits sink below an amount z from the maximum value they have reached. The dynamic optimization layer has the job of optimizing the system's parameters to improve the risk-return profile. These parameters include those mentioned here from the previous layer, x, y and z, and parameters from the basic RRL layer. The ARL system was tested on 2 years of EUR/USD historical data, from January 2000 to January 2002, with 1 minute granularity, achieving an average 26% annual return. Dempster and Leemans [43] note that profits diminish with time, speculating that this may be due to increased market efficiency.

All these implementations of RRL simply use a number of past returns, the simplest form of technical analysis. However, Zhang and Maringer [45] in 2013 showed with the use of a genetic algorithm as a pre-screening tool to search suitable indicators that the inclusion of volatility, which can be measured by the standard deviation of prices for example, in addition to past returns can improve the risk-adjusted profit obtained by the RRL trader. Unfortunately this study relied solely on stock trading data.

Value-based Reinforcement

Value-based reinforcement is the type of approach used in this thesis, which relies on estimating the state value function or action value function. It has not been as popular as the direct reinforcement approaches, particularly for foreign exchange. Cumming [44] in 2015 introduced a RL trading algorithm based on least-squares temporal difference, a technique that estimates the state value function. Their state signal relies on technical analysis: the first, highest, lowest and last prices (bid only) from the last 8 periods are included, where each period covers a minute. The reward given to the agent is purely the profit from each transaction. Training and testing used one minute data from 2014-01-02 to 2014-12-19. The reported annualized profit for the EUR/USD pair was 1.64%.

In their 2007 paper, Lee et al. [46] use 2-layered Q-networks with a multiagent approach. Rather than one agent executing all the decisions, they divide the task by four different specialized agents as depicted in Figure 2.7. The first two agents, which were named buy and sell signal agents, respectively,

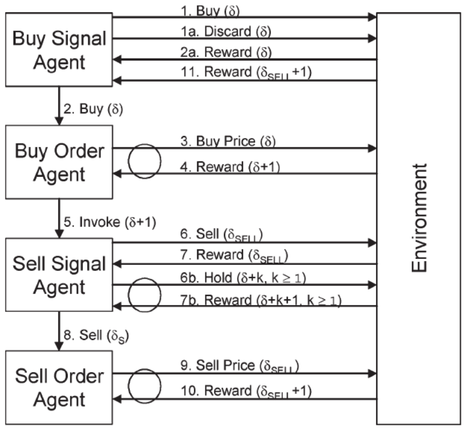

Figure 2.7: Multiagent Q-learning. [46]

attempt to determine the right day to buy and sell based on global trend prediction. These agents are rewarded based on the profit of the whole transaction. The other two agents, which were named buy and sell order agents agents, deal with the intraday time frame to carry out the order on the day chosen by the previous agents, and are rewarded according to how close the chosen price was to the optimum price of the day. All four agents use simple technical analysis indicators as their input for price prediction. This approach was successful for stock trading, but unfortunately was not tested on the foreign exchange market.

Chapter 3

Implementation

One problem of designing a training system is the lack of a solid theoretical framework for financial trading. Although not to the same degree, neural networks still being a developing field, suffers from similar problems. LeCun et al. [25] stated on the subject of backpropagational[1] neural networks:

> Backpropagation is very popular because it is conceptually simple, computationally efficient, and because it often works. However, getting it to work well, and sometimes to work at all, can seem more of an art than a science. Designing and training a network using backpropagation requires making many seemingly arbitrary choices such as the number and types of neurons, layers, learning rates, training and test sets, and so forth. These choices can be critical, yet there is no foolproof recipe for deciding them because they are largely problem and data dependent.

Thus we are applying computational tools that are largely problem and data dependent, to a field that contains little theoretical basis to guide us. This means we have to make up for theoretical insights with empirical testing during the design process. As there is no way to simulate or create market data for such tests, we have to use data drawn from the same historical source used to subsequently assess the performance of the system, which could lead to data dredging issues.

A black box system such as a Q-network is less susceptible to data dredging than other approaches, as it does not allow direct tinkering, but still, to contain some possible contamination of the data we based our design decisions and our hyper-parameter selection only on three specific EUR/USD datasets selected a priori. All remaining data was ”vaulted” and untouched while developing the system described in this chapter.

3.1 Overview

The core of the system is a feedforward backpropagational neural network acting as a Q-network. This network has three hidden layers of 20 ReLU neurons each, followed by an output layer of 3 linear

[1] A network that learns under the backpropagation / gradient descent approach described in the previous chapter.

neurons. The topology of the hidden layers was set empirically, while the three linear output neurons are intrinsic to our system's design: each of them represent the Q-value of a given action.

This network interacts with a simulated market environment in discrete steps $t = 0, 1, 2, ...$ At each of those steps it receives a state vector S_t as input. After a forward propagation, each of the three linear neurons output the Q-network's current estimate for an action value $Q_{a_n}(S_t, \mathbb{W}_k)$ for each of three possible actions $n \in [0, 1, 2]$, where $\mathbb{W}_k$ is the set of network weights after k updates. The estimates $Q_{a_n}(S_t, \mathbb{W}_k)$ are fed to a ϵ-greedy action selection method which selects the action choice for step t as either $A_t = \arg\max_a Q_a(S_t, \mathbb{W}_k)$ or, with probability ϵ, a random exploratory action $A_t \in [a_0, a_1, a_2]$.

$\mathbb{A}(s)$, $\forall s \in \mathbb{S}$ is made up of just these three action signals due to our discretization of the action space. There is an external imposition on the agent to invest $position\_size$ of the chosen asset at a time, a value set by the user, which leaves it with five different actions: open long position, open short position, close long position, close short position and do nothing. By interpreting a_n depending on whether there is a currently open position, as described in Table 3.1, these can be represented with three signals.

Action Signal	**Current Open Position**	**Action Description**
a_0	None	Nothing
	Short	Hold
	Long	Hold
a_1	None	Open Long
	Short	Close Short
	Long	Hold
a_2	None	Open Short
	Short	Hold
	Long	Close Long

Table 3.1: Interpretation of each action signal a_n.

The chosen action A_t is then received by the simulated market environment. Its role is to provide a faithful simulation of the foreign exchange market and coordinate the flow of information that reaches the system so that it follows the reinforcement learning paradigm. Thus, after receiving A_t from the network it answers with a new state S_{t+1} and the reward R_{t+1} for the chosen action.

Each state drafted by the environment includes the following information:

- Type of currently open position;
- Value of any open position in light of simulated market's current prices, Bid_i and Ask_i, where i is an index over the entries in the dataset used by the market environment;
- Current size of the trading account;
- Feature vector F_i;

The features in F_i are created using the market data entries preceding i by a preprocessing stage inspired by the typical technical analysis approach. The feature vector's purpose is to provide the network with price prediction capabilities needed to find useful action value estimates and thus perform profitable decisions. As for the reward given to the network, each action is rewarded as follows:

- Opening a position is rewarded by the unrealized profit it creates;
- Keeping a position open is rewarded by the fluctuation of the position's unrealized profit;
- Closing a position is rewarded with the acquired profit;
- Doing nothing receives zero reward.

After each step the Q-network can use the experience $e_t = (S_t, A_t, R_{t+1}, S_{t+1})$ to improve its action value estimates using an adaptation of the Q-learning algorithm to a backpropagational neural network's method of learning by updating $\mathbb{W}_k$. Figure 3.1 summarizes the interactions described above.

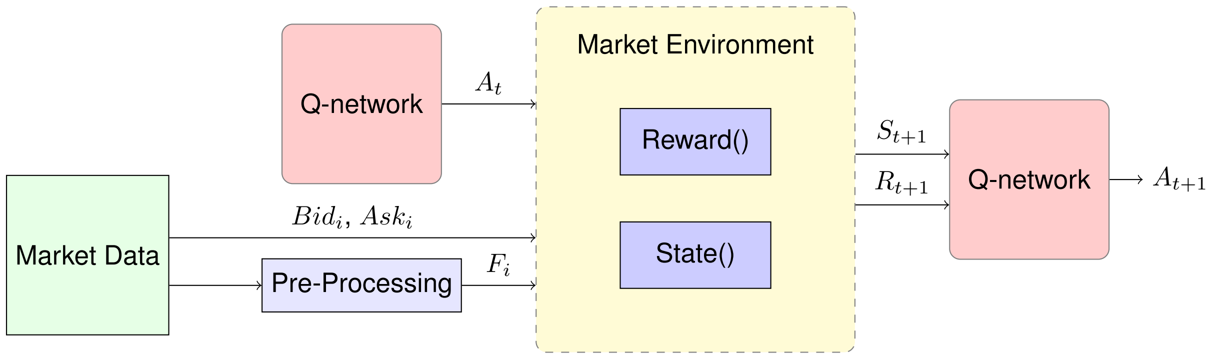

Figure 3.1: Flow of information between the three main components of the system: preprocessing stage, market simulation and Q-network.

The three main components of this system have thus been introduced, which the next three sections explain in further detail: Data preprocessing in section 3.2, market simulation in section 3.3 and the Q-Network in section 3.4.

3.2 Preprocessing

As discussed in section 2.1 this trading system uses tick data. Each tick T_i can be stored in an array:

$$T_i = \begin{bmatrix} B_i & A_i & Vb_i & Va_i \end{bmatrix}, \tag{3.1}$$

where B_i, A_i are the bid price and ask price at the time T_i was put out and Vb, Va were the volume of units traded at those respective prices. Figure 3.2 shows a segment of tick data for the EUR/USD pair. The frequency at which ticks are put out strongly depends on market volatility and liquidity, for the segment of data represented in Figure 3.2, the mean time difference between ticks is 1.11 ± 2.43 seconds[2].

We want our system to make a decision when the market is at tick T_i, the reference tick, using information from the preceding market ticks. Without preprocessing if we want to include information

[2]Excluding weekend gap.

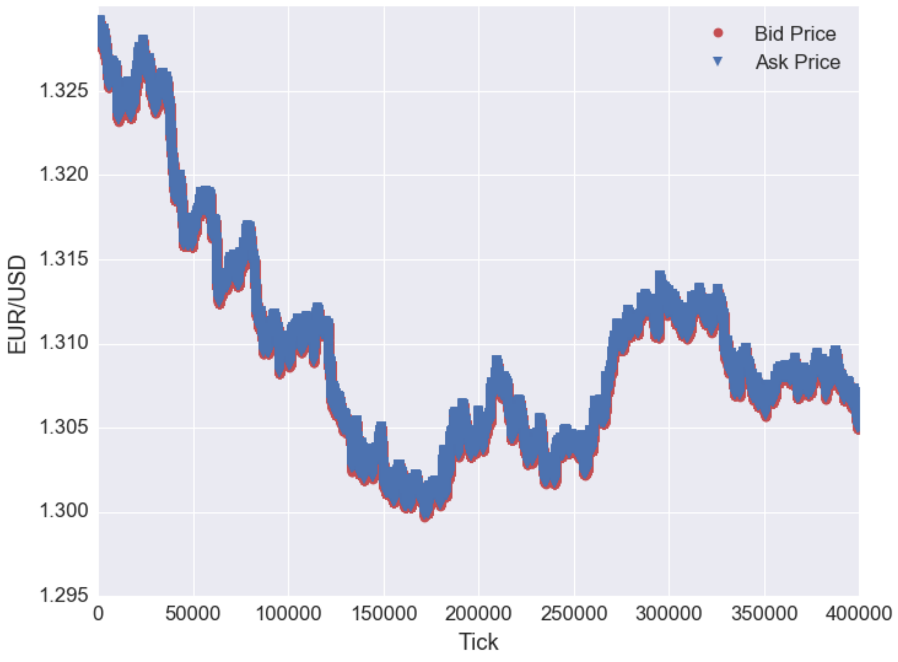

(a)

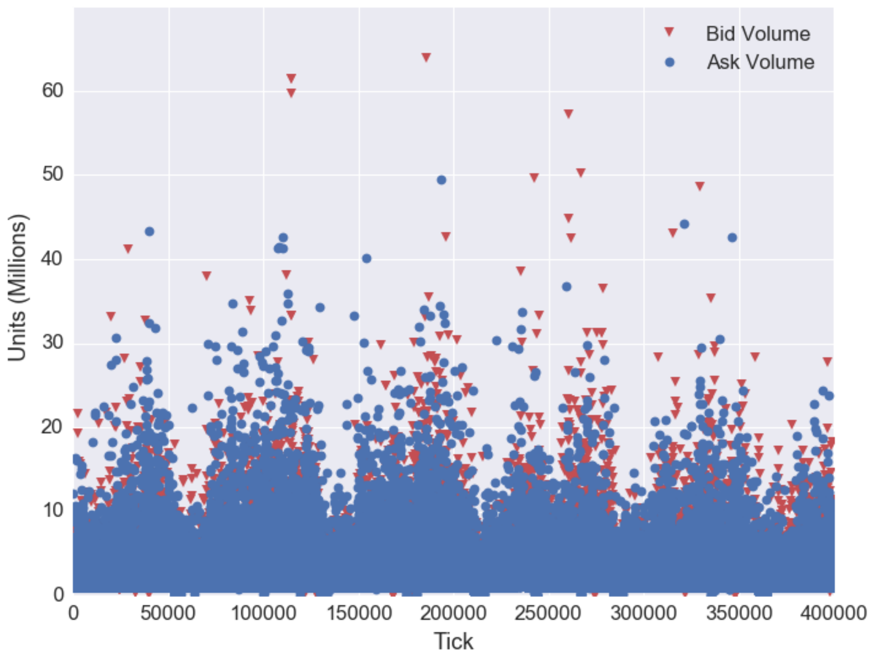

(b)

Figure 3.2: 400,000 ticks (2013.01.02 - 2013.01.09) of EUR/USD pair market data from Duskacopy broker: (a) bid and ask price values (b) bid and ask volume in millions of units.

from L previous ticks in our input we simply concatenate all those arrays, giving us a $L \times 4$ element history array:

$$H_i = \begin{bmatrix} B_i & A_i & Vb_i & Va_i \\ B_{i-1} & A_{i-1} & Vb_{i-1} & Va_{i-1} \\ B_{i-2} & A_{i-2} & Vb_{i-2} & Va_{i-2} \\ \vdots & \vdots & \vdots & \vdots \\ B_{i-L} & A_{i-L} & Vb_{i-L} & Va_{i-L} \end{bmatrix}$$

However, there are many characteristics of H_i that would make it difficult for the Q-Network to learn using it as input. First of all considering how fast ticks are put out, H_i can grow to a very large number of elements while including information from a relatively small time window. A widely discussed subject in machine learning is what has been dubbed ”the curse of dimensionality” [22], whereby as the input grows in number of dimensions (number of elements in the input array) the input space grows exponentially and thus a machine learning method has more difficulty in extracting meaningful relationships between inputs. An in depth discussion of this subject is beyond the scope of this thesis, suffice it to say that while neural networks are less affected by this ”curse” than other methods [47], it is still to our advantage to reduce dimensionality. Higher input dimensionality also requires greater computational resources, leading to a slower training process, which is an important limiting factor in our system development.

Furthermore, to facilitate learning H_i should, in so far as possible, have:

- Uncorrelated input variables;
- Input variables with a similar range;
- Input variables with an average over the training dataset close to zero for each input variable.

These characteristics make gradient learning faster, more stable and less prone to getting stuck in local minima [48, 25]. For the remainder of this section we focus on our preprocessing of H_i through feature extraction and standardization to better comply with the desired attributes of a neural network input.

3.2.1 Feature Extraction

Looking at Figure 3.2 we can tell the bid and ask prices are very close to perfectly correlated, and thus bring a lot of redundant information. In fact, the only relevant information that can be extracted by including both rather than just one is the spread, the difference between them, which acts as a time-varying commission (see Figure 3.3). So we make the job easier for our neural network by replacing in H_i the ask price A_i with the spread $S_i \equiv A_i - B_i$.

Our second change to H_i concerns its high dimensionality, we want to find a more compact representation for the information it contains. Our approach consists of splicing H_i along L into N windows $H_i^n \subset H_i$, $n \in \{1, N\}$. The size of each window is described by a parameter TW, an array whose

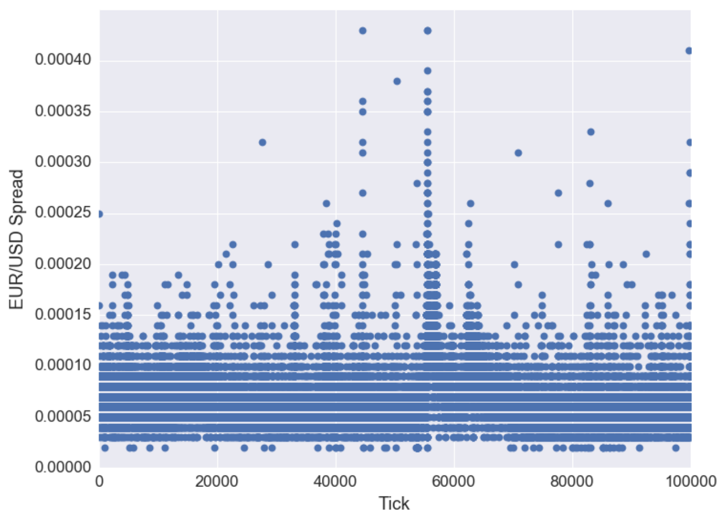

Figure 3.3: Bid-Ask spread for the first 100,000 ticks of the data segment from 3.2. Spread varies between a few well defined levels reflecting the broker's assessment of market conditions.

elements are the beginning and ending of a window in number of ticks preceding the reference tick:

$$TW = \begin{bmatrix} TW_0 = 0 & TW_1 & TW_2 & \dots & TW_{N-1} & TW_N = L \end{bmatrix}$$

so that the n^{th} window, where $n \in [1, 2, ..., N]$, includes the ticks T_k with $k \in [i - TW_{N-1}, i - TW_N]$. For the ticks in each window:

$$H_i^n = \begin{bmatrix} B_{i-TW_n} & S_{i-TW_n} & Vb_{i-TW_n} & Va_{i-TW_n} \\ B_{i-TW_n-1} & S_{i-TW_n-1} & Vb_{i-TW_n-1} & Va_{i-TW_n-1} \\ B_{i-TW_n-2} & S_{i-TW_n-2} & Vb_{i-TW_n-2} & Va_{i-TW_n-2} \\ \vdots & \vdots & \vdots & \vdots \\ B_{i-TW_{n+1}} & S_{i-TW_{n+1}} & Vb_{i-TW_{n+1}} & Va_{i-TW_{n+1}} \end{bmatrix}$$

we compute the mean, maximum, minimum and standard deviation for $\begin{bmatrix} B & A & Vb & Va \end{bmatrix}$. The resulting feature array F_i^n is used as the compact representation of the contents that window:

$$F_i^n = \begin{bmatrix} \underset{k\in[i-TW_n,i-TW_{n+1}]}{\mu} B_k & \underset{k\in[i-TW_n,i-TW_{n+1}]}{\mu} S_k & \underset{k\in[i-TW_n,i-TW_{n+1}]}{\mu} Vb_k & \underset{k\in[i-TW_n,i-TW_{n+1}]}{\mu} Va_k \\ \underset{k\in[i-TW_n,i-TW_{n+1}]}{\max} B_k & \underset{k\in[i-TW_n,i-TW_{n+1}]}{\max} S_k & \underset{k\in[i-TW_n,i-TW_{n+1}]}{\max} Vb_k & \underset{k\in[i-TW_n,i-TW_{n+1}]}{\max} Va_k \\ \underset{k\in[i-TW_n,i-TW_{n+1}]}{\min} B_k & \underset{k\in[i-TW_n,i-TW_{n+1}]}{\min} S_k & \underset{k\in[i-TW_n,i-TW_{n+1}]}{\min} Vb_k & \underset{k\in[i-TW_n,i-TW_{n+1}]}{\min} Va_k \\ \underset{k\in[i-TW_n,i-TW_{n+1}]}{\mathrm{std}} B_k & \underset{k\in[i-TW_n,i-TW_{n+1}]}{\mathrm{std}} S_k & \underset{k\in[i-TW_n,i-TW_{n+1}]}{\mathrm{std}} Vb_k & \underset{k\in[i-TW_n,i-TW_{n+1}]}{\mathrm{std}} Va_k \end{bmatrix}$$

The features in this compact representation follow the technical analysis approach of a descriptive statistic applied to segments of market data as seen in subsection 2.1.1. The rationale is that by giving the building blocks of technical analysis to our Q-Network, it should be able to use them to develop its own internal technical rules. Thus our history H_i for tick T_i is represented by a feature array $F_i = F_i^1 \cup F_i^1 \cup \cdots \cup F_i^N$, reducing the dimensionality of our input from $L \times 4$ to $N \times 4 \times 4$.

However, looking at the plot of bid prices in Figure 3.2a it is apparent the price distribution is strongly non-stationary, there is a large slow-varying underlying bias value around which prices fluctuate. This means that the features $\mu_{k \in [i-TW_n, i-TW_{n+1}]} B_k$, $\max_{k \in [i-TW_n, i-TW_{n+1}]} B_k$ and $\min_{k \in [i-TW_n, i-TW_{n+1}]} B_k$ extracted from the N windows included in F_i will be strongly correlated amongst themselves. Furthermore, the range of values of these features observed while training could be completely different from those found on the dataset where the system would be subsequently tested, which would make generalization of acquired knowledge more difficult as illustrated in Figure 3.4.

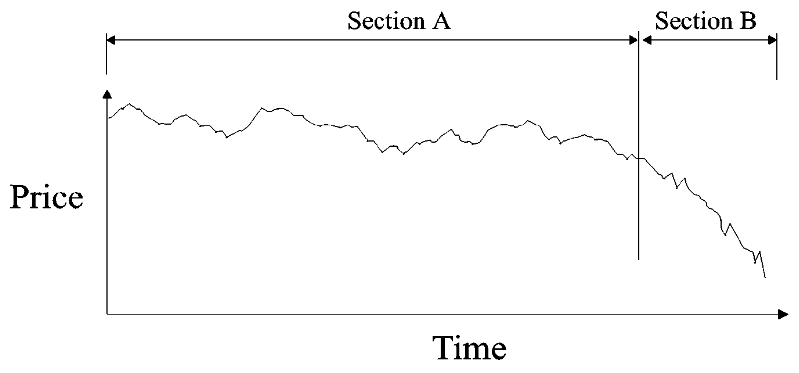

Figure 3.4: Generalization to section B from the training data in section A is difficult because the model has not been trained with inputs in the range covered by section B. [49]

We ameliorate these problems by subtracting from these features an estimate of the underlying bias: the bid value of the reference tick B_i. Figure 3.5 visually expounds the problem and our proposed solution on a segment of market data. With this change our feature array for tick T_i becomes:

$$F_i = \begin{bmatrix}
\underset{k\in[i,i-TW_1]}{\mu} B_k - B_i & \underset{k\in[i,i-TW_1]}{\mu} S_k & \underset{k\in[i,i-TW_1]}{\mu} Vb_k & \underset{k\in[i,i-TW_1]}{\mu} Va_k \\
\underset{k\in[i,i-TW_1]}{\max} B_k - B_i & \underset{k\in[i,i-TW_1]}{\max} S_k & \underset{k\in[i,i-TW_1]}{\max} Vb_k & \underset{k\in[i,i-TW_1]}{\max} Va_k \\
\underset{k\in[i,i-TW_1]}{\min} B_k - B_i & \underset{k\in[i,i-TW_1]}{\min} S_k & \underset{k\in[i,i-TW_1]}{\min} Vb_k & \underset{k\in[i,i-TW_1]}{\min} Va_k \\
\underset{k\in[i,i-TW_1]}{\text{std}} B_k & \underset{k\in[i,i-TW_1]}{\text{std}} S_k & \underset{k\in[i,i-TW_1]}{\text{std}} Vb_k & \underset{k\in[i,i-TW_1]}{\text{std}} Va_k \\
\vdots & \vdots & \vdots & \vdots \\
\underset{k\in[i-TW_{N-1},i-L]}{\mu} B_k - B_i & \underset{k\in[i-TW_{N-1},i-L]}{\mu} S_k & \underset{k\in[i-TW_{N-1},i-L]}{\mu} Vb_k & \underset{k\in[i-TW_{N-1},i-L]}{\mu} Va_k \\
\underset{k\in[i-TW_{N-1},i-L]}{\max} B_k - B_i & \underset{k\in[i-TW_{N-1},i-L]}{\max} S_k & \underset{k\in[i-TW_{N-1},i-L]}{\max} Vb_k & \underset{k\in[i-TW_{N-1},i-L]}{\max} Va_k \\
\underset{k\in[i-TW_{N-1},i-L]}{\min} B_k - B_i & \underset{k\in[i-TW_{N-1},i-L]}{\min} S_k & \underset{k\in[i-TW_{N-1},i-L]}{\min} Vb_k & \underset{k\in[i-TW_{N-1},i-L]}{\min} Va_k \\
\underset{k\in[i-TW_{N-1},i-L]}{\text{std}} B_k & \underset{k\in[i-TW_{N-1},i-L]}{\text{std}} S_k & \underset{k\in[i-TW_{N-1},i-L]}{\text{std}} Vb_k & \underset{k\in[i-TW_{N-1},i-L]}{\text{std}} Va_k
\end{bmatrix}$$

Due to their frequency and small variance we expect ticks to be prone to containing redundant information, and thus it should be possible to keep most of the useful information while reducing dimensionality by optimizing the parameter TW to strike a balance between the level of detail (number of ticks

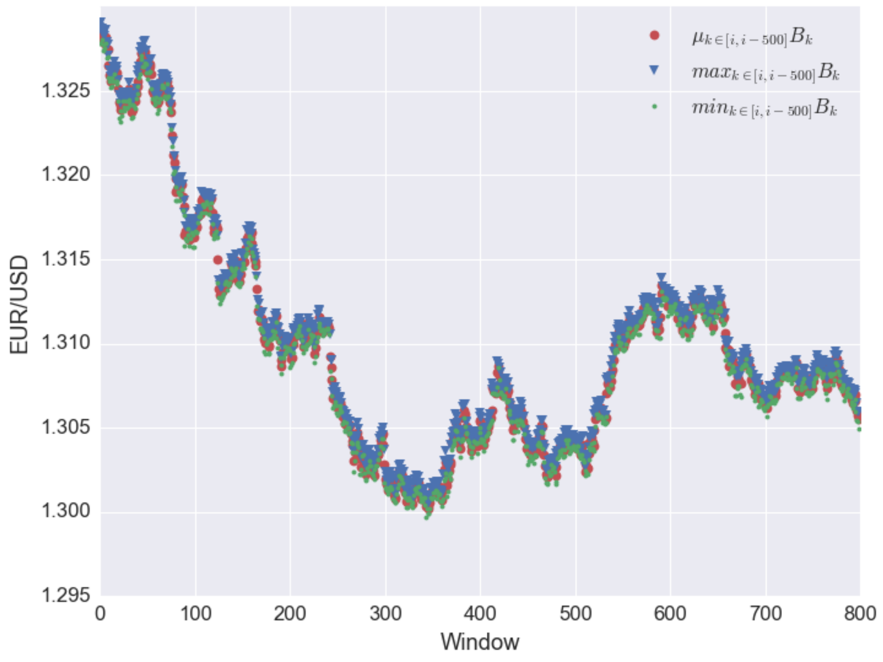

(a)

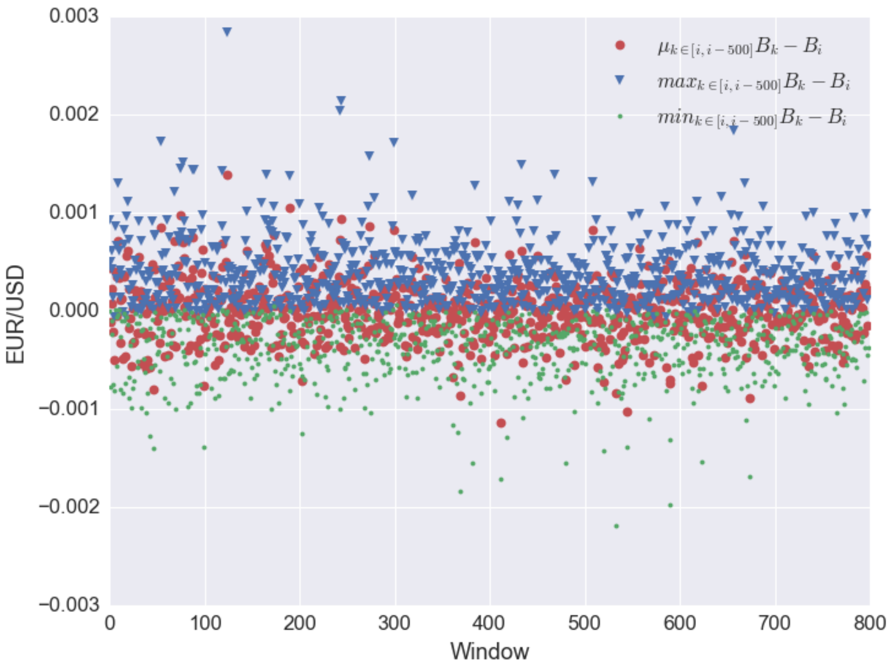

(b)

Figure 3.5: Features extracted from the same segment of data as Figure 3.3, divided into 500-tick windows. (a) shows the original features and (b) depicts our solution to the non-stationarity.

per window), the scope (total number of ticks included) and the dimensionality (number of windows) of our compact representation of history H.

A final addition to the feature array, is the time at which tick T_i was put out. The market behaves slightly differently according to the hour of the day mainly due to the working hours of the major trading capitals: Sydney, Tokyo, London and New York. This can result in consistently higher volume and volatility at certain times, and thus we want to relay that information to the system to aid in its interpretation of the market. We use the following two input variables to encode the hour:

$$time_i^1 = \sin(2\pi \frac{seconds_i}{86400}) \tag{3.2}$$

$$time_i^2 = \cos(2\pi \frac{seconds_i}{86400}) \tag{3.3}$$

where $seconds_i$ is the time when the reference tick was put out converted to seconds. This encoding method effectively conveys the cyclical nature of hours to the neural network.

3.2.2 Standardization

We aim to standardize the variables in the feature array to meet the criteria introduced above. We do this via a linear transformation known as min-max normalization:

$$\begin{aligned} \text{midrange} &= \frac{\max_i x_{k,i} + \min_i x_{k,i}}{2}, \\ \text{range} &= \max_i x_{k,i} - \min_i x_{k,i}, \\ f_{k,i} &= \frac{x_{k,i} - \text{midrange}}{\text{range}/2}. \end{aligned} \tag{3.4}$$

where $x_{k,i}$ is the k^{th} element of F_i and $s_{k,i}$ is its normalized counterpart[3].

While min-max does not ensure that the mean of each variable over the training dataset will be zero, as a z-score normalization would, it keeps the range of input variables thoroughly predictable in the range $f_k \in [-1, 1], \forall i$ which is very helpful for stability and debugging of gradient descent learning. Also, it keeps the distribution of each input variable intact making no assumptions or requiring any model for market behavior. It is not robust to outliers however, any large outlier will skew the main body of the distribution, which becomes confined to a small slice of the available range. This would lead to a loss of sensitivity that could render the neural network unable to extract meaning from that input variable.

This is problematic since we expect large outliers in most foreign exchange datasets. Firstly because retail level currency trading stops during the weekend but the interbank market continues to trade. Since the first closely follows the second, when trading resumes prices and volumes may be significantly changed as if there were two days of trading, although from a retail perspective the last tick before the weekends and the first one after are contiguous. Features extracted from tick windows that include this gap can become outliers, particularly for standard deviation features and for our bid price features due

[3]Note that the hour features are normalized by default.

to a possible subtraction with a price that effectively occurred two days after. Secondly, significant real world events or movements by big players may trigger rare spikes of extreme volume accompanied by sharp spread changes from the broker. Figure 3.6 shows the distribution of all the features introduced in the previous section, excluding the time, extracted from 500-tick windows over roughly one year of market data.

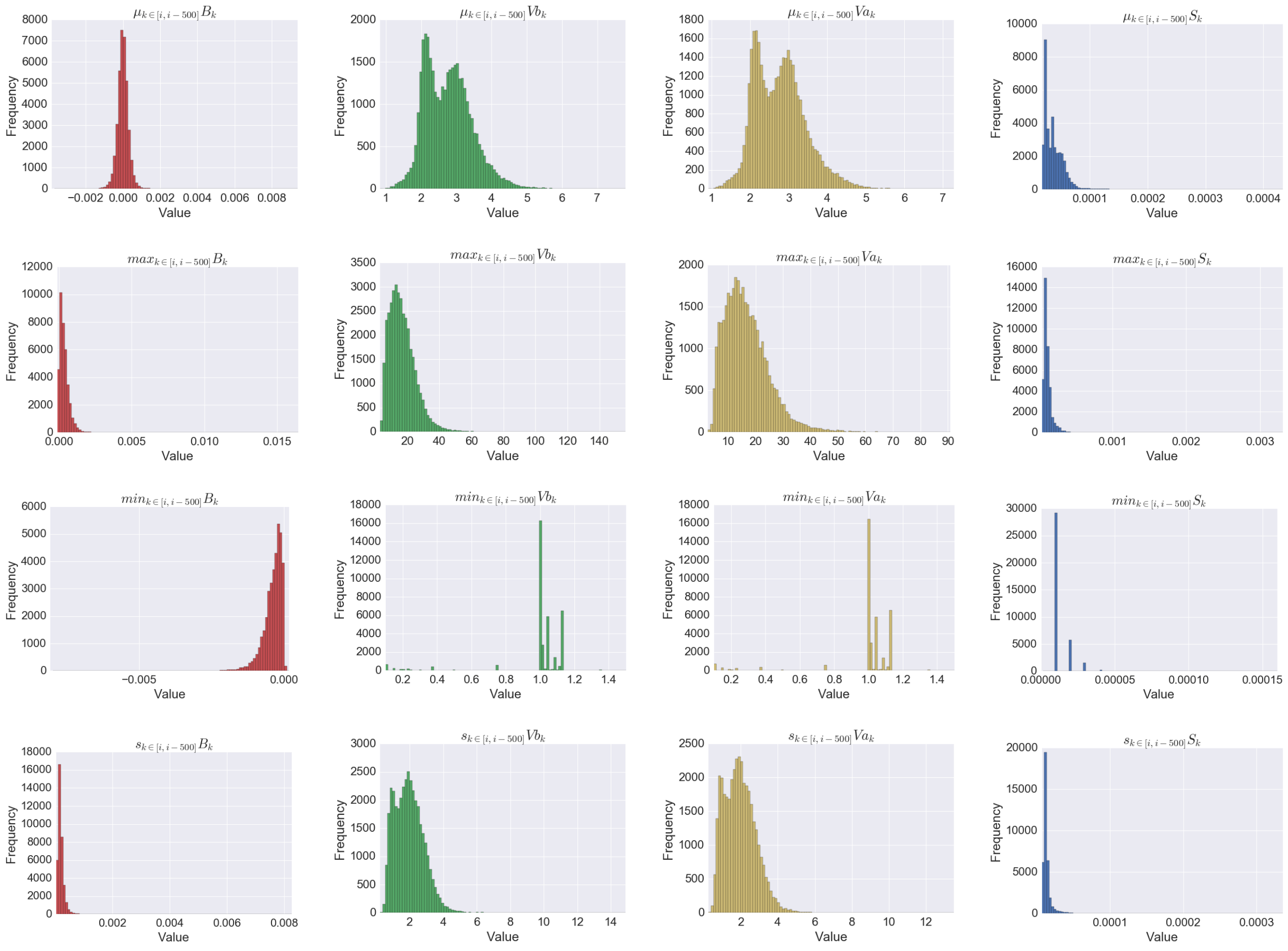

Figure 3.6: Distribution of the unstandardized feature variables extracted from 500 tick windows from roughly one year of bid (red), bid volume (green), ask volume (cyan) and spread (blue) data. X-axis of each distribution is bounded to the maximum and minimum value, so all values depicted have at least one occurrence even if not visible on the Y-axis due to scale. Raw data from the EUR/USD pair during 2013 from Duskacopy broker.

As expected it is clear that in most cases there are a number, albeit minute, of occurrences far outside the range occupied by the rest of the distribution. Since we simply want to curtail the impact of these occurrences while maintaining the distribution mostly intact, we apply a simple percentile-based filter. The q^{th} percentile of feature x_j, $q^{th}(x_j)$, is computed as the value $\frac{q}{100}$ of the way from the minimum to the maximum of a sorted copy of an array containing all entries of the feature for a dataset. The filter rule used is:

$$x_{j,i} = \begin{cases} (1-q)^{th}(x_j), & \text{if } x_{j,i} < (1-q)^{th}(x_j) \\ q^{th}(x_j), & \text{if } x_{j,i} > q^{th}(x_j) \\ x_{j,i}, & \text{otherwise} \end{cases} \tag{3.5}$$

where q should be set conservatively to only target the most outlying values. The price for this filtering is loss of sensitivity within these extreme values. Applying this filter, followed by the normalization described in Equation 3.4 we obtain the final features, whose distributions for the same conditions as above are shown in Figure 3.7.

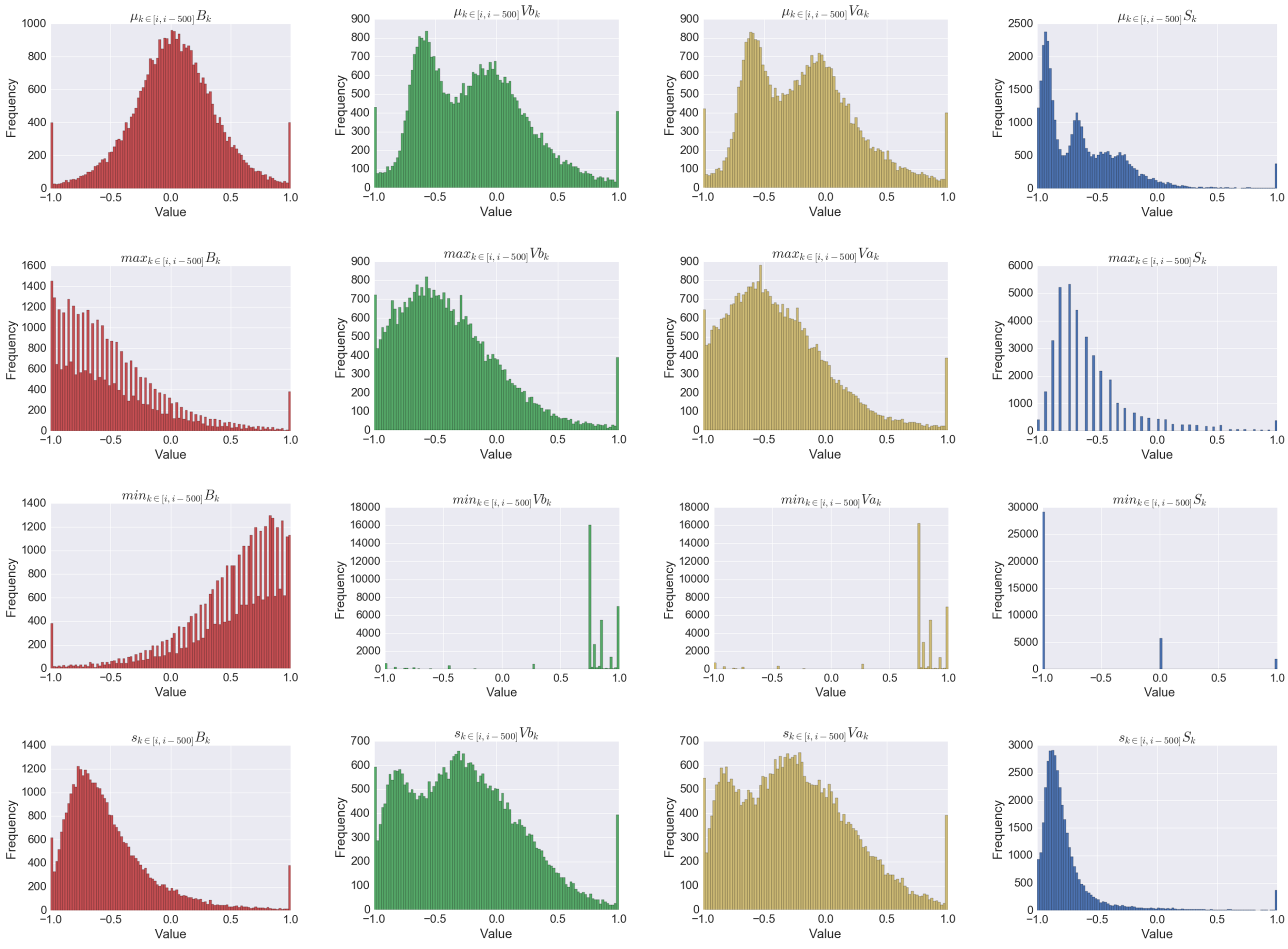

Figure 3.7: Distribution of feature variables, extracted from the same raw data as Figure 3.6, filtered, with $q = 99$, and standardized. Bid (red), bid volume (green), ask volume (cyan) and spread (blue) data.

Upon inspection of Figure 3.7 and empirical testing, features $\min\limits_{k\in[i-TW_{N-1},i-L]} S_k$, $\min\limits_{k\in[i-TW_{N-1},i-L]} Vb_k$ and $\min\limits_{k\in[i-TW_{N-1},i-L]} Va_k$ were removed from the feature array as they appear to not contain useful information and simply contributed to overfitting.

3.3 Market Simulation

With the market simulation we want to create an environment to coordinate the flow of information that reaches the system so that it follows the reinforcement learning paradigm, which means supplying the system with a state, receiving its response in the form of an action and answering with a new state and a reward. Also, this process must be consistent with trading in the real foreign exchange market, so that its learned behavior and our measure of its performance would translate to real trading.

The market simulation follows prices from a tick dataset $\mathbb{T} = \{T_0, .., T_D\}$. The system is only allowed to make a decision every $time\_skip$ ticks. At each step/interaction[4] t the market environment is at the price in tick $T_{i=t \cdot time\_skip+b}$, where b is the chosen starting tick for the first interaction, and sends the system the state S_t. The parameter $time\_skip$ and starting point b are further explained in subsection 3.3.1.

A response is received in the form of an action signal A_t, after which the market environment skips to the price in T_{i+time_skip} and drafts a new state S_{t+1} and a scalar reward R_{t+1} for the action A_t, which are sent to the system. State and reward signals are produced with the functions described in subsection 3.3.2 and subsection 3.3.3 respectively.

These interactions continue until the end of dataset is reached, completing what is referred to as a pass through the dataset. There are two types of passes, firstly training passes where the actions selected by the system have an exploratory component and observed experiences $e_t = (S_t, A_t, R_{t+1}, S_{t+1})$ are stored and used to update the network weights. Secondly, test passes where the system always chooses what it believes to be the best action and no updates are performed to the Q-network. While training passes always use a training dataset, test passes are performed on both a training dataset and a validation dataset for assessing quality of learning, as described in subsection 3.3.4, and on a test dataset to estimate real financial performance, as described in chapter 4.

3.3.1 time_skip and nr_paths

Most trading systems use hourly, daily, weekly or monthly data, which means they make decisions with a hourly, daily, weekly or monthly time gap. As we are using tick data, without a $time\_skip$ parameter it would make a decision with the time gap of a tick. Since ticks can happen extremely fast this is impractical. The latency of the connection between system and broker is much too high for realistic execution of such orders. Also, a system allowed to trade at such velocity would have a larger effect on the market, even in one as liquid as this one, and the assessment of performance would lose predictive value.

Thus we only allow the system to make a decision at every $time\_skip$ ticks. We chose $time\_skip = 5000$, which on average is somewhat less than two hours for 2013 EUR/USD tick data, since it fits with our aim of a short term speculator without being so high frequency as to be too affected by practical concerns such as latency and lack of broker liquidity. This value was chosen a priori, with no optimization involved, and treated as a trader's preference choice since the process to optimize the system for a variety of trading frequencies would be too lengthy with our computational resources. Other users could simply adjust $time\_skip$ to suit their own trading frequency preference, although the rest of our system's parameters were optimized with $time\_skip = 5000$ in mind and would likely require readjustment.

Intuitively, an advantage of using ticks with a $time\_skip$ parameter rather than directly use data with the desired time gap, is that with this approach the periodicity of decision-making is not a fixed interval as for most systems in the literature. When the market is more active, $time\_skip$ represents a smaller interval of time, while for periods of little activity $time\_skip$ is a much larger time gap between decisions.

[4]Which only happen every $time\_skip$ ticks.

This means that the system, for lack of a better term, pays more attention to the market when it should be paying more attention.

A more significant advantage is the possibility of carving different paths through the data. By changing the starting point of a training or testing pass through the data to T_b with:

$$b \in \{\, x \cdot \frac{time\_skip}{nr\_paths} \mid x \in \mathbb{N}_0,\, x < nr\_paths \,\}, \tag{3.6}$$

we change the whole set of market states visited on that pass, as shown schematically in Figure 3.8.

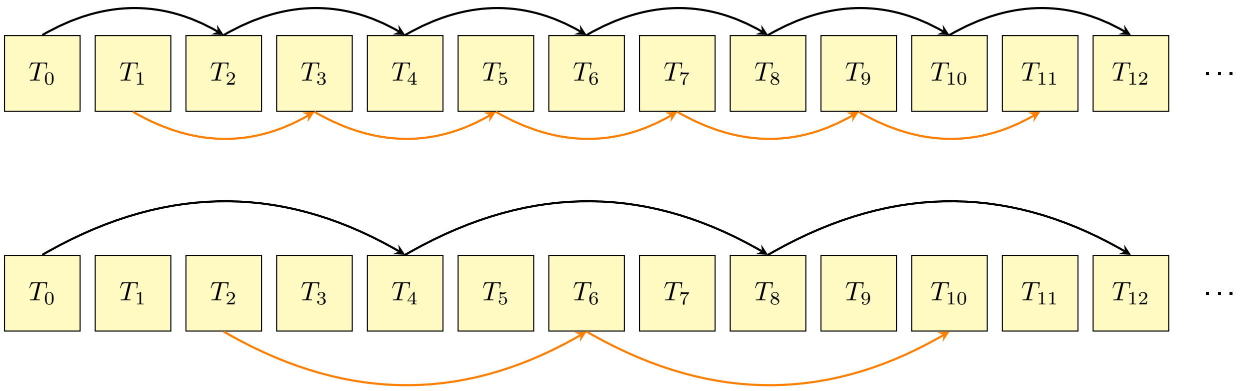

T_0 T_1 T_2 T_3 T_4 T_5 T_6 T_7 T_8 T_9 T_{10} T_{11} T_{12} $\cdots$
T_0 T_1 T_2 T_3 T_4 T_5 T_6 T_7 T_8 T_9 T_{10} T_{11} T_{12} $\cdots$

Figure 3.8: Schematic of a dataset of ticks and how the market environment sequentially visits those ticks through two different paths, in orange and black. Top: $time\_skip = 2$, Bottom: $time\_skip = 4$. These paths would be very similar, but for larger values of $time\_skip$ the distance between ticks visited in different paths increases and so does the quality of information added by having different paths.

By using a different path through the data each time we train the network, we supply the system with a larger variety of data. Neural networks are known to require large amounts of data, especially as their complexity increases, thus this approach helps mitigate overfitting and increases generalization capability. Figure 3.9[5] exemplifies this effect: performance in the validation dataset improves and overfitting is delayed and less severe.

This advantage also extends to testing the system. The standard testing approaches deliver a path-dependent distribution of gains thus increasing the chances of a ”lucky” trading strategy. This is regarded as a serious problem in testing trading systems [50], which we also mitigate through this various paths approach. For each test we perform a number of test passes through different paths and use the resulting average as the result of that test. It stands to reason that a system performing well through a variety of initial conditions is a better predictor of future success. This also provides rigor to testing, as the standard deviation of performance over the different paths gives us a measure of the uncertainty of these tests.

nr_paths linearly increases computational time and it has diminishing returns as paths become more similar between them and thus increasingly redundant. We have found $nr\_paths = \frac{time\_skip}{500}$, meaning a distance of 500 ticks between paths, is a balanced value for both testing and training passes, and use it throughout this work. We define nr_paths to keep a certain tick distance between paths rather than as a fixed value, ie. $nr\_paths = 2$, to allow a user to seamlessly lower or increase trading frequency,

[5]Note this figure was obtained as part of the optimization process and does not use the last iteration of the system.

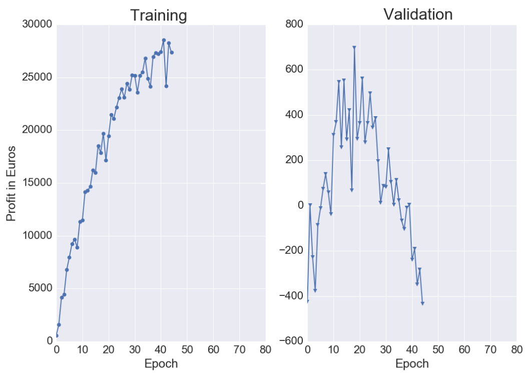

(a) With $nr\_paths = 1$.

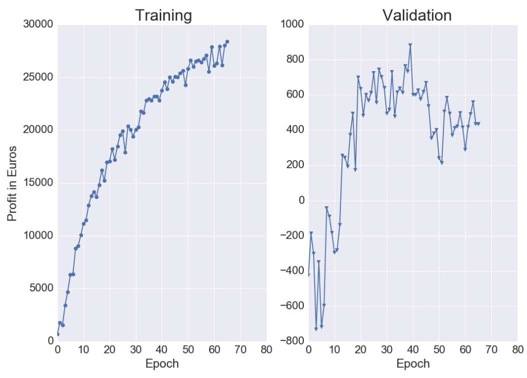

(b) With $nr\_paths = 10$.

Figure 3.9: Example of learning curves with and without the nr_paths dynamic. Training dataset: 01/2011 to 01/2012. Validation dataset: 01/2012 to 07/2012. How these learning curves are produced is further explained in subsection 3.3.4.

by changing $time\_skip$, while keeping the amount of ”unique” data the Q-network is trained on constant. This opens the door to training the Q-network to trade at frequencies that would otherwise not offer enough data points, within certain limits of course, the data thus generated has some redundancy, it is not of the same quality as truly new data.

3.3.2 Reward Signal

The initial approach for the reward signal was to use only the profit obtained from each transaction. This approach is intuitive, simple to implement and imposes no constraints to the system on how to achieve profitability. However, tests revealed it introduced consistent behavioral flaws. Since the system was not punished for holding positions with negative unrealized profits, but was punished at moment of their closing, it learned to keep a position open until its unrealized profit bounced back to positive values however long that may take, as observed in Figure 3.10.

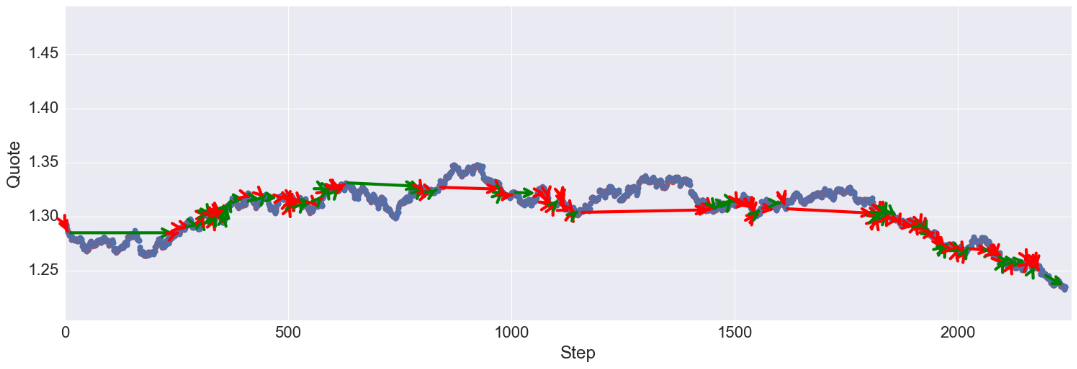

Figure 3.10: Behaviour with the initial reward approach on a 6 month validation dataset from 2012.01 to 2012.06. Each step skips 5000 ticks. Green arrows are long positions and red arrows are short positions.

Obviously, this is a critical flaw, the asset may never regain its former value or take so long to do so as to make the system inviable. To solve this issue a new reward component was added: the variation of unrealized profit, to which we refer as the return. Actions A_t that create a return, opening a position and holding a position open, are rewarded with the magnitude of that return: the difference between the unrealized profit in the state S_t in which they were taken and the unrealized profit in the state S_{t+1} to which they lead. Both approaches obtain similar profit, but various tests showed the second approach effectively corrects for the behavior flaws previously observed as exemplified in Figure 3.11, which means that profit is obtained with less risk. Furthermore, its seems that the increase in feedback given to the system alleviates the credit assignment problem as various tests show the system's learning curve develops in a significantly smaller number of epochs.

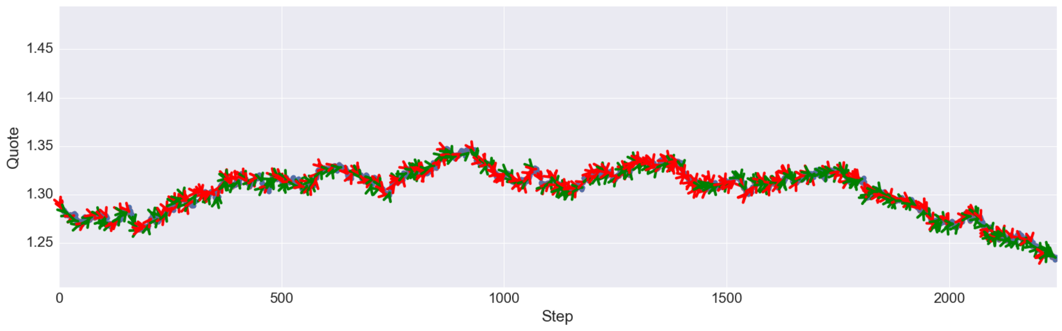

Figure 3.11: Example of behaviour with the final approach to reward on a 6 month validation dataset from 2012.01 to 2012.06. Each step skips 5000 ticks. Green arrows are long positions and red arrows are short positions.

We saw in section 2.4 that some systems use risk-adjusted profit as their reward. The most common methods to adjust for risk are the Sharpe ratio, which divides the profit by the standard deviation of unrealized profit, and its modification the Sortino ratio, which divides profits by the downside deviation of unrealized profit. Both aim to penalize large variations of unrealized profit which are interpreted as risk. Our reward system is in essence very similar, especially to the Sortino ratio since positive volatility is not punished, as is the case with the Sharpe ratio, but rewarded. The difference is that rather than introduce the punishment/reward at the end of the transaction by adjusting the profit, it is spread out over its life with the return at each step, which has the empirically observed benefit of speeding up the learning process, possibly by alleviating the credit assignment problem.

Algorithm 1 describes in pseudocode the implementation of a function that creates such a reward signal. Notice that the reward derived from the profit or the return is, through min-max normalization, always in the range $[-1, 1]$ for each dataset $\mathbb{T}$. This makes learning more stable by limiting the size of the cost function gradients [6]. Also, it becomes easier to find suitable hyper-parameters for the system and allows the use of those same hyper-parameters across a variety of datasets with different profit/return distributions and with different $position\_size$.

Also, similarly to the standardization performed in subsection 3.2.2, we apply a percentile filter to values above a certain percentile $return\_percentile$ of absolute return before normalizing them with the min-max method, since weekend-gaps in $\mathbb{T}$ create returns that significantly skew the distribution as observed in Figure 3.12. This is not an issue for the profit reward, to which we simply apply a min-max normalization directly. The use of the $return\_percentile^{th}$ also allows us to control how much importance

Algorithm 1 Compute reward R_{t+1} for action A_t in state S_t

```
Precondition: $max\_r$ is the $return\_percentile^{th}$ percentile of the absolute distribution of returns in the
    training dataset.
Precondition: $max\_p$ is the maximum possible profit in the training dataset.
 1: function REWARD($unrealized\_profit_t, unrealized\_profit_{t+1}, A_t$)
 2:     if $A_t$ = Open Long or $A_t$ == Open Short or $A_t$ == Hold Position then
 3:         $return \leftarrow unrealized\_profit_{t+1} - unrealized\_profit_t$
 4:         $R_{t+1} \leftarrow sign(return) * min(abs(return/max\_r), 1)$
 5:     else if $A_t$ == Close Long or $A_t$ == Close Short then
 6:         $R_{t+1} \leftarrow sign(unrealized\_profit_t) * min(abs(unrealized\_profit_t/max\_p), 1)$
 7:     else
 8:         $R_{t+1} \leftarrow 0$
 9:     end if
10:     return $R_{t+1}$
11: end function
```

the system gives to return rewards compared to profit rewards, as a tighter percentile filter equates to larger return rewards.

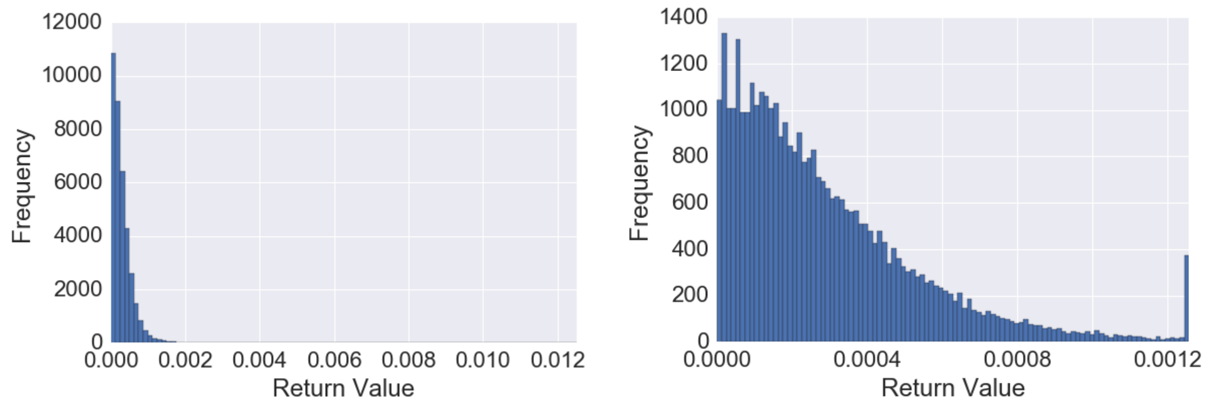

(a) Without percentile filter. (b) With $return\_percentile = 99$.

Figure 3.12: Distribution of possible returns in a EUR/USD Duskacopy dataset of the year 2013, with $time\_skip = 500$.

3.3.3 State Signal

In this section we describe the state signal created by the market environment. A pseudocode implementation is provided in algorithm 2.

The dataset $\mathbb{T} = T_0, .., T_D$ used by the market environment to set the prices has a counterpart $\mathbb{F} = F_0, .., F_D$ created from it by the preprocessing procedure described in section 3.2. Its element $F_{i=t \cdot time\_skip+b}$, containing the compact representation of the market history associated with the current tick T_i, is a component of the state S_t.

A second component of S_t is an integer scalar h_t with three discrete values, whose purpose is telling

Algorithm 2 Assemble state S_t

```
Precondition: $max\_p$ is the maximum possible profit in the training dataset.
Precondition: $Bid_k$ and $Ask_k$ are the Bid and Ask prices from the $k^{th}$ tick in the dataset.
Precondition: $F_k$ is the feature array for the $k^{th}$ tick in the current dataset.
function STATE($S_t, A_t, \mathbb{T}, \mathbb{F}$)
    $S_{t+1} \leftarrow [0, 0, 0, 0]$
    if $A_t$ == Open Long then
        $S_{t+1}[0] \leftarrow 1$
        $Ask_{open} \leftarrow Ask_{t \cdot time\_skip+b}$
    else if $A_t$ == Open Short then
        $S_{t+1}[0] \leftarrow -1$
        $B_{open} \leftarrow B_{t \cdot time\_skip+b}$
    else if $A_t$ == Hold or $A_t$ == Idle then
        $S_{t+1}[0] \leftarrow S_t[0]$
    else if $A_t$ == Close Long or $A_t$ == Close Short then
        $S_{t+1}[0] \leftarrow 0$
        $acc\_size \leftarrow acc\_size + unrealized\_profit_t$
    end if
    if $S_{t+1}[0] == 1$ then
        $unrealized\_profit_{t+1} \leftarrow position\_size \cdot (Bid_{(t+1) \cdot time\_skip+b} - Ask_{open})$
    else if $S_{t+1}[0] == -1$ then
        $unrealized\_profit_{t+1} \leftarrow position\_size \cdot (Bid_{open} - Ask_{(t+1) \cdot time\_skip+b})$
    else if $S_{t+1}[0] == 0$ then
        $unrealized\_profit_{t+1} \leftarrow 0$
    end if
    $S_{t+1}[1] \leftarrow sign(unrealized\_profit_{t+1}) \cdot min(abs(unrealized\_profit_{t+1}/max\_p), 1)$
    $S_{t+1}[2] \leftarrow min(max(-1, 2 \cdot (((acc\_size + unrealized\_profit_{t+1})/init\_acc\_size - failure)/(safe - failure) - 1), 1)$
    if $S_{t+1}[2] == -1$ then
        Flag $S_{t+1}$ as terminal.
    end if
    $S_{t+1}[3] \leftarrow F_{(t+1) \cdot time\_skip+b}$
    return $S_{t+1}$
end function
```

the system if it currently has a position open and of which kind:

$$h_t = \begin{cases} 1, & \text{if long position open} \\ 0, & \text{if no position open} \\ -1, & \text{if short position open} \end{cases} \tag{3.7}$$

A third component is a float scalar v_t containing the unrealized profit of the currently open position, normalized in the same manner as the profit reward described in subsection 3.3.2. Thus v_t is meant to convey the system how much reward it will receive by closing the currently open position.

The fourth and final component of the state signal is a float scalar c_t which tells the system the current size of the account, including the unrealized profit of any open position, compared to the initial size. This value is normalized and clipped to the range $[-1, 1]$, where the maximum and minimum represent, respectively, a $safe$ level and a $failure$ level, both set by the user:

$$c_t = \begin{cases} 1, & \text{if } \frac{AccountSize}{InitialAccountsize} > safe \\ -1, & \text{if } \frac{AccountSize}{InitialAccountsize} < failure \\ 2 \cdot (\frac{AccountSize}{InitialAccountsize} - failure)/(safe - failure) - 1, & \text{otherwise.} \end{cases} \tag{3.8}$$

The goal of this component is to introduce a condition for a terminal state. In RL the terminal state is the last in a chain of interactions, and thus is state with a precisely known Q-value: the reward obtained in that state, since no further rewards will be earned. It can thus act as an anchor for learning. Should the current account size reach the $failure$ threshold, the system flags it as a terminal state[6]. After a state is flagged as terminal, the account size is reset to the initial value and training continues.

The terminal state condition was added for its value anchoring effect and to further punish strings of consecutive bad decisions, common in the early stages of training. Empirically we verified that a $failure$ threshold closer to 1, meaning more instances of terminal states, does increase learning speed. But if it is set too close to 1 it diminishes leaning quality. Thus, we set $failure$ to 0.8, which modestly increases learning speed while safely out of the range where learning quality starts to suffer. The $safe$ threshold is simply for normalization purposes, and was set to 2.

3.3.4 Training Procedure

The training procedure is structured into epochs. Each epoch has four distinct phases, a learning phase and three phases to assess learning progress:

- Training pass over a training dataset (learning phase);
- Evaluation of Q-values over random set of states (first metric);
- Test over the training dataset (second metric);
- Test over the validation dataset (third metric).

The procedure, excluding the first metric, is depicted schematically in Figure 3.13. For the first metric, states are collected by running a random policy through the training dataset and then at each epoch we assess the Q-Network's average estimated Q-value for that set of states. A smooth growth in this metric, with no divergence, suggests that the Q-Network is learning and stable. This metric is useful for debugging in early stages of system development where learning is still unstable and design choices must be taken to improve its stability, but in later stages it is no longer necessary and was eventually put aside to speed up training execution. Thus this metric does not feature throughout the rest of the thesis and is mentioned here simply for completeness.

For the second and third metrics the profit generated over the test is recorded and the evolution of that profit over the epochs is the indicator of how well the system is learning. In the case of the third metric, we are testing on data, the validation dataset, that the system does not access while training.

[6]See algorithm 3 for the implementation.

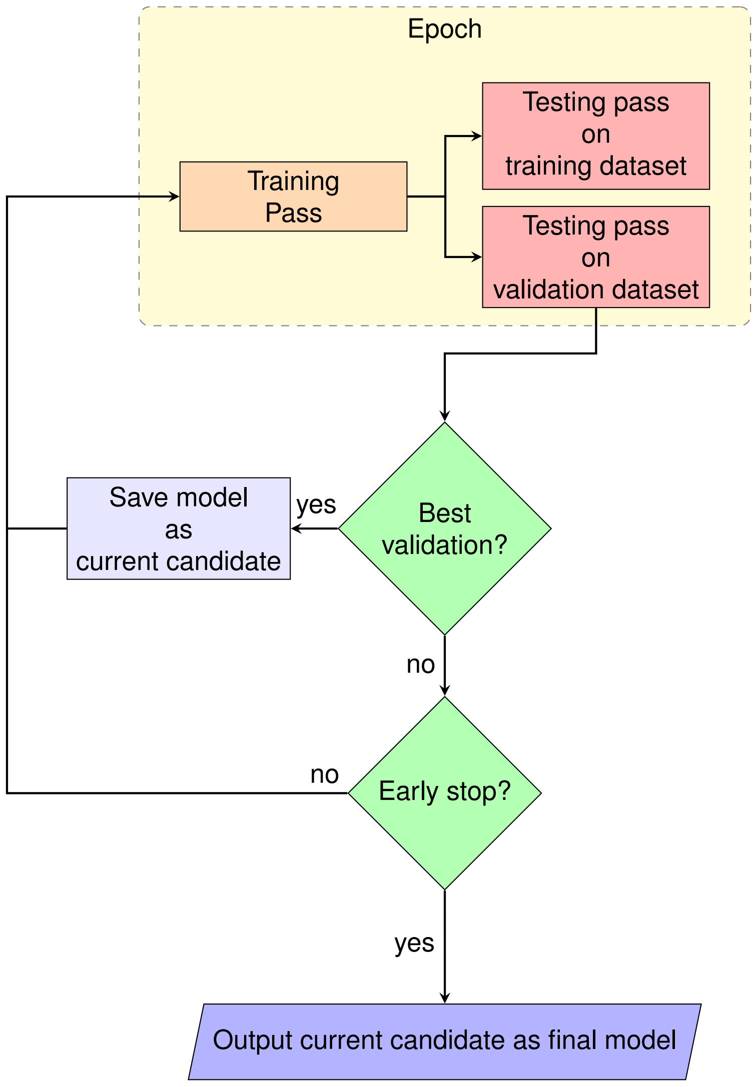
Epoch
Training Pass
Testing pass on training dataset
Testing pass on validation dataset
Best validation?
yes
Save model as current candidate
no
Early stop?
no
yes
Output current candidate as final model

Figure 3.13: Training Procedure.

The validation dataset corresponds to a period of time immediately following the training dataset. The aim is to make sure that what our system is not only learning how to behave when confronted with the training dataset, but that what it learns will generalize to data it has not seen during training. Relying only on training dataset performance could be misleading as it is possible that the progress observed for the training dataset comes from learning the idiosyncrasies of that dataset, its noise, rather than the underlying relationships, an issue known as overfitting. This metric is the crux of the learning process, since it is performance on previously unseen data that we truly want when subsequently applying the system to live training. We rely on the validation performance curve to tell us when to stop training i.e. how many epochs to train for, via the early stopping approach.

With early stopping, each time the performance assessment on the validation reaches a new high we save the current model[7] as our candidate to final model and a counter is started. This counter is reset when a new candidate appears, but if that counter reaches predefined limit then the training process is

[7]By model we mean the Q-network with a given set of weights. After each epoch that set of weights has changed and so we consider it a new model.

stopped early and the current saved candidate is our final model. This is an inexpensive way to avoid strong overfitting even if the other hyper-parameters would yield to overfitting [32].

3.3.5 Example

In this section we aim to make clearer how the procedures introduced so far interact to create the market environment for our Q-network. To do so, we provide a slightly scaled down example with $TW = [0, 4000, 6000]$, $time\_skip = 5000$, $nr\_paths = 10$, $init\_acc\_size = position\_size = 10000$, a training dataset with 5,000,000 ticks and a validation dataset with 1,000,000 ticks.

According to the parameter TW, 6,000 ticks are necessary to create a feature vector thus our market simulation has to start each pass, at the earliest, from tick $T_{i=6000}$. This is simply a practical detail and was overlooked in the notation introduced in the sections above to avoid further cluttering. Firstly, the training pass starting from step $t = 0$. The initial tick is T_b with $b \in \{x \cdot 500 \mid x \in \mathbb{N}_0, x < 10\}$, and thus for this first pass training pass we start from T_0, which is actually T_{6000} due to the aforementioned practical consideration. Preprocessing creates the first feature array F_{6000}:

$$\begin{bmatrix}
\underset{k\in[6000,2000]}{\mu} B_k - B_{6000} & \underset{k\in[6000,2000]}{\mu} S_k & \underset{k\in[6000,2000]}{\mu} Vb_k & \underset{k\in[6000,2000]}{\mu} Va_k \\
\underset{k\in[6000,2000]}{\max} B_k - B_{6000} & \underset{k\in[6000,2000]}{\max} S_k & \underset{k\in[6000,2000]}{\max} Vb_k & \underset{k\in[6000,2000]}{\max} Va_k \\
\underset{k\in[6000,2000]}{\text{std}} B_k & \underset{k\in[6000,2000]}{\text{std}} S_k & \underset{k\in[6000,2000]}{\text{std}} Vb_k & \underset{k\in[6000,2000]}{\text{std}} Va_k \\
\underset{k\in[6000,2000]}{\min} B_k - B_{6000} & \underset{k\in[2000,0]}{\mu} B_k - B_{6000} & \underset{k\in[2000,0]}{\mu} S_k & \underset{k\in[2000,0]}{\mu} Vb_k \\
\underset{k\in[2000,0]}{\mu} Va_k & \underset{k\in[2000,0]}{\max} B_k - B_{6000} & \underset{k\in[2000,0]}{\max} S_k & \underset{k\in[2000,0]}{\max} Vb_k \\
\underset{k\in[6000,2000]}{\max} Va_k & \underset{k\in[2000,0]}{\text{std}} B_k & \underset{k\in[2000,0]}{\text{std}} S_k & \underset{k\in[2000,0]}{\text{std}} Vb_k \\
\underset{k\in[2000,0]}{\text{std}} Va_k & \underset{k\in[2000,0]}{\min} B_k - B_{6000} & time^1_{6000} & time^2_{6000}
\end{bmatrix}$$

which is fed to the state function from the market environment. The state function adds to the feature array the components $h_0 = 0$ and $v_0 = 0$, since there is no position open, and $c_0 = 2 \cdot (1 - 0.8)/(2 - 0.8) - 1 = -0.667$, creating the state:

$$S_0 = \begin{bmatrix} 0 & 0 & -0.667 & F_{6000} \end{bmatrix}$$

.

The Q-network is initialized with a random set of weights $\mathbb{W}_0$. It performs a forward propagation with S_0 and outputs its estimation for the action value of each possible action $Q(S_t, a_n; \mathbb{W}_0)$, with $n \in [0, 1, 2]$. The ϵ-greedy algorithm selects one of the actions action based on these values. Since there is no position open: a_0 represents opening doing nothing, a_1 opening a long position and a_2 opening a short position. For this example let us assume the action selection chose $A_0 = a_1$, thus opening a long position.

This action is passed on to the market environment. It is now step $t = 1$, and per the $time\_skip$

parameter the market is now in tick T_{11000}. The chosen action A_0 is given to the reward function, so R_1 can be drafted. The reward for opening a long position is the variation of unrealized profit, which was 0 before, normalized to the range $[-1, 1]$ in regard to max_r, the $return\_percentile^{th}$ percentile of the training dataset's possible returns. The order to open a position was given in tick T_{6000} when the ask price was 1.32655, for example, and we are now in T_{11000} where the bid price is 1.32454. Assuming $max\_r = 0.012$ in this dataset:

$$R_1 = \frac{return}{max_r} = \frac{position\_size \cdot B_{11000} - A_{6000}}{position\_size \cdot max\_r} = \frac{-0.00201}{0,012} = -0,1675 \tag{3.9}$$

A new state S_1 is also drafted. Preprocessing creates the new feature array F_{11000}:

$$\begin{bmatrix}
\underset{k\in[11000,7000]}{\mu} B_k - B_{11000} & \underset{k\in[11000,7000]}{\mu} S_k & \underset{k\in[11000,7000]}{\mu} Vb_k & \underset{k\in[11000,7000]}{\mu} Va_k \\
\underset{k\in[11000,7000]}{\max} B_k - B_{11000} & \underset{k\in[11000,7000]}{\max} S_k & \underset{k\in[11000,7000]}{\max} Vb_k & \underset{k\in[11000,7000]}{\max} Va_k \\
\underset{k\in[11000,7000]}{\operatorname{std}} B_k & \underset{k\in[11000,7000]}{\operatorname{std}} S_k & \underset{k\in[11000,7000]}{\operatorname{std}} Vb_k & \underset{k\in[11000,7000]}{\operatorname{std}} Va_k \\
\underset{k\in[11000,7000]}{\min} B_k - B_{11000} & \underset{k\in[7000,5000]}{\mu} B_k - B_{11000} & \underset{k\in[7000,5000]}{\mu} S_k & \underset{k\in[7000,5000]}{\mu} Vb_k \\
\underset{k\in[7000,5000]}{\mu} Va_k & \underset{k\in[7000,5000]}{\max} B_k - B_{11000} & \underset{k\in[7000,5000]}{\max} S_k & \underset{k\in[7000,5000]}{\max} Vb_k \\
\underset{k\in[7000,5000]}{\max} Va_k & \underset{k\in[7000,5000]}{\operatorname{std}} B_k & \underset{k\in[7000,5000]}{\operatorname{std}} S_k & \underset{k\in[7000,5000]}{\operatorname{std}} Vb_k \\
\underset{k\in[7000,5000]}{\operatorname{std}} Va_k & \underset{k\in[2000,0]}{\min} B_k - B_{11000} & time^1_{11000} & time^2_{11000}
\end{bmatrix}$$

to which the state function adds $h_1 = 1$ and, assuming $max_p = 1000$, $v_1 = \frac{-20.1}{1000} = -0.02$, since there is a Long position open, and $c_1 = 2 \cdot (0.998 - 0.8)/(2 - 0.8) - 1 = -0.670$ so that:

$$S_1 = \begin{bmatrix} 1 & -0.02 & -0.670 & F_{11000} \end{bmatrix}$$

With S_1 and R_1 the Q-network has the first experience $e_0 = (S_0, A_0, R_1, S_1)$ with which to learn. S_1 is inputted to the network which performs a forward propagation and starts a new interaction. This cycle is repeated until tick T_{499600}, step $t = 998$, when it is no longer possible to skip 5000 ticks. This concludes the first training pass.

After a training pass the market environment performs test passes on the training dataset. The interaction cycle is exactly the same, except that ϵ is set to 0 so that the action with best Q-value is always chosen, and observed experiences e_t are not used for Q-network updates. When it reaches the end of the pass, tick T_{499600} or step $t = 998$, it restarts from a new path, meaning a new initial tick T_b with $b \in \{\, x \cdot 500 \mid x \in \mathbb{N}_0,\ x < 10 \,\}$ is chosen. It performs this new pass starting from T_{6500}, then another starting from T_{7000}, until a final pass starting from T_{10500}, while recording the profit obtained from each of those passes.

After the last test pass with the training dataset, it is time for test passes on the validation dataset. The same cycle as above, a pass starting from T_{6000} and finishing at T_{996000}, or $t = 198$. Then another pass starting from T_{6500}, T_{7000}, etc. recording the profit from each. After all validation test passes, the first epoch is complete.

A second epoch starts with a new training pass. The only difference between this training pass and the one from the previous epoch, is that this one starts from, T_{6500}, the second path. The training pass in the third epoch will start from T_{7000}, in the fourth it starts from T_{7500}, etc. eventually goes back to starting T_{6000}, then T_{6500} again and so on. This allows for the Q-network to always learn from data it has not seen in a number of epochs, making it more difficult to "memorize" and thus overfit, while being tested on all data to ensure more accurate assessment of performance. Epoch after epoch this repeats itself, until the early stop procedure stops it.

3.4 Q-Network

So far, we have gone into detail about the environment surrounding the trading system, and how it controls the flow of information into it. Now we take take a closer look at the system itself. Its core is a fully connected backpropagational neural network, depicted schematically in Figure 3.14. This network is tasked with computing a function $Q(s; \mathbb{W}_k)$, where $\mathbb{W}_k$ is the set of weights and biases of the network at iteration k.

The input layer has a number of neurons defined by the elements in our representation of the state s of the market, which per the hyper-parameter TW chosen in section 3.5 results in 148 input neurons. This input layer is followed by three hidden layers with 20 ReLU neurons each.

The ReLu activation function was chosen due to its documented superiority for training multi-layer neural networks [51] over other widely used activations, such as hyperbolic tangent and logistic sigmoid. Future developments in the field of neural networks may bring change, but currently the number of hidden neurons and layers has to be determined empirically (see [32] for practical recommendations). We did so using the datasets described in Table 3.2, used for all hyper-parameter selection. This process was performed in tandem with the choice of parameter TW to make sure there was a balance between power of the network and number of input variables. We found this balance hard to achieve and very precarious, with the Q-network easily slipping into overfitting. This is not surprising given the noisy nature of financial data.

Tests were performed with L1 regularization, L2 regularization and dropout regularization to help prevent overfitting, but they were not successful and these methods were not included in the final architecture. We found significant performance gain from the three hidden layer topology versus a two hidden layer or a single hidden layer with the same number of total neurons, although adding a fourth layer made training difficult and resulted in decayed performance.

Finally, the output layer has three neurons with linear activations:

$$a_j^4 = net_j^4 = \sum_{i=1}^{n} a_i^3 \cdot w_{ji}^4 + b_j^4, \tag{3.10}$$

since they are meant to represent action values which may take any real value.

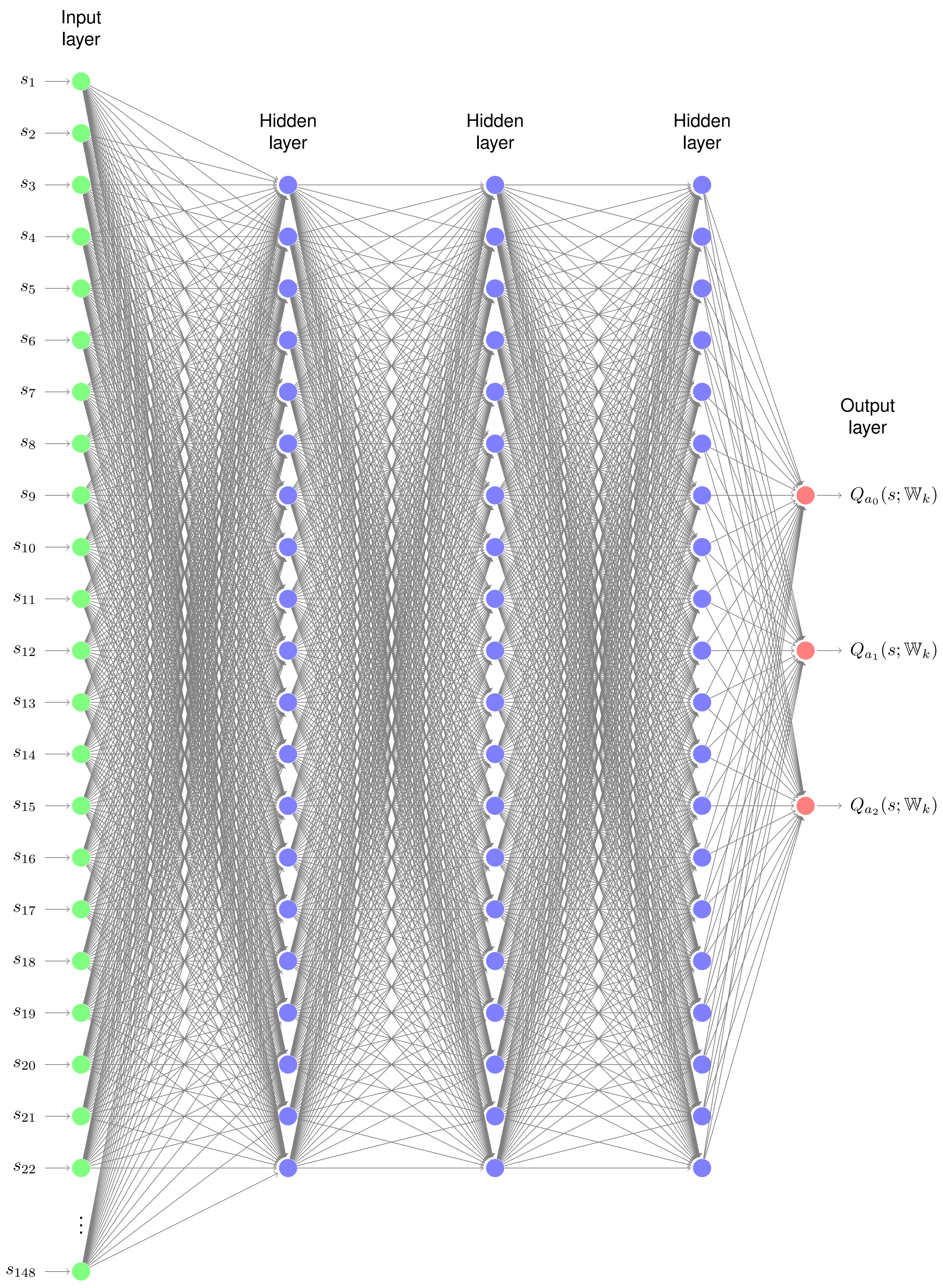

Figure 3.14: Schematic of the trading system's Q-network. s_n is the n^{th} element of the vector representing the state s. Hidden and output neurons have ReLU and Linear activations respectively.

With this topology have chosen to approximate the optimal action value function in its vectorial form:

$$Q(s;\mathbb{W}_k) := (Q_{a_0}(s;\mathbb{W}_k), Q_{a_1}(s;\mathbb{W}_k), Q_{a_2}(s;\mathbb{W}_k)) \approx q_*(s) := (q_*(s,a_0), q_*(s,a_1), q_*(s,a_2)), \quad (3.11)$$

rather than the arguably more intuitive:

$$Q(s,a_n;\mathbb{W}_k) \approx q_*(s,a_n). \quad (3.12)$$

The reasoning is that the second option would require a forward propagation to obtain the Q-value of each action a_n, while this approach, first proposed by Mnih et al. [6], gives us all action values in a single forward propagation, saving computational resources.

The above-described Q-network is initialized with a random set of weights where each weight is drawn from an independent normal distribution with range $[-1,1]$. Obviously this means its outputs are initially completely random, and we need a process through which they can become better approximations of π_*. As per the interactions between system and environment described in section 3.3, the Q-network collects experience at each step t in the form of transitions e_t:

$$e_t = (S_t, A_t, R_{t+1}, S_{t+1}). \quad (3.13)$$

Looking back at standard tabular implementation of Q-learning (subsection 2.2.4), we would have a arbitrarily initialized table which after observing a transition e_t would use that experience to iteratively update its tabulated estimate of q_* for state S_t and action A_t, $Q_k(S_t,A_t)$, towards $(R_{t+1} + \gamma \max_a Q_k(S_{t+1},a))$:

$$Q_k(S_t,A_t) \leftarrow (1-\alpha)Q_k(S_t,A_t) + \alpha[R_{t+1} + \gamma \max_a Q_k(S_{t+1},a)]. \quad (3.14)$$

Our network aims to play the role of such a table, thus we apply the same concept in improving our neural network's approximation of q_*, but through the learning mechanisms of neural networks i.e. updating the set of weights with backpropagation/gradient descent. e_t is given to a learning function which performs these updates as described in subsection 3.4.1, an implementation specialized for stable Q-Network learning.

3.4.1 Learning Function

The role of the learning function is to receive the transitions e_t observed during learning passes and use them to change the Q-Network's weights in a way that improves its approximation of q_*. A direct adaptation of Equation 3.14 to the neural network learning methods introduced in the previous chapter would suggest performing backpropagation/gradient descent updates, Equation 2.28 and Equation 2.32, with a cost function such as:

$$E_t(\mathbb{W}_k) = \|\mathbf{a}^L_{t,k} - \mathbf{d}_t\|^2 = (Q_{A_t}(S_t,\mathbb{W}_k) - (R_{t+1} + \gamma \max_a Q_a(S_{t+1},\mathbb{W}_k)))^2. \quad (3.15)$$

Note that $\mathbf{d_t}$ is defined in such a way that outputs representing Q-values of the actions other than the one responsible for transition e_t do not contribute to $E_t(\mathbb{W}_k)$ and, by the extension, to the weight update. This is generally the approach we take, but using a modified version of $\mathbf{d_t}$ and an alteration to the typical minibatch gradient descent implementation. Algorithm 3 describes our approach via pseudocode.

Algorithm 3 Use observed transitions to improve Q-Network

```
Precondition: $e = [s, a, r, s']$ is an observed transition.
 1: Initialize replay buffer with maximum capacity $N$
 2: Initialize $updates = 0$ and $transitions = 0$
 3: function LEARN($e_t$)
 4:     $transitions \leftarrow transitions + 1$
 5:     if buffer is not full then
 6:         Append $e_t$ to buffer
 7:     else
 8:         Replace oldest element in the buffer with $e_t$
 9:     end if
10:     if $transitions$ % $update\_q$ == 0 then
11:         Sample random mini-batch $\mathbb{S}_{updates}$ of size $B$ from buffer with elements $e_p = [s^p, a^p, r^p, s'^p]$
12:         for each $e_p$ do
13:             if $s^p$ is terminal then
14:                 set $\mathbf{d}_p = r^p$
15:             else
16:                 set $\mathbf{d}_p = r^p + \gamma Q_A(s'^p, \mathbb{W}^-)$, with $A = \arg\max_a Q_a(s'^p, \mathbb{W}_{updates})$
17:             end if
18:         end for
19:         Compute $\sum_{p=1}^{B} \frac{E_p(\mathbb{W}_{updates})}{B}$
20:         Perform backpropagation and RMSProp for $\mathbb{W}_{updates}$.
21:         $updates \leftarrow updates + 1$
22:     end if
23:     if $updates$ % $update\_q^-$ == 0 then
24:         $\mathbb{W}^- \leftarrow \mathbb{W}_{updates}$
25:     end if
26: end function
```

We introduce an auxiliary Q-Network, $Q(s; \mathbb{W}^-)$, topologically identical to the original Q-Network, whose weights $\mathbb{W}^-$ are static and periodically copied from the original set $\mathbb{W}_k$ every $update\_q^-$ updates. This auxiliary Q-network is used to generate the targets for updates:

$$E_t(W_k) = (Q_{A_t}(S_t, W_k) - (R_{t+1} + \gamma \max_a Q_a(S_{t+1}, W^-)))^2. \tag{3.16}$$

The issue is that the original targets $\max_a Q_a(s_{t+1}, \mathbb{W}_k)$ are constantly shifting in a correlated manner with the Q-value estimations, which made learning more difficult and could easily spiral out of control through feedback loops. This approach, first proposed by Mnih et al. [8], improves Q-Learning performance and stability. We further improved upon Equation 3.16 through a variation known as double Q-learning, suggested by van Hasselt et al. [11]:

$$E_t(\mathbb{W}_k) = (Q_{A_t}(S_t, \mathbb{W}_k) - (R_{t+1} + \gamma Q_a(S_{t+1}, \mathbb{W}^-)))^2, \text{ with } a = \arg\max_n Q_n(S_{t+1}, \mathbb{W}_k). \tag{3.17}$$

The aim of this change is to decouple, even if only partially, the action choice from the target Q-value generation which is known to introduce a bias in the action value estimation resulting in poorer policies.

A final learning mechanism that has been found to by very helpful for Q-network learning, deals with the composition of minibatch $\mathbb{S}_k$ used in the gradient descent algorithm (see Equation 2.32). Typically the minibatch updates would happen in an online fashion, meaning that as training progresses the system would sequentially collect $|\mathbb{S}_k|$ gradients, perform an update, discard them and then collect $|\mathbb{S}_{k+1}|$ more and so on, synchronized with the stream of experience. However, this leads to two problems [52]:

- strongly correlated updates resulting in inefficient learning;
- the rapid forgetting of possibly rare experiences that would be useful later on.

For this reason we use a method known as experience replay [53] was introduced, whereby each experience e_t obtained is stored in a sliding window buffer of size N, from which a selection of B experiences are randomly drawn every $update\_q$ steps to perform a minibatch update. This ameliorates the issues above and generally reduces the amount of experience required to learn.

3.5 Hyper-parameter Selection

Optimization of the system is based on the observed learning curves, particularly on the validation datasets as they provide insight into the generalization power of the acquired knowledge. This means that to assess each configuration of hyper-parameters we have to fully train the network. Depending on the size of the dataset, the number of neurons in the Q-network and the parameters $time\_skip$ and nr_paths it can take anywhere from a couple of hours to almost a whole day for a single test. Testing on a single dataset is not enough since results are too dataset dependent and need to be confirmed. Also, there is a large number hyper-parameters to tune and they are related to each other in complex ways: by changing one of them, a number of the others may no longer be optimal. These factors have made it impossible for us to perform a systematic grid search for the optimal set of hyper-parameters.

Instead, the values of hyper-parameters were selected by performing an informal search using the three datasets described in Table 3.2, with the goal of obtaining the most stable learning curve with the highest generalization capability, as measured by peak performance on the validation dataset. The size and number of datasets was a compromise between testing on a meaningful amount of data and completing the tests in a realistic time frame.

	Dataset A		**Dataset B**		**Dataset C**	
	Training	Validation	Training	Validation	Training	Validation
Begins	01/2011	01/2012	01/2012	01/2013	01/2013	01/2014
Ends	01/2012	06/2012	01/2013	06/2013	01/2014	06/2014
Nr. Ticks	25,786,841	11,507,313	23,467,196	8,723,458	18,643,628	5,884,697

Table 3.2: The three datasets used for hyper-parameter selection.

Hyperparameter	Value	Description
q	99	Percentile filter applied to extracted features.
$time\_skip$	5000	Number os ticks skipped between steps t and $t+1$.
nr_paths	$\frac{time\_skip}{500}$	Number of different paths carved through the data in training and testing passes.
$return\_percentile$	90	Percentile filter applied to the distribution of returns in the dataset.
$failure$ / $safe$	0.8 / 2.0	Parameters used in normalizing the account size for the state signal and flagging terminal states.
$update\_q$	8	Number of observed transitions between gradient descent updates.
$update\_q^-$	5000	The frequency, in number of gradient descent updates, with which the target network Q^- is updated.
$\|\mathbb{S}\| = B$	60	Number of elements in minibatch used for gradient descent.
N	60000	Size of experience buffer from which minibatches are randomly drawn.
γ	0.99	Discount factor used in the Q-learning algorithm.
α	0.001	Learning rate used in the RMSProp algorithm.
ϵ_0 / ϵ_f	1 / 0.3	Initial and final value of the decaying ϵ in ϵ-greedy
$init\_acc\_size$	10000	Initial size of the trading account, in units of the base currency.
$position\_size$	10000	Number of units of base currency invested in each transaction.

Table 3.3: Hyper-parameters chosen for the trading system.

The hyper-parameters thus selected are detailed in Table 3.3, some of which merit some further discussion. The purpose of having distinct account size and position size parameters in the system is to allow for future implementation of a variable position size scheme to optimize profitability. Tests performed in chapter 4 do not include such optimization, thus we set $init\_acc\_size = position\_size$ so that profits can be easily interpreted in relation to the initial available capital, which was was given the placeholder value of 10,000. The RL discount rate parameter γ is close to 1, meaning future rewards are weighed heavily. This reflects the fact that a successful transaction requires future-oriented decision making. Parameter ϵ from ϵ-greedy action selection is made to decay over the training process so that the system takes advantage of acquired knowledge proportionally to the quality of that knowledge.

As for the parameter TW, the array whose elements are the beginning and ending of each window from which to extract features in number of ticks preceding the reference tick, the following values were selected:

$$TW = \begin{bmatrix} 0 & 1 & 2 & 3 & 4 & 5 & 6 & 7 & 8 & 9 & 10 & 60 \end{bmatrix} \cdot \frac{time\_skip}{2}$$

, thus defined to allow a seamless transition to other $time\_skip$ values. With that being said, in an ideal situation, TW would be re-optimized for different trading frequencies.

Using this hyper-parameter configuration on the datasets described in Table 3.2 yielded the learning curves shown in Figure 3.15. Three main observations can be made from these learning curves. Firstly,

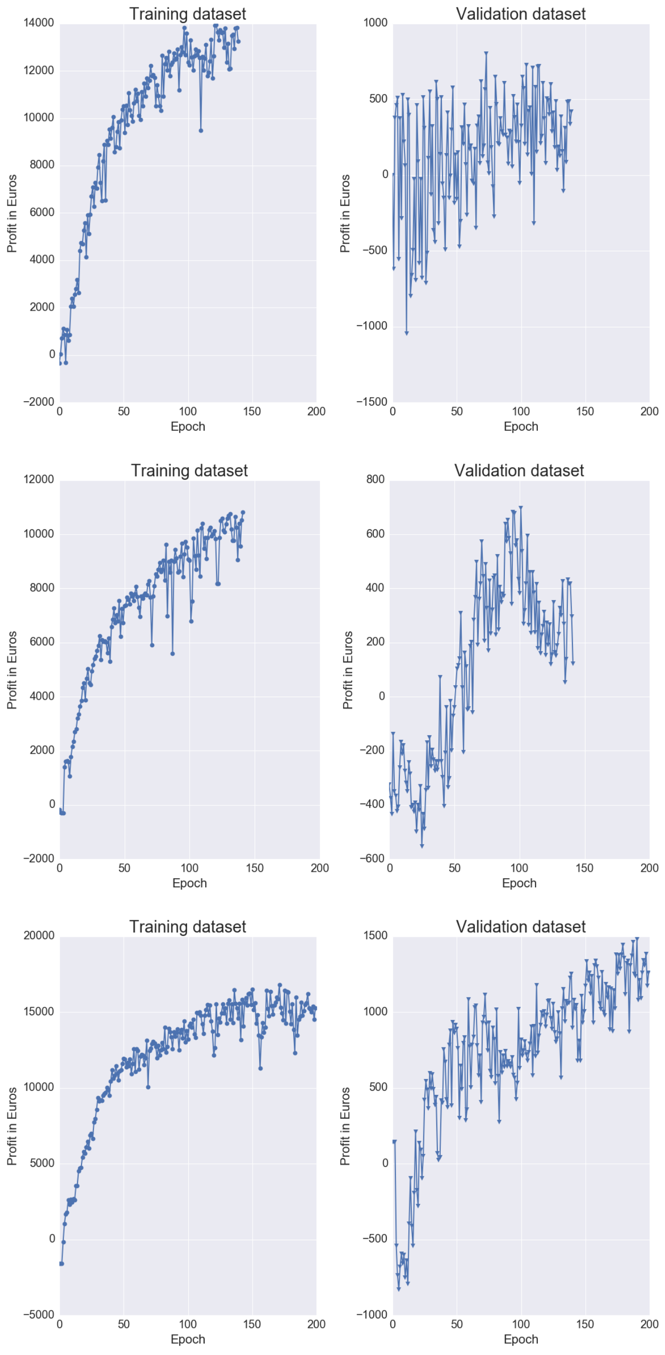

Figure 3.15: Learning curves for dataset A (top), B (middle) and C (bottom) with $position\_size = 10000$.

learning is strongly dataset dependent, clearly some datasets generalize better to their validation than others. In dataset A and B a peak validation profit of 795 ± 287[8] and 680 ± 233 is reached before learning is interrupted by the early stopping procedure. For dataset C on the other hand, a much higher validation profit of 1458 ± 260 is reached, and by the end of the preset 200 epochs limit the system still appeared

[8]Error bars are not included in the validation curves to avoid excessive cluttering.

to be learning with generalization, with the early stopping mechanism not being triggered.

Secondly, there is a clear overfit to the training dataset. If we take into account that the validation datasets are only 6 months long and thus extrapolate their results, we obtain yearly validation profitability of $15.9 \pm 5.74\%$, $13.6 \pm 4.6\%$ and $29.2 \pm 5.2\%$ for datasets A, B and C respectively while training profitability for those same datasets is 115.8 ± 6.4, 78.0 ± 3.9 and 179.7 ± 6.6. This was expected given the nature of financial data.

The third and most important remark, is that training the Q-network does in fact translate into improved out-of-sample financial performance over the epochs, otherwise the validation curve would simply be a random collection of points with no overarching positive direction. Knowing that our system is able to learn and that what it learns is reflected in out-of-sample data allows us to proceed and test the system on the previously vaulted data in an attempt to assess if it produces a positive expectation of financial performance.

Chapter 4

Testing

In this chapter we test our system, implemented as described in the previous chapter, on the EUR/USD currency pair. While performance on the validation dataset is a measure of generalization power, it cannot be used to estimate performance during actual live trading. During the training procedure we are observing the evolution of performance on the validation dataset, and purposefully choose the model that offers best performance. This is obviously not possible for live trading, there is only the chance to try one model. Thus, a test dataset is introduced to serve as an unbiased estimator of live trading performance. After the training procedure takes place, the model with the best generalization power as measured by the validation dataset is chosen and tested on the test dataset.

The premise is that a model that has learned to perform well on the training dataset and subsequently also performs well on a validation dataset, is more likely to then be profitable on the test dataset. However, markets are known to be non-stationary [49] and if market dynamics change too much from the training/validation period to the testing period, the model will not perform as expected.

While this risk is unavoidable, it can be ameliorated by having the training and validation dataset as temporally close as possible to the test dataset so that market conditions have a smaller chance to have significantly changed. To this effect, rather than simply dividing the whole span of the available data into a single training, validation and test dataset, we perform the tests using a rolling window as described in Figure 4.1.

Theoretically, the smaller we make each step forward of the rolling window, or in other words, the smaller we make the size of the test dataset, the better we tackle the non-stationarity issue. However, this does entail greater computational effort as a greater number of tests must be performed to cover the same amount of time. Considering the running time of each test with our resources, we decided on a test dataset size of 4 months.

The size of the training and validation datasets must also be considered. If they are smaller, the data the network learns (training dataset) and the filter through which the model is selected (validation dataset) should be more similar to the test dataset and thus suffer less from non-stationarity. On the other hand, since market data is remarkably noisy, if the training dataset is too small it will simply learn noise and lose generalization power, and if the validation dataset is too small, the overall performance

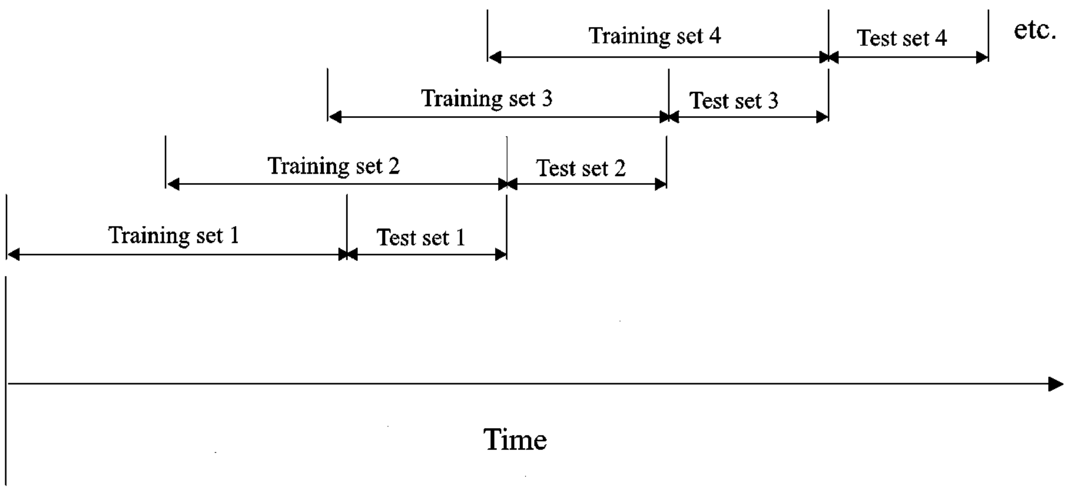

Figure 4.1: Rolling window approach to testing. Note that the training set includes both training dataset and validation dataset, while the test set is where the final model obtained with the training procedure is applied to assess its ”true” performance. [49]

on the dataset is more easily influenced by noisy unpredictable events and will tend to select models that randomly perform well on those events rather than those that truly generalize well. Moody [10] refers to these opposing effects as the noise/non-stationarity trade-off. A training and validation dataset size of 24 and 6 months was chosen through informal testing with data from the year 2013.

In section 4.1 we describe the results of testing the system on post-2008 crisis EUR/USD pair data: from 2010 to 2017. These tests are meant to assess the hypothetical validity of the trading system, to confirm it has a positive expectation of gain, rather than trying to accurately project its revenue potential. This means we are not trying to optimize execution: position sizing was set a priori and kept constant, and no stop-loss or take-profit orders were used. Also, while bid-ask spread commission is included, the volume commission is not, because the rates depend strongly on the specific trader’s resources.

4.1 5,000 time_skip

4.1.1 Results

Below are the results obtained by our Q-network trading system for the EUR/USD currency pair in the time period of 2010-2017 for $time\_skip = 5000$. In Table 4.1 each of the test datasets is described and in Figure 4.2 a portion of the learning curves responsible for the selection of the final model for each of the tests is displayed, with the rest included in appendix A.

A couple of exceptions to the standard size of 24 months of training and 6 months validation datasets were made. For the three 2010 test datasets we curtailed the training and validation dataset size to avoid including data from the 2008 crisis. For the 2011 p.3 test, the standard training/validation dataset size resulted in the learning curves depicted in Figure 4.3. The validation performance only worsens with training, making it difficult to select a candidate for testing. Simply halving the validation to a 3 month period solved this issue, suggesting a portion of the removed 3 months was incompatible with the training

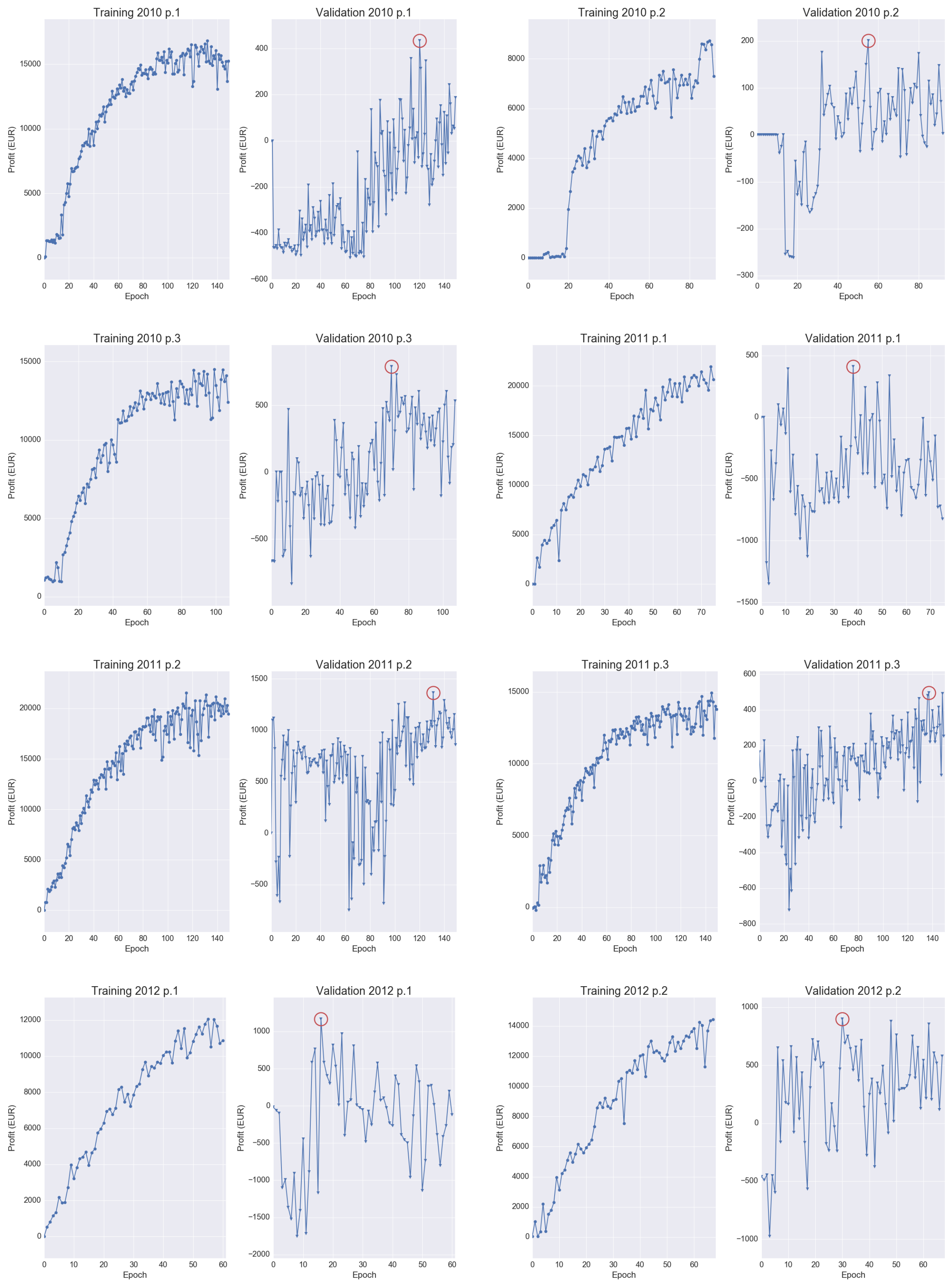

Figure 4.2: Learning curves for $time\_skip = 5000$. Red circle marks the chosen model. Remaining learning curves were placed in Appendix A.

Test Name	Begins	Ends	Nr. Ticks
2010 p.1	01/2010	05/2010	2,461,601
2010 p.2	12/2011	12/2011	2,475,378
2010 p.3	12/2012	12/2012	3,339,173
2011 p.1	01/2011	05/2011	6,564,138
2011 p.2	05/2011	09/2011	9,371,840
2011 p.3	09/2011	01/2012	9,866,644
2012 p.1	01/2012	05/2012	9,101,708
2012 p.2	05/2012	09/2012	8,497,184
2012 p.3	09/2012	01/2013	5,945,955
2013 p.1	01/2013	05/2013	7,013,688
2013 p.2	05/2013	09/2013	6,454,267
2013 p.3	09/2013	01/2014	5,945,955
2014 p.1	01/2014	05/2014	4,549,733
2014 p.2	05/2014	09/2014	4,932,296
2014 p.3	09/2014	01/2015	7,538,760
2015 p.1	01/2015	05/2015	8,237,522
2015 p.2	05/2015	09/2015	8,419,406
2015 p.3	09/2015	01/2016	7,532,748
2016 p.1	01/2016	05/2016	9,779,630
2016 p.2	05/2016	09/2016	15,969,628
2016 p.3	09/2016	01/2017	19,281,366

Table 4.1: A description of the test datasets. Each one is referred to by year followed by quadrimester.

dataset. The final exception was the 2016 p.2 test. Inspection of Table 4.1 shows there was a marked increase in tick density over the year 2016. We could not ascertain the reason for this increase, most likely an internal change in the broker's method of producing tick data. We halved the validation dataset size for the 2016 p.2 test to include, proportionally, more data with the altered tick density so it would select a candidate that performs well in these new conditions.

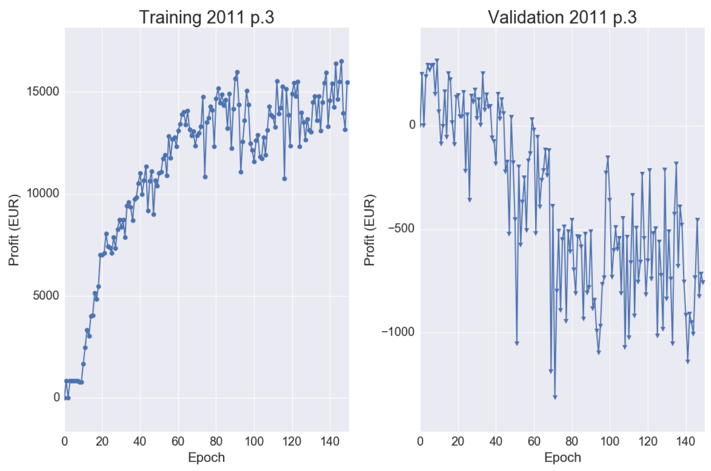

Figure 4.3: Learning curves for the 2011 p.3 test using the standard 24/6 months training/validation.

Choosing the candidate from each learning curve is straightforward for most cases, the one with best validation performance. But in a few cases we have to take into account validation performance peaks which arise from the fact that the neural network is randomly initialized and that learning with Q-networks is a noisy procedure, as exemplified by Figure 4.4, taken from the original Atari playing Q-network paper. This effect is exacerbated in the much noisier trading environment. Thus, to ensure the chosen model is the product of actual learning rather than random oscillations or initialization, we ignore the first 10 epochs as candidates for final model. This is relevant for the 2014 p.3, 2015 p.3 and 2016 p.3 curves and would have been in the case in 2011 p.1 and 2012 p.3 if the chosen peaks were slightly lower.

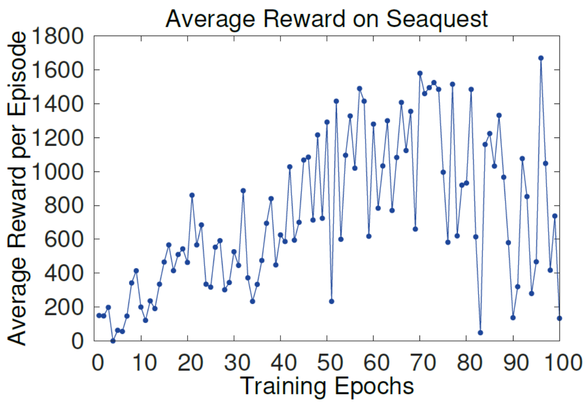

Figure 4.4: A Q-network's learning curve from the original Atari playing system on 'Seaquest'. [8]

Table 4.2 details the test results in both absolute profit and profit relative to the initial account size. Note that results shown are an average of 10 test passes from different initial points following the nr_paths methodology, and their uncertainty is the standard deviation over those passes.

Test Name	**Size (months)**		**Test Profit**	
	Training	Validation	Abs. (EUR)	Rel. (%)
2010 p.1	12	1	605±312	6.1±3.1
2010 p.2	12	1	159±368	1.6±3.7
2010 p.3	18	3	322±377	3.2±3.8
2011 p.1	24	6	1011±75	10.1±0.8
2011 p.2	24	6	36±228	0.4±2.3
2011 p.3	24	3	320±343	3.2±3.4
2012 p.1	24	6	70±87	0.7±0.9
2012 p.2	24	6	323±218	3.2±2.2
2012 p.3	24	6	-327±78	-3.3±0.8
2013 p.1	24	6	388±231	3.9±2.3
2013 p.2	24	6	342±173	3.4±1.7
2013 p.3	24	6	434±69	4.3±0.7
2014 p.1	24	6	249±70	2.5±0.7
2014 p.2	24	6	296±141	3.0±1.4
2014 p.3	24	6	841±51	8.4±0.5
2015 p.1	24	6	767±36	7.7±0.4
2015 p.2	24	6	131±112	1.3±1.1
2015 p.3	24	6	328±227	3.3±2.3
2016 p.1	24	6	962±131	9.6±1.3
2016 p.2	24	3	-264±311	-2.6±3.1
2016 p.3	24	6	-212±222	-2.1±2.2

Table 4.2: Overview of the test results for $time\_skip = 5000$.

The system is profitable in all but three tests, 2012 p.3, 2016 p.2 and 2016 p.3, although in two other cases, 2011 p.2 and 2012 p.1, it just about breaks even. This means it generated significant profit in roughly 75% of the tests, and significant losses in only 14%, a good indicator of its validity.

The simple and compounded total test results are concisely described in Table 4.3. By simple, we mean that profits are not reinvested, after each test whatever profits there may be are put aside and the following test starts from the same initial conditions. From a financial perspective, investments are more often judged based on their compounded profit. Some trading systems use continuous compounding, by including profits from a given trade in the position size of the next trade. We chose to use a fixed position size during each test and compound between tests, ie. change the fixed position size at the onset of a test by including the total profit of the previous tests in the account. Compounding increases the overall profit, but also increases uncertainty ie. the risk of the trading system.

Compounding	Total Absolute Test Profit (EUR)	Total Relative Test Profit (%)	Yearly Avg. Test Profit (%)
None	6782±977	67.8±9.8	9.7±1.4
Yearly	8982±1690	89.8±16.9	12.8±2.4
Triannual	9247±1802	92.5±18.4	13.2±2.6

Table 4.3: Simple and compounded total test profit for $time\_skip = 5000$.

In Table 4.4 we look at the trades individually for a better insight into the behaviour of the system. It is apparent that the system generally relies on a large number of small trades, roughly 550 trades per year with 0.2% profit/loss per trade, which are profitable 53.5% of the time. There is a very slight tendency to favor the Short position in general, especially in trades that end up being profitable. This can be explained by looking at the plot of EUR/USD prices in Figure 4.6, the Euro has on average been losing value relative to the Dollar. The duration that each position stays open is similar in both profitable and unprofitable trades, showing that the system has no problem cutting its losses and does not overly wait for rebounds.

	Trades		
	Total	Profitable	Unprofitable
Nr.	39287	21038	18249
Avg. profit (%)	0.017±0.384	0.215±0.337	-0.211±29.9
Avg. Duration	34788±87867	33679±96107	36066±77264
% Longs	49.2	48.8	49.6

Table 4.4: Trade-by-trade analysis for $time\_skip = 5000$. Note that trades from all 10 paths are included. Duration is in number of ticks.

Figure 4.5 provides a sample of the system's behavior in three different tests. For the most part the system behaves as described, small trades in large numbers. However, that appears to change when it detects a trend, switching to larger trade durations in a attempt to follow that trend, as observed 2011

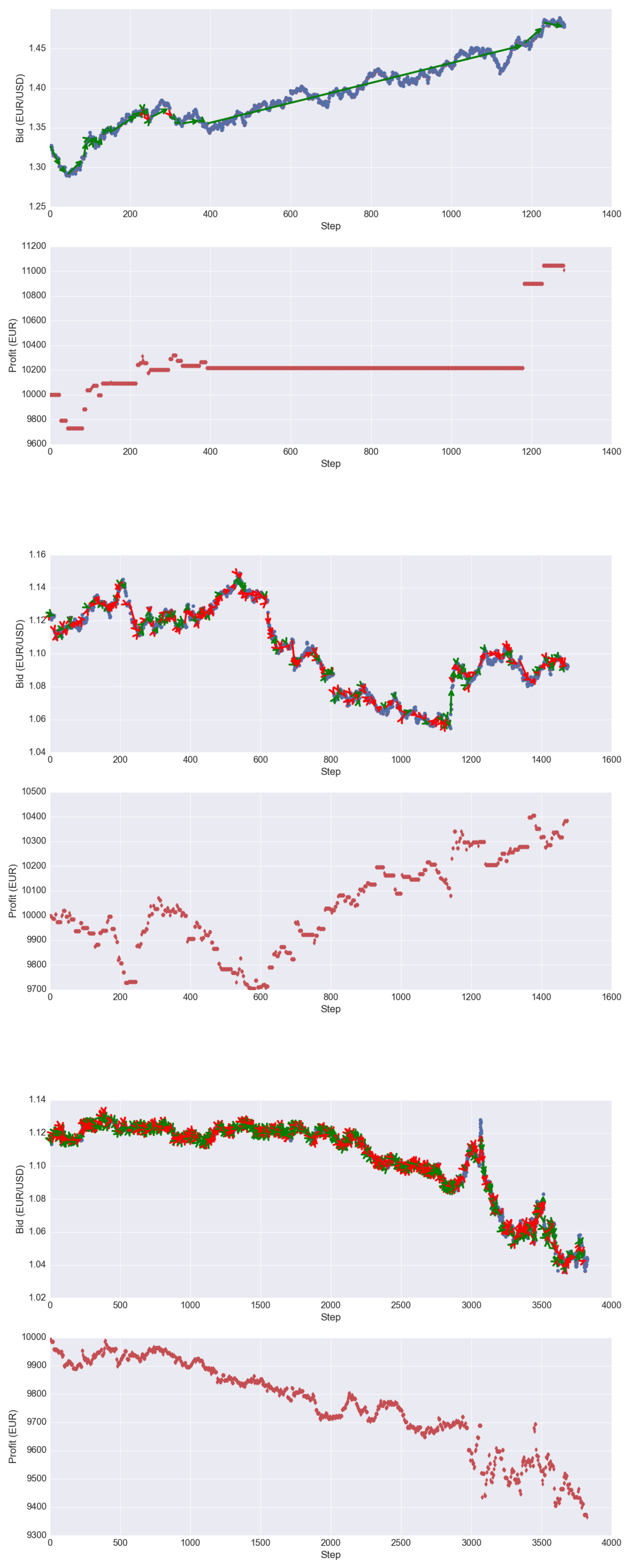

Figure 4.5: System behaviour from 2011 p.1 (top), 2015p.3 (middle) and 2016 p.3 (bottom). Green and red arrows represent Long and Short positions respectively. Each step is 5,000 ticks apart.

p.1. In 2016 p.3 we can see how it displays an unusually large number of trades, leading to a gradual accumulation of losses.

4.1.2 Result Analysis

In this section we take a closer look at the results presented above. We start by looking at the relationship between validation and test performances. To that effect Table 4.5 contains the annualized results for each validation/testing dataset pair. Annualized profit is an extrapolation of the profit obtained in a dataset to what they would be over a year, assuming the same rate of gains, meant to allow comparisons between datasets of different sizes.

Test Name	Validation Profit		Test Profit	
	Abs. (EUR)	Annualized	Abs. (EUR)	Annualized
2010 p.1	441±173	52.9±20.8%	605±312	18.2±9.4%
2010 p.2	200±117	24.0±14.0%	159±368	4.8±11.0%
2010 p.3	806±320	32.2±12.8%	322±377	9.7±11.3%
2011 p.1	409±408	8.2±8.2%	1011±75	30.3±2.3%
2011 p.2	1387±211	27.7±4.2%	36±228	1.1±6.8%
2011 p.3	495±320	19.8±12.8%	320±343	9.6±10.3%
2012 p.1	1166±169	23.3±3.4%	70±87	2.1±2.6%
2012 p.2	897±184	17.9±3.7%	323±218	9.7±6.5%
2012 p.3	655±213	13.1±4.2%	-327±78	-9.8±2.3%
2013 p.1	655±234	15.6±4.7%	388±231	11.6±6.9%
2013 p.2	520±151	10.4±3.0%	342±173	10.3±5.8%
2013 p.3	643±231	12.8±4.6%	434±69	13.0±2.1%
2014 p.1	196±38	3.9±0.8%	249±70	7.5±2.1%
2014 p.2	748±145	15.0±2.9%	296±141	8.9±4.2%
2014 p.3	461±89	9.2±1.8%	841±51	25.2±1.5%
2015 p.1	1189±51	23.8±0.1%	767±36	23.0±1.1%
2015 p.2	1267±76	25.3±1.5%	131±112	3.9±3.4%
2015 p.3	-57±306	-1.1±6.1%	328±227	9.8±6.8%
2016 p.1	745±210	14.9±4.2%	962±131	28.9±3.9%
2016 p.2	921±140	27.6±4.2%	-264±311	-7.9±9.3%
2016 p.3	275±421	5.5±8.4%	-212±222	-6.4±6.7%

Table 4.5: Comparison between validation and test results for $time\_skip = 5000$.

As expected, validation performance is for the most part superior to subsequent test performance. Furthermore, simple observation of Table 4.5 seems to suggest that validation profit is not a good predictor of test profit. This is confirmed by a Pearson correlation coefficient of -0.28 at p-value significance of 0.2, indicating no correlation between annualized validation and test profits. It is clear that the training process creates a positive expectation for profits in a test setting, but results are too dataset dependent to create an expectation on the magnitude of those profits.

On the other hand, the standard deviation between different paths obtained by the model in the validation dataset compared to that of the test dataset has a Pearson correlation coefficient of 0.73 with p-value significance 0.0002. This means that we can actually select stabler candidates based on the validation process. Considering our total profit, with triannual compounding, has an uncertainty of almost 20%, our choice of candidate solely through peak validation performance was misguided, and exploring this correlation could be an important avenue for improving the system's performance.

We continue our result analysis by looking at equity growth trajectory. By equity we mean the current size of the account plus the value of any currently open positions, relative to the initial account size. As important as the final profit is, it is equally important the manner in which that profit level is reached. If equity grows smoothly the risk the trading system presents is lower and the use of leverage can be considered. On the other hand, if the equity growth curve contains large, frequent drawdowns, our confidence in the trading system diminishes and the use of leverage must be kept to a minimum or none at all. Drawdown is the difference between the equity size at a certain point and the size at the last equity peak. It is one of the main measures of risk in financial trading. A drawdown of just 20% would empty a trader's account if he were to be using $L = 5$ leverage. Figure 4.6 shows the equity curve obtained by our system, with the bid price over the 7 years of testing for context.

The equity curve is somewhat regular, with no extreme drawdowns at any point. This is made more clear with Figure 4.7, which displays all drawdowns graphically, and Table 4.6 which discretizes the maximum drawdown for each year along with that year's test profit. The maximum drawdown was -9.9±12.1, without compounding, and -16.6±20.0% with triannual compounding. These are relatively low values, albeit with a large uncertainty due to how uncertainty is propagated, accumulating the uncertainty from both the peak and the drought. This amount of drawdown would allow for a comfortable use of leverage $L = 2$, which would have doubled our final profit.

Year	**Test Profit**		**Maximum Drawdown**	
	Abs. (EUR)	Rel. (%)	Abs. (EUR)	Rel. (%)
2010	1086±612	10.9±6.1%	-365±7270	-3.7±7.3
2011	1367±419	13.7±4.2%	-825±1060	-8.2±10.6
2012	66±247	0.7±2.5%	-900±1104	-9.0±11.0
2013	1164±297	11.6±3.0%	-332±1115	-9.9±11.2
2014	1386±165	13.9±1.7%	-258±1206	-2.6±12.1
2015	1226±256	12.3±2.6%	-987±1213	-9.9±12.1
2016	487±404	4.9±4.0%	-790±1359	-7.9±13.6

Table 4.6: Simple yearly profit and maximum drawdown for $time\_skip = 5000$.

It is hard to pin point the exact reasons why the year of 2012 stands apart from the the others in terms of performance since a Q-network is a black box system. However, a closer look at Figure 4.6 can provide some speculation. Note that in 2012 there is for the most part no overall trend to the price

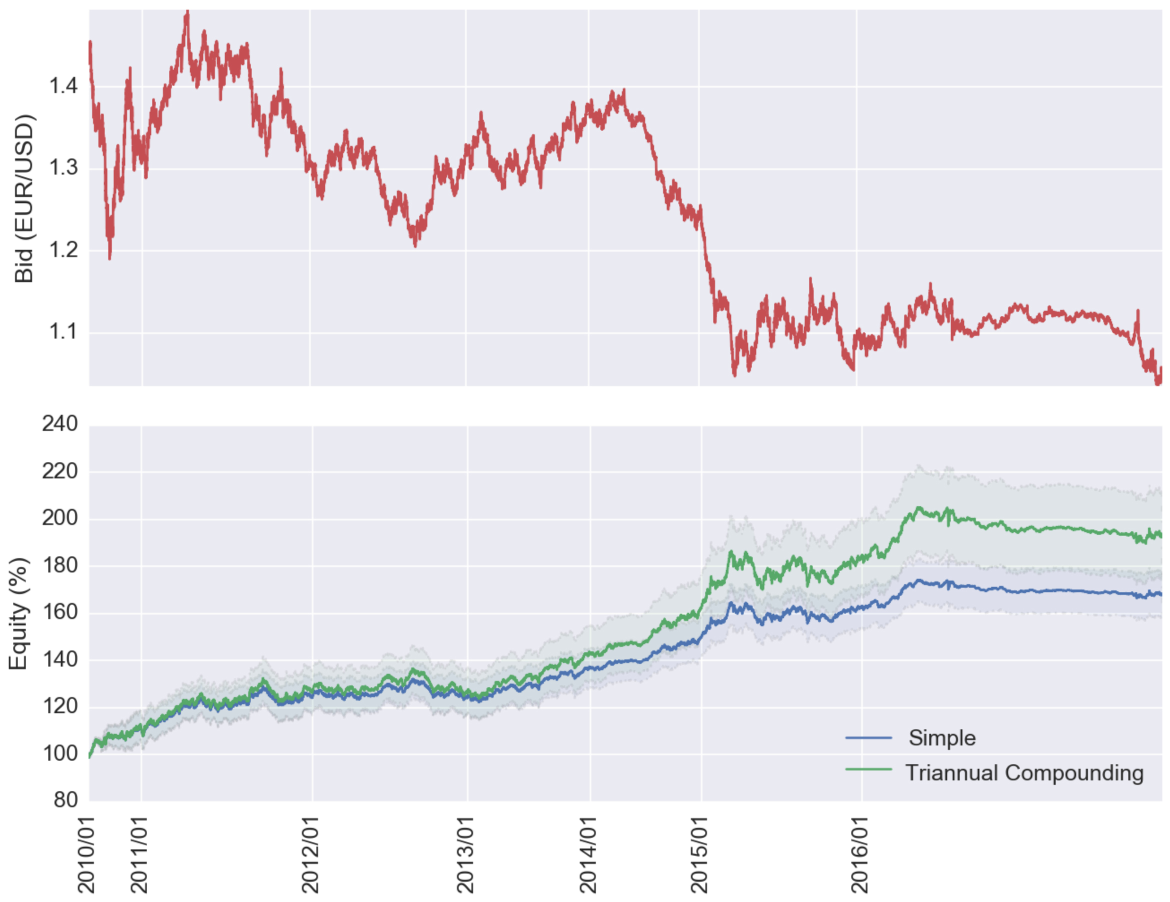

Figure 4.6: Bid prices for EUR/USD pair (top) and equity growth curve with and without compounding (bottom) for $time\_skip = 5000$. Light area around equity curves represents their uncertainty. X-axis is in units of ticks.

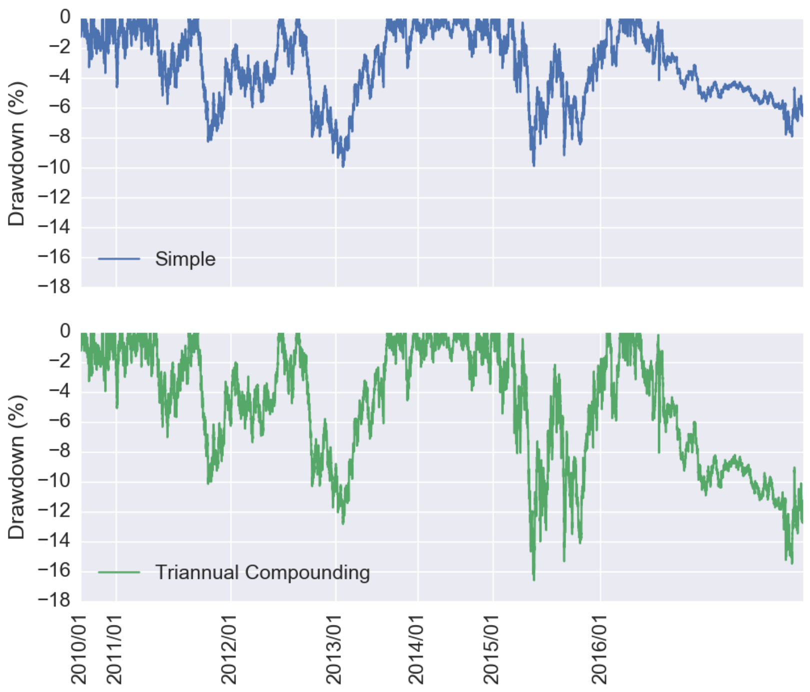

Figure 4.7: Average drawdowns for $time\_skip = 5000$, uncertainty was not included for clarity. X-axis is in units of ticks.

changes, it mostly fluctuates inside a range and finishes the year close to the same value where it starts. There is an exception in the middle of the year with a downwards trend followed by an upwards trend where the equity grows, but it accumulates losses again with the sideways movement at the end of the year. We can observe that this is mirrored in the year 2011 and 2015. While they are overall successful years, those profits come from the beginning and the end of the year where there are clear trends. In the middle part of both those years, where there is mostly sideways movement, there is little to no equity growth. Possibly, when the market has a clear downward or upward trend there are distinguishing patterns in the input features that allow exploitation, while more indecisive sideways periods result in noisier inputs and poorer decisions.

The problem with the two final datasets, 2016 p.2 and 2016 p.3, is slightly different. While there is also the problem of a mostly sideways moving market, it is exacerbated by the change in tick density by the broker. Due to how our system is designed, larger tick frequency leads to larger trading frequency, as Figure 4.5 showed. Thus, we have a system forced to trade much more frequently than intended in a market context where it has been shown to struggle, which unsurprisingly results in losses.

This could be easily corrected by increasing the $time\_skip$ parameter to 10,000 once the larger tick frequency was detected. Rather than repeating only these two tests with $time\_skip = 10000$ we decided to experiment with the rest as well. The reason for these tests is two-fold, firstly it serves as another test to the system's capabilities, should it obtain positive performance working under conditions it was not optimized for, system's validity is further supported. Secondly, in 2010 the tick density is roughly half the rest of the datasets and the system performed well, which may indicate lowering trading frequency could be beneficial.

4.2 10,000 time_skip

For these tests with $time\_skip = 10000$, training and validation datasets as well as all other hyper-parameters were unchanged from the previous approach. The exception is the nr_paths parameter which was defined in the previous chapter to keep the distance between paths at 500 ticks, and thus also doubles to $nr\_paths = \frac{10000}{500} = 20$.

4.2.1 Results

Figure 4.8 shows a portion of the learning curves responsible for the selection of the final model for each of the tests, with the rest included in the appendix A. These learning curves were obtained using the same training and validation datasets from the $time\_skip = 5000$ tests. The only difference is that the year of 2010 is not included. Those tests used a much smaller training dataset to avoid 2008 data. Furthermore this older data has less tick density. It was thus observed that, even with the nr_paths dynamic, there was difficulties in training the network at the $time\_skip = 10000$ frequency due to insufficient datapoints.

In choosing the candidate from these learning curves the same consideration explained subsection 4.1.1

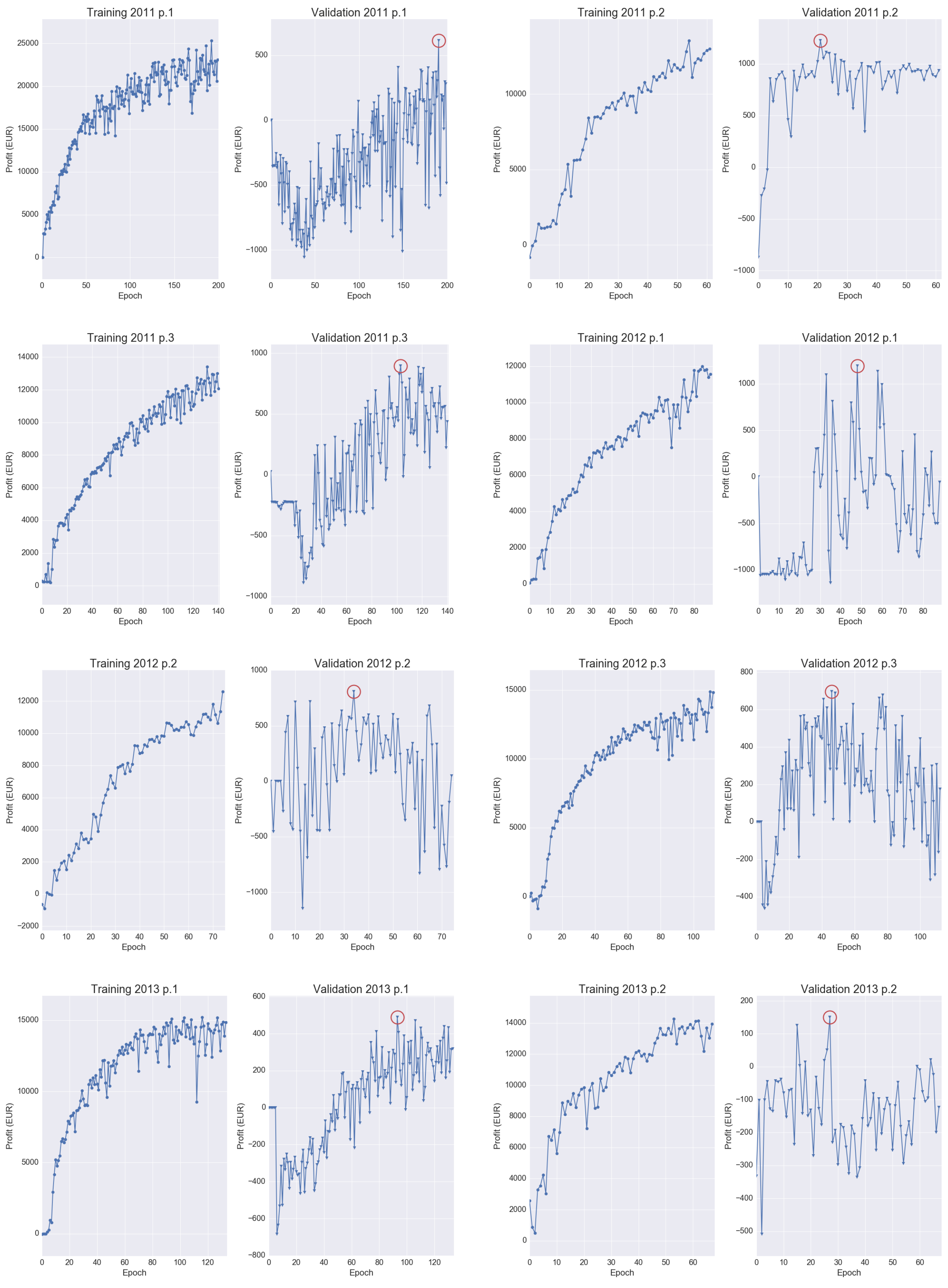

Figure 4.8: Learning curves for $time\_skip = 10000$. Red circle marks the chosen model. Remaining learning curves were placed in Appendix A, as appendix.

Test Name	**Size (months)**		**Test Profit**	
	Training	Validation	Abs. (EUR)	Rel. (%)
2011 p.1	24	6	1021±83	10.2±0.8
2011 p.2	24	6	-123±137	-1.2±1.4
2011 p.3	24	3	-26±364	-0.3±3.6
2012 p.1	24	6	58±299	0.6±3.0
2012 p.2	24	6	450±318	4.5±3.2
2012 p.3	24	6	-341±105	-3.4±1.1
2013 p.1	24	6	225±89	2.3±8.9
2013 p.2	24	6	485±181	4.9±1.8
2013 p.3	24	6	399±7	4.0±0.1
2014 p.1	24	6	173±47	1.7±0.5
2014 p.2	24	6	-392±61	-3.9±0.6
2014 p.3	24	6	722±76	7.2±0.8
2015 p.1	24	6	412±199	4.1±2.0
2015 p.2	24	6	143±258	1.4±2.6
2015 p.3	24	6	268±255	2.7±2.6
2016 p.1	24	6	445±276	4.5±2.8
2016 p.2	24	3	251±220	2.5±2.2
2016 p.3	24	6	337±198	3.4±2.0

Table 4.7: Overview of the testing procedure results for $time\_skip = 10000$.

applied in the case of 2016 p.3. Note that the disregarded validation performance peak in this case is slightly out of the 10-epoch range we defined. Since each epoch contains a single learning pass, and each pass with $time\_skip = 10000$ is smaller than $time\_skip = 5000$, it is actually within the range in the measure that truly counts: amount of updates to the network. This is probably the same reason why most learning curves with $time\_skip = 10000$ appear better behaved than their $time\_skip = 5000$ counterparts, each epoch or point in the graph represents a smaller number of updates smoothing the behavior changes between epochs.

Table 4.7 details the performance obtained in both absolute profit and profit relative to the initial account size. Considering that 2011 p.3 and 2012 p.1 just about break even, the system generated significant profit in roughly 72% of the tests and significant losses in 16%. Once again, these numbers suggest the validity of our trading system.

The simple and compounded total test results are concisely described in Table 4.3. Overall the results are frankly inferior to the previous trading frequency, which is not particularly unexpected considering the whole system was optimized with $time\_skip = 5000$ in mind. But they are nevertheless positive, 9.1±1.9% per year is still superior to most available financial applications.

With Table 4.4 we look at the trades individually while Figure 4.9 provides a sample of the system's behavior in three different tests. The system behaves very similarly to the $time\_skip = 5000$ case, with two key differences. As expected the duration of each trade is roughly double that of the $time\_skip =$

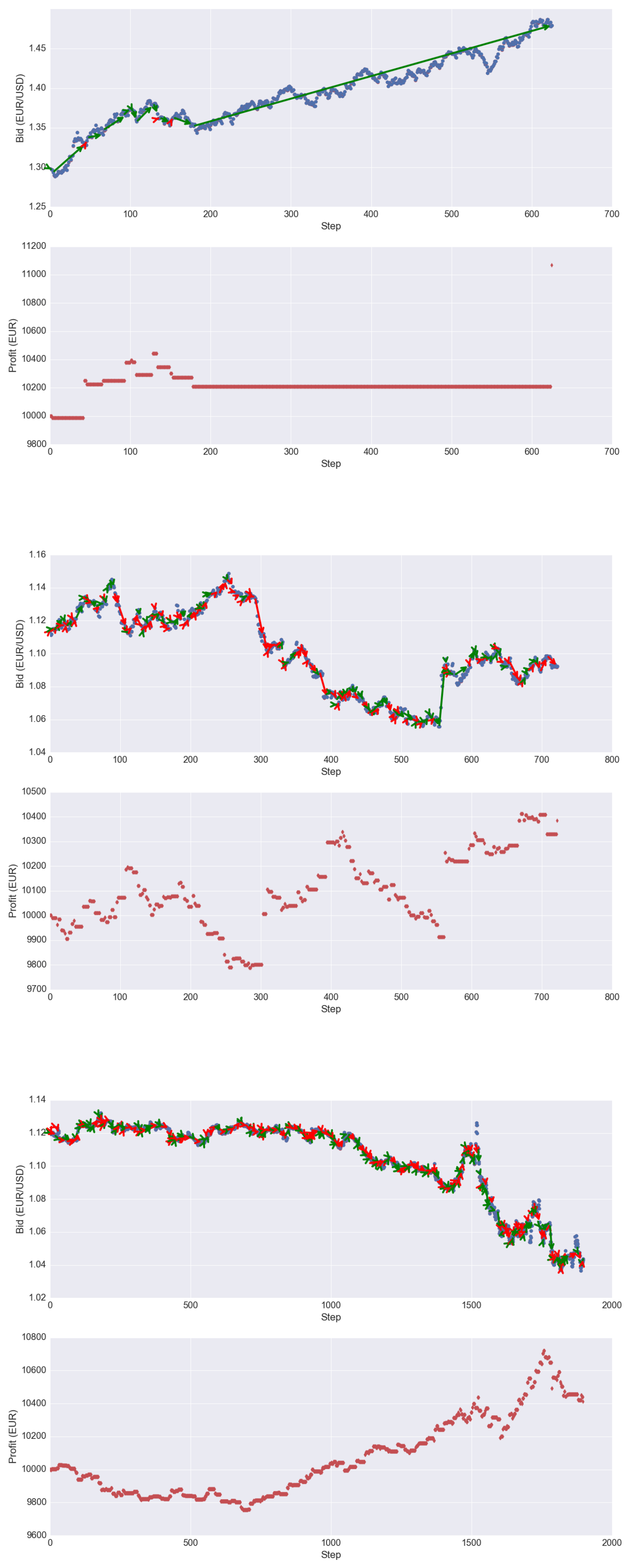

Figure 4.9: System behaviour from 2011 p.1 (top), 2015p.3 (middle) and 2016 p.3 (bottom). Green and red arrows represent Long and Short positions respectively. Each step is 10,000 ticks apart.

Compounding	Total Absolute Test Profit (EUR)	Total Relative Test Profit (%)	Yearly Avg. Test Profit (%)
None	4507±864	45.1±8.6	7.5±1.4
Yearly	5400±1244	54.0±12.4	9.0±2.1
Triannual	5457±1140	54.6±11.4	9.1±1.9

Table 4.8: Simple and compounded total test profit for $time\_skip = 10000$.

5000 system, which results in a larger average profit/loss per trade. And the total number of trades is also roughly halved. With 2016 p.3 its seems that solving its excessive number of trades allowed the system to become profitable once the market stopped moving sideways. The tendency to favor the Short position is also more pronounced with this trading frequency. As we mentioned before, the overall trend of EUR/USD has been for the Euro to lose value, and the overall trend becomes more important at lower trading frequencies, which explains this growing asymmetry.

	Trades		
	Total	Profitable	Unprofitable
Nr.	34445	17923	16522
Avg. profit (%)	0.026±0.517	0.299±0.471	-0.270±0.385
Avg. Duration	74364±220261	79445±263958	68852±159697
% Longs	47.2	47.4	46.9

Table 4.9: Trade-by-trade analysis for $time\_skip = 10000$. Note that trades from all 20 paths are included. Duration is the number of ticks during which a position was kept open.

4.2.2 Result Analysis

Table 4.5 contains the annualized results for each validation/testing dataset pair. The relationship between validation and test performances observed with $time\_skip = 5000$ still holds for this new trading frequency. There is a Pearson correlation coefficient of -0.31 at p-value significance of 0.21, once again indicating that validation performance is not a good predictor of test performance. A correlation coefficient of 0.67 at p-value significance of 0.002 for the uncertainties confirms the possibility of selecting stabler candidates based on the validation process.

There is a significant correlation between validation performance from both trading frequencies, Pearson coefficient of 0.65 with 0.004 significance, and testing performance from both trading frequencies, with a coefficient of 0.66 at 0.003 significance. This once again suggests that some datasets, ie. some time periods of market behaviour, are inherently more predictable from technical data than others, which is why test performance cannot be predicted by validation performance.

We continue our result analysis by looking at equity growth trajectory. Figure 4.6 shows the equity

Test Name	Validation Profit		Test Profit	
	Abs. (EUR)	Annualized	Abs. (EUR)	Annualized
2011 p.1	613±233	12.3±4.7	1021±83	30.6±2.5
2011 p.2	1225±264	24.5±5.3	-123±137	-3.7±4.1
2011 p.3	893±279	35.7±11.2	-26±364	-0.8±10.9
2012 p.1	1191±294	23.8±5.9	58±299	1.7±9.0
2012 p.2	807±196	16.1±3.9	450±318	13.5±9.5
2012 p.3	695±235	13.9±4.7	-341±105	-10.2±3.2
2013 p.1	488±247	9.8±4.9	225±89	6.8±2.7
2013 p.2	150±213	3.0±4.3	485±181	14.6±5.4
2013 p.3	442±116	8.8±2.3	399±7	12.0±0.2
2014 p.1	778±82	15.6±1.6	173±47	5.2±1.4
2014 p.2	474±110	9.5±2.2	-392±61	-11.8±1.8
2014 p.3	438±107	8.8±2.1	722±76	21.7±2.3
2015 p.1	1139±129	22.8±2.6	412±199	12.4±6.0
2015 p.2	1232±175	24.6±3.5	143±258	4.3±7.7
2015 p.3	820±434	16.4±8.7	268±255	8.0±7.7
2016 p.1	822±312	16.2±6.2	445±276	13.3±8.3
2016 p.2	900±145	27.0±4.4	251±220	7.5±6.6
2016 p.3	397±315	7.9±6.3	337±198	10.1±5.9

Table 4.10: Comparison between validation and test results.

curve obtained by our system, with the bid price over the 6 years of testing for reference. The equity curve confirms our previous observations that the system has its worst periods when the market is moving sideways. This is clear in the middle of 2011, in 2012 with the exception of some growth when there are clear trends in the middle, in the middle of 2015 and in the middle of 2016. The big difference is that during the middle of 2016 it is no longer forced to trade at double the desired frequency, thus it manages to break even rather than accumulate losses, and then make some gains at the end of the year when a trend emerges.

Figure 4.7 displays all drawdowns graphically. Overall the drawdowns are very similar in magnitude to the higher frequency system. The maximum drawdown was -10.9±4.2%, without compounding and -11.9±4.5% with triannual compunding. The uncertainty is much smaller since the largest drawdown occurs near the beginning of the equity growth curve, before the possible paths have diverged too much. Again, these are low values which would probably allow for the use of a small amount of leverage.

To conclude this analysis, we look to the main motivation of testing the system with $time\_skip = 10000$, the two final datasets where tick density doubles. In Figure 4.12 we depict the equity growth

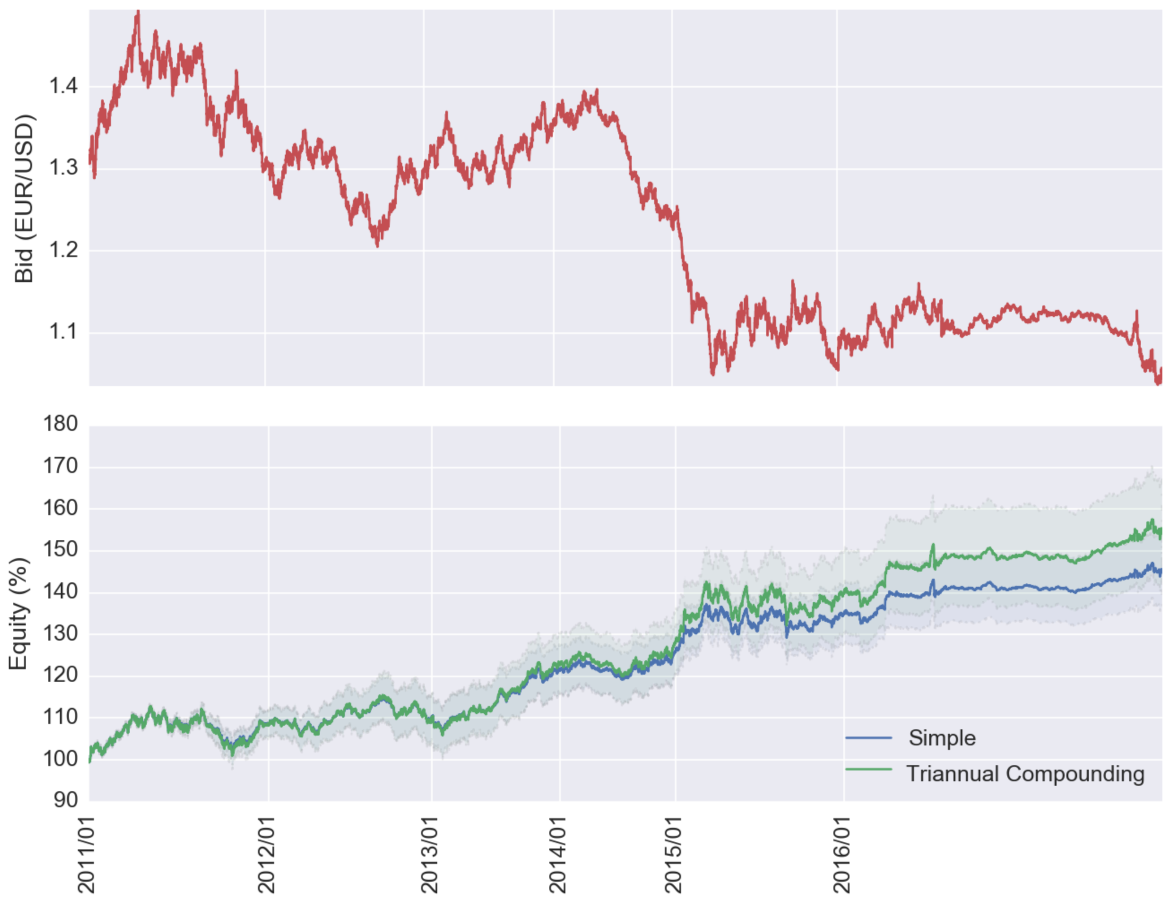

Figure 4.10: Bid prices for EUR/USD pair (top) and equity growth curve with and without compounding (bottom) for $time\_skip = 10000$. Light area around equity curves represents their uncertainty. X-axis is in units of ticks.

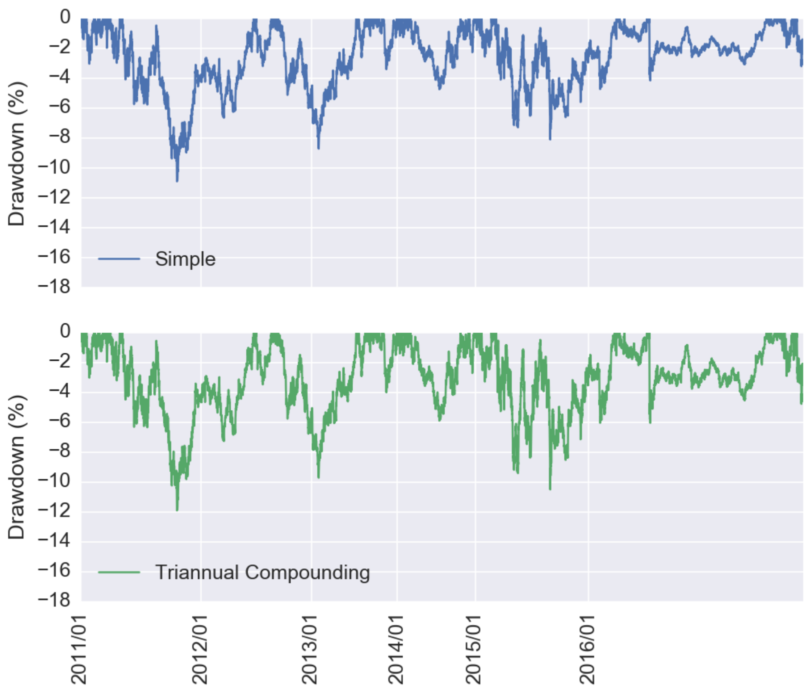

Figure 4.11: Average drawdowns for $time\_skip = 10000$, uncertainty was not included for clarity. X-axis is in units of ticks.

curve of an approach where the original $time\_skip = 5000$ is mixed with $time\_skip = 10000$ for the last two datasets.

Table 4.11 further describes the results that this approach yields. We consider these results a realistic depiction of what the trading system designed in this thesis would have obtained. It is only natural that upon realizing the change in tracking tick data by the broker, $time\_skip$ would be accordingly adjusted to maintain a trading frequency that had so far yielded results.

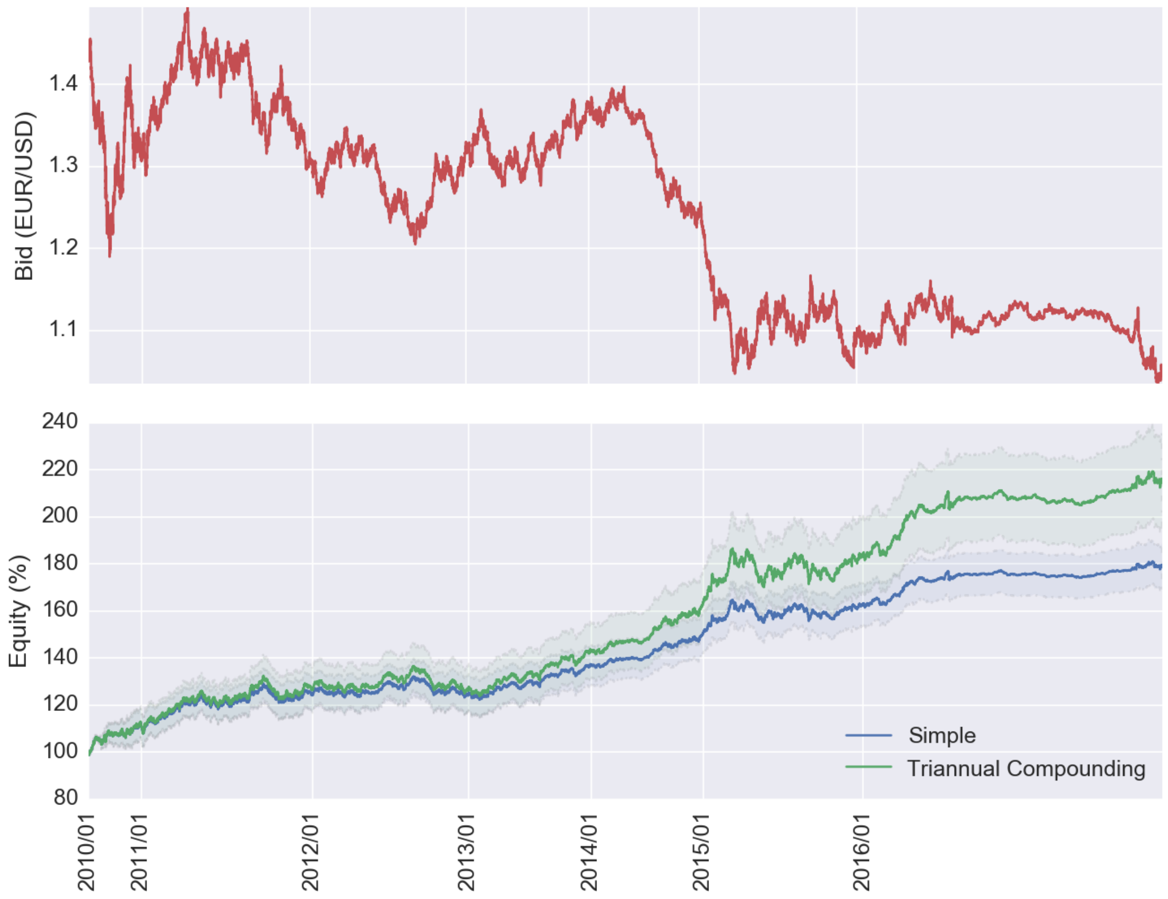

Figure 4.12: Bid prices for EUR/USD pair (top) and equity growth curve with and without compounding (bottom) for a mix of 5,000 and 10,000 $time\_skip$. Light area around equity curves represents their uncertainty. X-axis is in units of ticks.

Compounding	Total Absolute Test Profit (EUR)	Total Relative Test Profit (%)	Yearly Avg. Test Profit (%)
None	7845±947	78.5±9.5	11.2±1.4
Yearly	10906±1777	109.1±17.8	15.6±2.5
Triannual	11399±1964	114.0±19.6	16.3±2.8

Table 4.11: Simple and compounded total test profit for a mix of 5,000 and 10,000 $time\_skip$.

Chapter 5

Conclusions

The main goals of this thesis were achieved. Learning in the training dataset is stable and it is apparent from a number of validation learning curves that the Q-network is indeed capable of finding relationships in financial data that translate to out-of-sample decision making. This speaks to the potential of the neural network / reinforcement learning combo: this noisy, non-stationary environment is a far cry from the deterministic Atari or Go environments, and still it was capable of learning performing policies. Furthermore, this learning capability was successfully leveraged to produce positive financial gain in a test setting.

It is difficult to compare our results with those obtained by other RL systems, being that there so few examples of RL traders applied to the foreign exchange. In Table 3.2, the only RL system that uses a modern dataset obtained a 1.64% profit for the year of 2014. For that same year we obtained 13,86% without compounding. As for the remaining three systems, all RRL traders, our profitability is somewhat in line with their results. Our results were obtained in a more challenging context however. Firstly our tests cover a much much larger timeframe, which requires a more robust system that performs well under a variety of market conditions. Secondly, as we saw in subsection 2.1.1, various sources indicate that profitability derived from technical analysis methods has been declining sharply. These RRL traders were tested with datasets ranging from 1996 to 2002, while our system was tested on contemporary datasets.

However, it is not an approach that works well ”out-of-the-box”, we found it is not very robust at all. Without a preprocessing stage and state function that ensured all inputs were within a contained range, learning did not happen. Before ensuring outliers did not distort input variable distribution, learning was unstable and out-of-sample performance was inconsistent, almost random. Reward normalization was also essential, many attempts resulted in unstable or non-existent learning. Although RMSProp gives it some robustness in terms of the learning rate parameter, other parameters concerning the network updates such as the batch size, frequency of the updates of the target network or size of the buffer all can easily derail learning if not appropriately set. Overall, it is a finicky, labour-intensive architecture.

Another drawback of this architecture, is that despite its success, it is difficult to extract insights as it is very much a black-box approach. The final product is a trained network that provides no equations or coefficients defining a relationship, beyond it's own internal mathematics. The network *is* the final equation of the relationship. It should be seen as an engineer's tool, something with which to obtain results since although there are efforts to 'gray the black-box' [54], for the most part neural networks with more than a couple of layers are as of now too complex to extract accurate insights. But the architecture's complexity may actually have played in its favour for this task. In subsection 2.1.1 we have seen that there is somewhat of a consensus that potential profitability from technical analysis methods has decreased over time, but more complex technical rules were more resistant to this efficiency of the market. A network with three hidden layers such as ours has the potential to create fairly complex internal technical rules, which may account for its continued profitability.

Overall, it is my opinion that this approach has a great deal of potential to be explored. There are a number of probably sub-optimal parameters, chief among them the TW parameter controlling feature extraction and the topology of the hidden layers. Furthermore there are design options, such as choice of cost function or activation function of the hidden layers, that were not fully explored due to lack of computational power to test configurations. These relatively small changes would certainly provide a performance boost without even changing the overall architecture laid out in this thesis. In section 5.1 more in depth changes are discussed.

5.1 Future Work

Besides the already discussed incomplete optimization, there are two main weaknesses in this trading system that should merit further work. Both concern how the displayed capacity to improve out-of-sample performance by training can be turned into a profitable trading system in a test setting:

- Traning/validation/testing dataset choice: a more interesting alternative based on identifying market regimes, for example, could be conjectured. Otherwise, our fixed size approach could be improved by exhaustive search rather than our limited informal testing.

- Model candidate selection: our approach to choose the model with highest validation performance was already shown to be overly simplistic in subsection 4.1.2, where it became clear that the uncertainty the model presents in the validation dataset should have been taken into account. The inclusion of this extra factor in the selection process would be a start, but more complex selection methods could be tested. For example, rather than using just one candidate the trading account could be split among a number of candidates which would help dilute the risk through diversification.

Other than changes to the system itself, some possible future work could focus on improving the financial facets of this work:

- Other types of financial data: the use of data classified as fundamental analysis, or simply market data from other assets that correlate to the target asset, could improve performance. This would not be a straightforward change however. Each extra input variable makes it easier for the system to overfit the training data. We struggled in this thesis to achieve a balance between the neural network's power and the number of input variables to prevent, in so far as possible, overfitting. Any additions to the input would have to contribute enough to overcome the extra overfit potential, and would probably entail finding a new balance with neural network topology.

- Diversification: this is the most straightforward avenue for further work. There is no reason, in theory, for this system not to work with other assets now that it has been shown to work with EUR/USD, although it would almost certainly entail parameter re-optimization. These could be other currencies or other financial objects altogether, from stocks to commodities, as long as there is a large quantity of historical data for training.
- Execution: a layer for optimized execution could be added to control risk and maximize profitability using, for example, variable position sizing and stop-loss/take-profit orders.

Bibliography

[1] A. P. Chaboud, B. Chiquoine, E. Hjalmarsson, and C. Vega. Rise of the machines: Algorithmic trading in the foreign exchange market. *The Journal of Finance*, 69(5):2045–2084, Oct. 2014.

[2] B. for International Settlements. Foreign exchange turnover in april 2016. *Triennial Central Bank Survey*, Sept. 2016.

[3] T. M. Mitchell. The discipline of machine learning. *SCS Technical Report Collection*, July 2006.

[4] Y. LeCun, B. Boser, J. S. Denker, D. Henderson, R. E. Howard, W. Hubbard, and L. D. Jackel. Backpropagation applied to handwritten zip code recognition. *Neural Computation*, 1(4):541–551, Mar. 1989.

[5] J. Stallkamp, M. Schlipsing, J. Salmen, and C. Igel. Man vs. computer: Benchmarking machine learning algorithms for traffic sign recognition. *Neural Networks*, 32:323–332, Mar. 2012.

[6] V. Mnih, K. Kavukcuoglu, D. Silver, A. A. Rusu, J. Veness, M. G. Bellemare, A. Graves, M. Riedmiller, A. K. Fidjeland, G. Ostrovski, S. Petersen, C. Beattie, A. Sadik, I. Antonoglou, H. King, D. Kumaran, D. Wierstra, S. Legg, and D. Hassabis. Human-level control through deep reinforcement learning. *Nature*, 518:529–533, Feb. 2015.

[7] G. Tesauro. Temporal difference learning and td-gammon. *Communications of the ACM*, 38(3): 58–68, Mar. 1995.

[8] V. Mnih, K. Kavukcuoglu, D. Silver, A. Graves, I. Antonoglou, D. Wierstra, and M. Riedmiller. Playing atari with deep reinforcement learning. *Computing Research Repository*, Apr. 2013.

[9] M. Krakovsky. Reinforcement renaissance. *Communications of the ACM*, 56(8):12–14, Aug. 2016.

[10] J. Moody. Forecasting the economy with neural nets: A survey of challenges and solutions. In *Neural Networks: Tricks of the Trade, This Book is an Outgrowth of a 1996 NIPS Workshop*, pages 347–371. Springer-Verlag, 1998.

[11] H. van Hasselt, A. Guez, and D. Silver. Deep reinforcement learning with double q-learning. *CoRR*, abs/1509.06461, 2015.

[12] Y.-W. Cheung and M. Chinn. Currency traders and exchange rate dynamics: a survey of the us market. *Journal of International Money and Finance*, 20(4):439–471, 2001.

[13] T. Gehrig and L. Menkhoff. Technical analysis in foreign exchange - the workhorse gains further ground. Hannover economic papers (hep), Leibniz Universität Hannover, Wirtschaftswissenschaftliche Fakultät, 2003.

[14] L. Menkhoff. The use of technical analysis by fund managers: International evidence. *Journal of Banking and Finance*, 34(11):2573–2586, Nov. 2010.

[15] C. J. Neely and P. A. Weller. Technical analysis in the foreign exchange market. Working papers, Federal Reserve Bank of St. Louis, 2011.

[16] C. J. Neely, P. A. Weller, and J. M. Ulrich. The adaptive markets hypothesis: Evidence from the foreign exchange market. Working papers, Federal Reserve Bank of St. Louis, 2006.

[17] C.-H. Park and S. H. Irwin. What do we know about the profitability of technical analysis? *Journal of Economicl Surveys*, 21(4):786–826, July 2007.

[18] Y.-W. Cheung and M. Chinn. Currency traders and exchange rate dynamics: a survey of the us market. *Journal of International Money and Finance*, 20(4):439–471, 2001.

[19] P.-H. Hsu, Y.-C. Hsu, and C.-M. Kuan. Testing the predictive ability of technical analysis using a new stepwise test without data snooping bias. *Journal of Empirical Finance*, 17(3):471–484, 2010.

[20] R. S. Sutton and A. G. Barto. *Reinforcement Learning, An Introduction*. The MIT Press, 1998.

[21] L. Liu. Reinforcement learning, 2012. URL `http://cse-wiki.unl.edu/wiki/index.php/Reinforcement_Learning`.

[22] R. Bellman. *Dynamic Programming*. Princeton University Press, Princeton, NJ, USA, 1 edition, 1957.

[23] C. J. Watkins and P. Dayan. Technical note: Q-learning. *Machine Learning*, 8(3):279–292, 1992.

[24] L. Buşoniu, R. Babuška, B. D. Schutter, and D. Erns. *Reinforcement Learning and Dynamic Programming using Function Approximators*. CRC Press, 2010.

[25] Y. LeCun, L. Bottou, G. Orr, and K. Muller. Efficient backprop. In G. Orr and M. K., editors, *Neural Networks: Tricks of the trade*. Springer, 1998.

[26] A. Karpathy. Lecture notes in 'convolutional neural networks for visual recognition', 2016. URL `http://cs231n.stanford.edu`.

[27] B. C. Csáji. Approximation with artificial neural networks. Master's thesis, Eötvös Loránd University, 2001.

[28] V.-T. Tran. Lecture notes in 'from neural networks to deep learning', 2015. URL `https://www.slideshare.net/microlife/from-neural-networks-to-deep-learning`.

[29] P. V. V. *Mathematical foundation for Activation Functions in Artificial Neural Networks*, 2016. URL `https://medium.com/autonomous-agents`.

[30] M. A. Nielsen. *Neural Networks and Deep Learning*. Determination Press, 2015.

[31] D. E. Rumelhart, G. E. Hinton, and R. J. Williams. Neurocomputing: Foundations of research. chapter Learning Representations by Back-propagating Errors, pages 696–699. MIT Press, 1988.

[32] Y. Bengio. Practical recommendations for gradient-based training of deep architectures. In *Neural Networks: Tricks of the Trade*, volume 7700 of *Lecture Notes in Computer Science*, pages 437–478. Springer, 2012.

[33] T. Tieleman and G. Hinton. Lecture 6.5-rmsprop: Divide the gradient by a running average of its recent magnitude. COURSERA: Neural Networks for Machine Learning, 2012.

[34] T. Schaul, I. Antonoglou, and D. Silver. Unit tests for stochastic optimization. *CoRR*, abs/1312.6055, 2013.

[35] I. Goodfellow, Y. Bengio, and A. Courville. *Deep Learning*. MIT Press, 2016. `http://www.deeplearningbook.org`.

[36] J. Schmidhuber. Deep learning in neural networks: An overview. *Neural Networks*, 61:85–117, 2015.

[37] Y. Bengio. Learning deep architectures for ai. *Foundations and Trends in Machine Learning*, 2(1): 1–127, Jan. 2009.

[38] R. Pascanu, G. Montufar, and Y. Bengio. On the number of response regions of deep feed forward networks with piece-wise linear activations. In *International Conference on Learning Representations 2014 (ICLR 2014), Banff, Alberta, Canada*, 2013.

[39] G. Montúfar, R. Pascanu, K. Cho, and Y. Bengio. On the number of linear regions of deep neural networks. In *Proceedings of the 27th International Conference on Neural Information Processing Systems*, NIPS'14, pages 2924–2932. MIT Press, 2014.

[40] X. Glorot and Y. Bengio. Understanding the difficulty of training deep feedforward neural networks. In *In Proceedings of the International Conference on Artificial Intelligence and Statistics (AISTATS'10). Society for Artificial Intelligence and Statistics*, 2010.

[41] J. Moody and M. Saffell. Learning to trade via direct reinforcement. *IEEE Transactions on Neural Networks*, 12(4):875–889, July 2001.

[42] C. Gold. Fx trading via recurrent reinforcement learning. *Computational Intelligence for Financial Engineering*, pages 363–370, Mar. 2003.

[43] M. A. H. Dempster and V. Leemans. An automated FX trading system using adaptive reinforcement learning. *Expert Systems with Applications*, 30(3):543–552, Apr. 2006.

[44] J. Cumming. An investigation into the use of reinforcement learning techniques within the algorithmic trading domain. Master's thesis, Imperial College London, jun 2015.

[45] J. Zhang and D. Maringer. Indicator selection for daily equity trading with recurrent reinforcement learning. *Proceedings of the 15th annual conference companion on Genetic and evolutionary computation*, pages 1757–1758, July 2013.

[46] J. W. Lee, J. Park, J. O, J. Lee, and E. Hong. A multiagent approach to q-learning for daily stock trading. *IEEE Systems, Man, and Cybernetics - Part A: Systems and Humans*, 37(6):864–877, Nov. 2007.

[47] Y. J. Choe. A statistical analysis of neural networks. Carnegie Mellon University, 2016.

[48] W. Sarle. Neural network faq, part 2 of 7: Learning. Periodic posting to the Usenet newsgroup comp.ai.neural-nets, 1997. ftp://ftp.sas.com/pub/neural/FAQ.html.

[49] C. L. Giles, S. Lawrence, and A. C. Tsoi. Noisy time series prediction using recurrent neural networks and grammatical inference. *Machine Learning*, 44(1):161–183, July 2001.

[50] P. Scholz. Size matters! How position sizing determines risk and return of technical timing strategies. CPQF Working Paper Series 31, Frankfurt School of Finance and Management, Centre for Practical Quantitative Finance (CPQF), 2012.

[51] X. Glorot, A. Bordes, and Y. Bengio. Deep sparse rectifier neural networks. In *Proceedings of the Fourteenth International Conference on Artificial Intelligence and Statistics (AISTATS-11)*, volume 15, pages 315–323. Journal of Machine Learning Research - Workshop and Conference Proceedings, 2011.

[52] T. Schaul, J. Quan, I. Antonoglou, and D. Silver. Prioritized experience replay. *CoRR*, abs/1511.05952, 2015. URL `http://arxiv.org/abs/1511.05952`.

[53] L.-J. Lin. *Reinforcement Learning for Robots Using Neural Networks*. PhD thesis, Pittsburgh, PA, USA, 1992. UMI Order No. GAX93-22750.

[54] T. Zahavy, N. Ben-Zrihem, and S. Mannor. Graying the black box: Understanding dqns. *CoRR*, abs/1602.02658, 2016.

Appendix A

Learning curves

This appendix contains the learning curves obtained during the testing procedure described in chapter 4, that were not included in said chapter. Figure A.1 and Figure A.2 were obtained using $time\_skip = 5000$ while Figure A.4 and Figure A.5 were obtained with $time\_skip = 10000$.

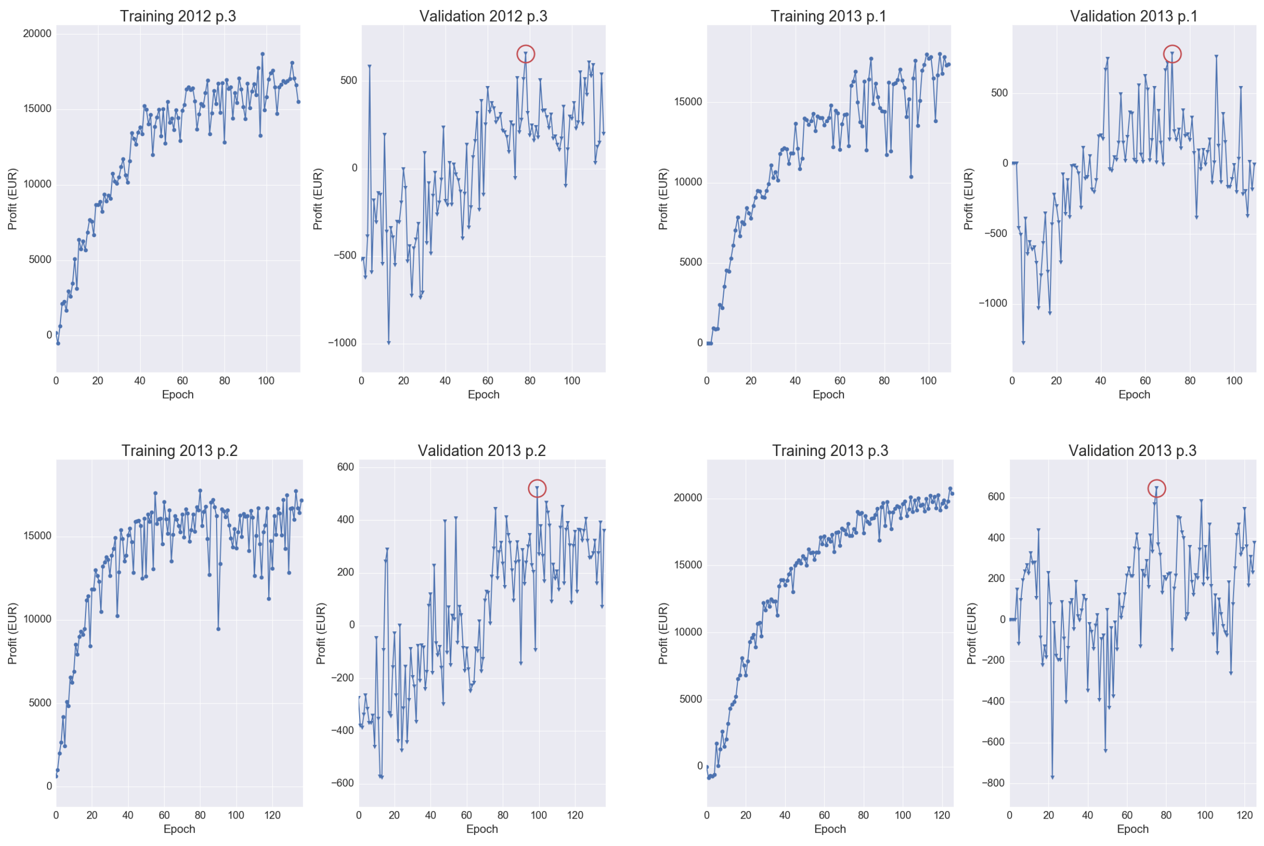

Figure A.1: Learning curves, $time\_skip = 5000$ (cont.) Red circle marks the chosen model.

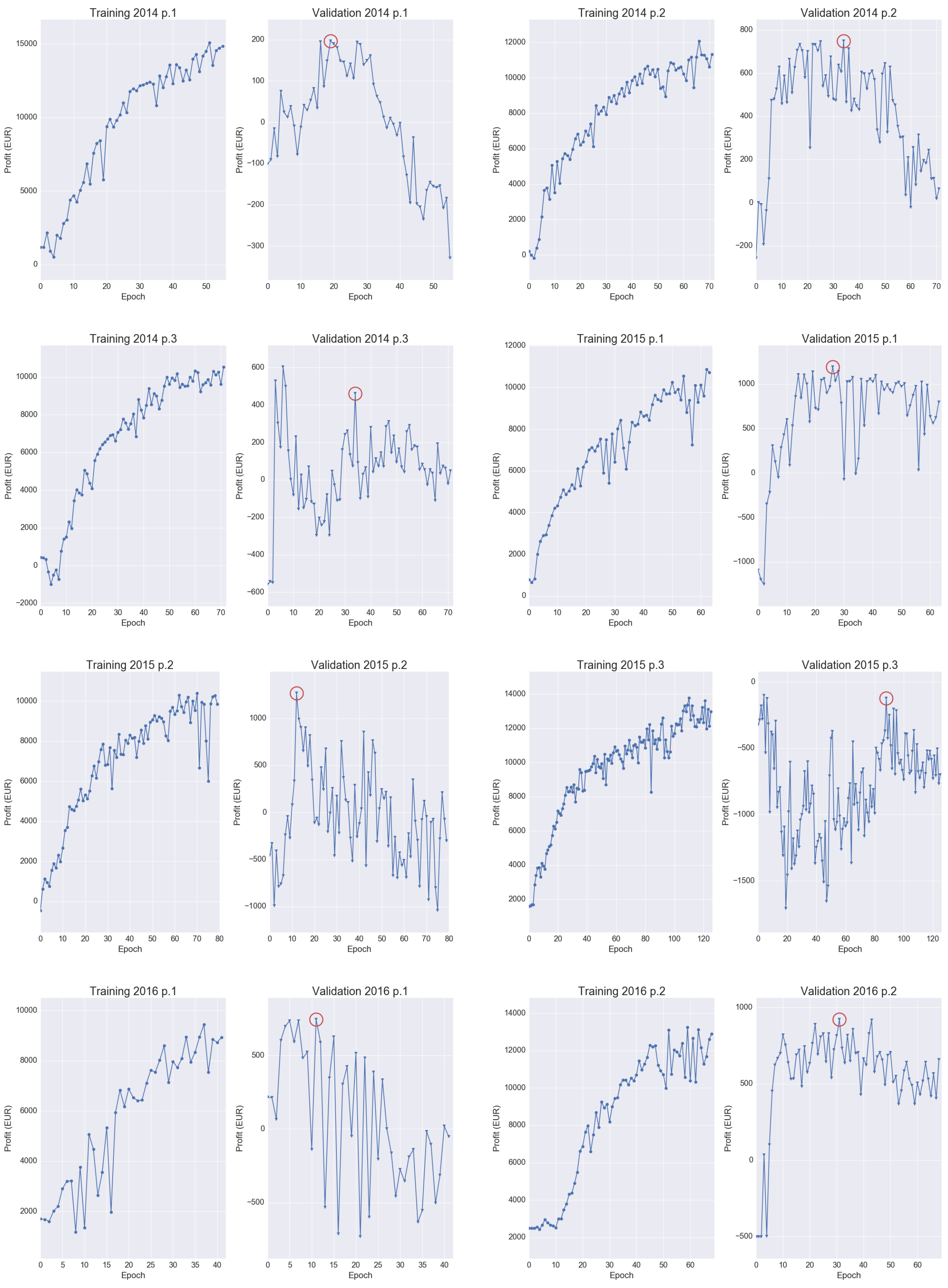

Figure A.2: Learning curves, $time\_skip = 5000$ (cont.) Red circle marks the chosen model.

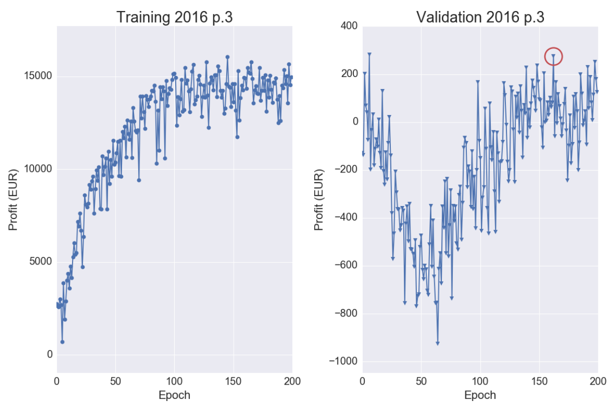

Figure A.3: Learning curves, $time\_skip = 5000$ (cont.) Red circle marks the chosen model.

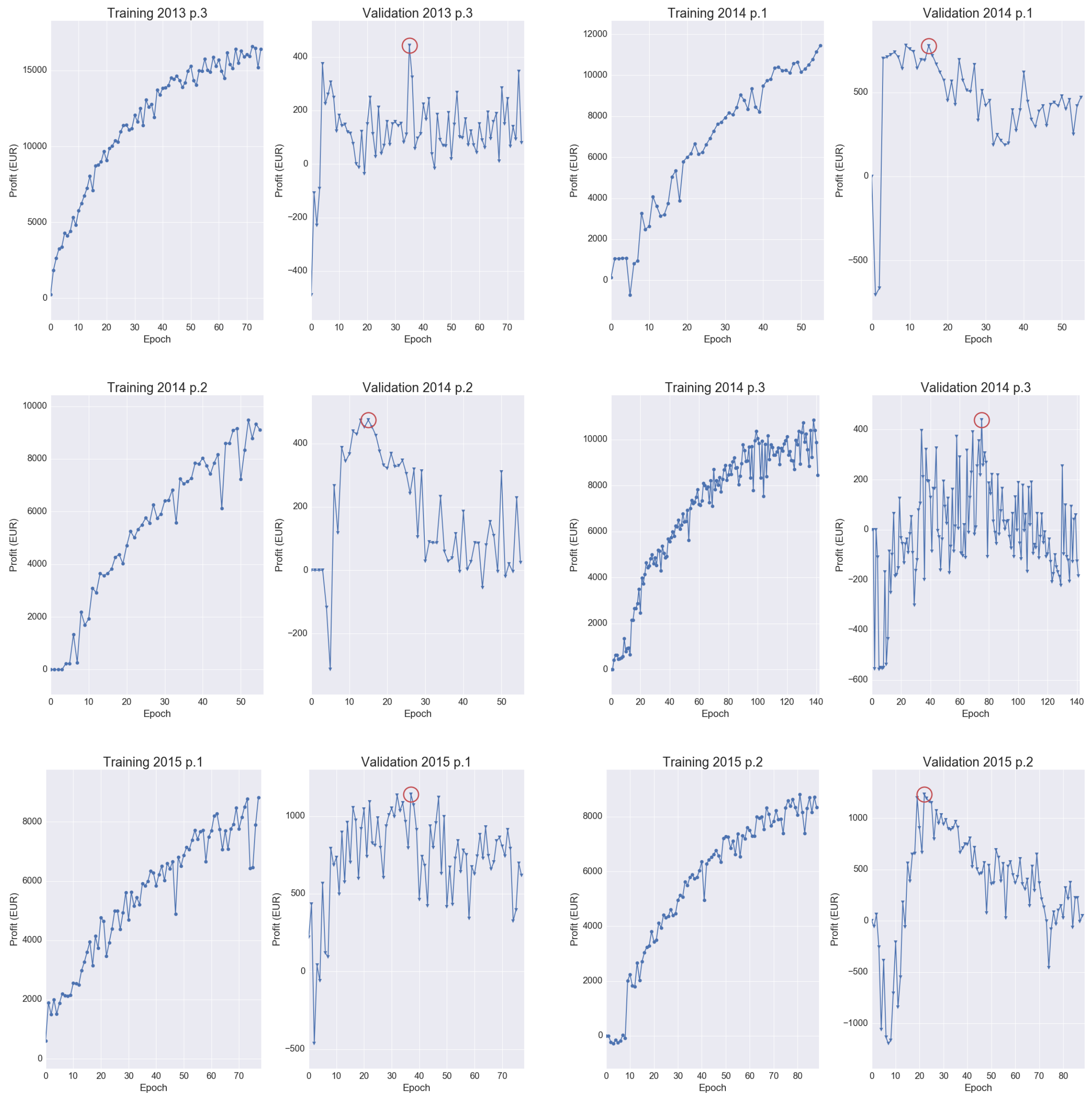

Figure A.4: Learning curves, $time\_skip = 10000$ (cont.) Red circle marks the chosen model.

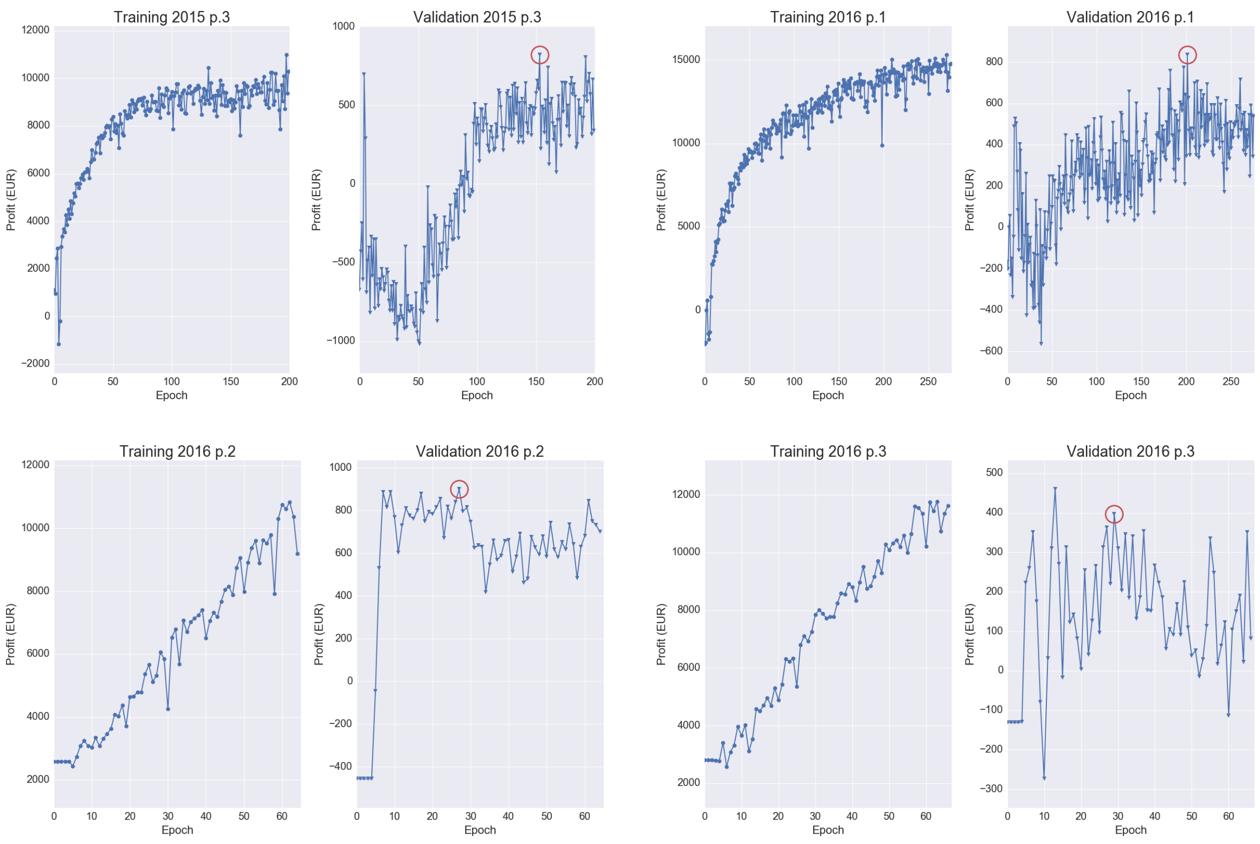

Figure A.5: Learning curves, $time\_skip = 10000$ (cont.) Red circle marks the chosen model.